

Environmental
Studies
Revolving
Funds

039 Inventory of Upslope and
Downslope Iceberg
Scouring

The Environmental Studies Revolving Funds are financed from special levies on the oil and gas industry and administered by the Canada Oil and Gas Lands Administration for the Minister of Energy, Mines and Resources, and by the Northern Affairs Program for the Minister of Indian Affairs and Northern Development.

The Environmental Studies Revolving Funds and any person acting on their behalf assume no liability arising from the use of the information contained in this document. The opinions expressed are those of the authors and not necessarily reflect those of the Environmental Studies Revolving Funds agencies. The use of trade names or identification of specific products does not constitute an endorsement or recommendation for use.

Environmental Studies Revolving Funds

Report No. 039

July, 1986

INVENTORY OF UPSLOPE AND DOWNSLOPE ICEBERG SCOURING

C.M.T. Woodworth-Lynas

D.W. Bass

J. Bobbitt

Centre for Cold Ocean Resources Engineering (C-CORE)

Memorial University of Newfoundland

St. John's, Newfoundland A1B 3X5

Scientific Adviser: Lorne Schoenthaler

The correct citation for this report is:

Woodworth-Lynas, C.M.T., Bass, D.W. and Bobbitt, J.,
1986. Inventory of upslope and downslope iceberg
scouring. Environmental Studies Revolving Funds
Report, No. 039. Ottawa, 103 p.

Published under the auspices
of the Environmental Studies
Revolving Funds

ISBN: 0-920783-38-4

© 1986 - Centre for Cold Ocean Resources Engineering

TABLE OF CONTENTS

	PAGE
LIST OF TABLES	vi
LIST OF ILLUSTRATIONS	vii
GLOSSARY OF TERMS	x
THE INVENTORY	xi
ACKNOWLEDGEMENTS	xii
SUMMARY	1
RESUME	2
INTRODUCTION	3
METHODS	5
Data sources	5
Sidescan mosaics	5
Scour maps	7
Radar iceberg trajectories	7
Inventory compilation	8
Orientation	8
Length	9
Shape	9
Depth	9
Bathymetric range	10
Change in width	10
RESULTS	10
Hekja North mosaic	10
Inventory results	10
Seabed slope and surficial geology	13
Currents	13
Rut mosaic	14
Inventory results	14
Seabed slope and surficial geology	14
Currents	18
Saglek East mosaic	21
Inventory results	21
Seabed slope and surficial geology	21
Currents	24
Saglek West mosaic	24
Inventory results	24
Seabed slope and surficial geology	28
Currents	28

Contents (continued)	PAGE
Iceberg Caroline mosaic	29
Inventory results	29
Seabed slope and surficial geology	33
Currents	33
Saglek Bank iceberg scours from radar	
Observations	33
Inventory results	33
Seabed slope and surficial geology	36
Currents	37
Nain Bank mosaic	37
Inventory results	37
Seabed slope and surficial geology	37
Currents	40
Bjarni wellsite scour map	40
Inventory results	40
Seabed slope and surficial geology	44
Currents	44
North Bjarni mosaic	47
Inventory results	47
Seabed slope and surficial geology	47
Currents	47
Snorri wellsite scour map	49
Inventory results	49
Seabed slope and surficial geology	49
Currents	53
Makkovik Bank iceberg scours from radar	
Observations	53
Inventory results	53
Seabed slope and surficial geology	53
Currents	57
DB Wellsite mosaic	59
Inventory results	59
Currents	59
East Harrison Bank mosaic	63
Inventory results	63
Seabed slope and surficial geology	63
Currents	63
Hibernia East mosaic	67
Inventory results	67
Seabed slope and surficial geology	67
Currents	67

Contents (continued)	PAGE
THEORETICAL MODELLING OF UPSLOPE, DOWNSLOPE SCOUR	71
Stability	71
Two-dimensional theoretical modelling	73
Unstable roll	73
Tilt	87
DISCUSSION AND POSSIBLE FUTURE WORK	95
REFERENCES	98

LIST OF TABLES

Table	PAGE
1. Mosaics and scour maps originally targeted for study	6
2. Range in scour depth along length of scours from the Saglek East mosaic	11
3. Probability of exceeding certain percentage draft increases for four typical trapezoidal icebergs	86

LIST OF ILLUSTRATIONS

Figure	PAGE
1. Location map of study areas	4
2. Hekja North mosaic scour map	12
3. Hekja North mosaic orientations of isobath-traversing scours	15
4. Location map of the Rut and Caroline mosaics	16
5. Rut mosaic scour map	17
6. Progressive current vector diagram illustrating looping motion of semi-diurnal tides, Saglek Bank	19
7. Rut mosaic orientations of isobath-traversing scours	20
8. Location map of the Saglek East and Saglek West mosaics	22
9. Saglek East mosaic scour map	23
10. Current directions and speeds on Saglek Bank	25
11. Saglek East mosaic orientations of isobath-traversing scours	26
12. Saglek West mosaic scour map	27
13. Saglek West mosaic orientations of isobath-traversing scours	30
14. Orientations of all scours from the 1978 Saglek East and Saglek West mosaics	31
15. Iceberg Caroline mosaic scour map	32
16. Iceberg Caroline mosaic orientations of isobath-traversing scours	34
17. Radar tracks of icebergs on Saglek Bank interpreted as grounded or scouring	35
18. Location map of the Nain Bank mosaic	38
19. Nain Bank mosaic scour map	39
20. Current directions and speeds on Nain Bank	41
21. Nain Bank mosaic orientations of isobath-traversing scours	42

Illustrations (continued)	PAGE
22. Bjarni Wellsite Scour Map	43
23. Location Map of Bjarni wellsite scour map and North Bjarni mosaic	45
24. Bjarni Wellsite scour map orientations of isobath-traversing scours	46
25. North Bjarni mosaic scour map	48
26. Current directions and speeds on Makkovik Bank ..	50
27. North Bjarni mosaic orientations of isobath-traversing scours	51
28. Snorri wellsite scour map	52
29. Location map of the Snorri wellsite scour map and also location of Nain Bank mosaic	54
30. Snorri wellsite scour map orientations of isobath-traversing scours	55
31. Radar tracks of icebergs interpreted as grounded or scouring on Makkovik Bank	56
32. DB wellsite mosaic scour map	60
33. Location map of the DB wellsite mosaic	61
34. Current directions and speeds on Hamilton Bank ..	62
35. DB wellsite mosaic orientations of isobath-traversing scours	64
36. East HB mosaic scour map	65
37. Location map of the East HB wellsite mosaic	66
38. East HB wellsite mosaic orientations of isobath-traversing scours	68
39. Hibernia East mosaic scour map	69
40. Iceberg profile showing node points	72
41. Trapezoidal representation of iceberg profile ...	74
42. Partial underwater profiles of typical icebergs	75
43. Melting of iceberg leads to near-neutral stability	77

Illustrations (continued)	PAGE
44. Iceberg profiles having similar bulge-width (BW) ratios but different bulge-depth ratios (BD)	78
45. Iceberg profile increases its draft by nearly 50% on Roll	80
46. Iceberg profile increases its draft by 15% on roll	81
47. Distribution of draft-to-height ratios for different types of icebergs	83
48. Trapezoidal iceberg of type (a,c)	85
49. Iceberg profile used in simulation	88
50. Scour depth versus distance travelled by a small keel	91
51. Scour depth versus distance travelled by a large keel	92
52. Scour by a rolling iceberg	93

GLOSSARY OF TERMS

- Upslope and downslope - These terms refer to iceberg scours that cross isobaths.
- Grounded - An iceberg that has ceased to drift because its keel is in contact with the seabed is referred to as grounded.
- Sub-parallel - Straight and curved lines or linear features (e.g., scours or contours) that are not quite parallel.
- Geostrophic - When gravity, pressure gradient, and coriolis force are the only forces involved in oceanic flow, accelerations involved in water motion are then said to be geostrophic.
- Semi-diurnal - Tides with a roughly 12-hour periodicity (i.e., a cycle of ebb, flow and ebb) are semi-diurnal. These tides are generally responsible for the looping trajectories of icebergs seen from the radar trajectory data.
- Relict scour - An iceberg scour that is visible through superimposed scours and/or the orientation of which appears to bear no relationship to modern oceanic current flow.
- Modern scour - An iceberg scour formed within historic time.
- Ablation - The wasting or erosion of an iceberg by melting or water action.
- Isobath - Line connecting points of the same water depth.
- Bathymetric range - In describing iceberg scours, this is the vertical range through which the scour passes.
- Berm - Linear to curvilinear mound of seabed material heaved up on either side of an iceberg scour trough by the action of a scouring keel.
- M₂ - The semi-diurnal lunar tidal component of a current, with a period of 12.42 solar hours.
- K₁ - The luni-solar diurnal tidal component of current, with a period of 23.93 solar hours.

THE INVENTORY

The inventory of upslope and downslope iceberg scouring contains statistics on scours which cross isobaths. These statistics include orientation, length, shape, bathymetric range and maximum and minimum width. The scour maps, illustrated in reduced form in this volume, are contained in the inventory and are at a scale of 1:10,000. The inventory is not included in this volume but is available as a Geological Survey of Canada Open File Report.

ACKNOWLEDGEMENTS

The authors would like to thank Lorne Schoenthaler of Mobil Oil who was the Scientific Adviser during this study for providing guidance and appropriate comments and criticism. We thank particularly John Miller of Petro-Canada Resources for initial help in obtaining access to some of the sidescan mosaics and also Alan Ruffman of Geomarine Associates Ltd. whose encouragement and speedy response to several requests for data are greatly appreciated. Thanks also to John Zevenhuizen of Orca Marine for preparing two excellent bathymetric maps. We extend our appreciation to Peter Wood, formerly of ESRF, who coached us through some of the elaborate ESRF paper work. Finally we extend our great appreciation to Carol Anne Coombs who spent many hours and late evenings typing, proofing, and arranging the manuscript, and to Desiree King for the excellent drafting of scour maps and other diagrams, and to Bill Collins who helped in compiling some of the database.

SUMMARY

Statistics on iceberg scours that cross isobaths have been gathered from ten sidescan mosaics, two scour maps, and also about ten seasons of iceberg trajectory information compiled from radar observations at exploration wellsites, at locations between southern Baffin Island and the Grand Banks of Newfoundland. A total of 5,118 scours and interpreted scour tracks (from iceberg radar-tracking data) have been analysed, of which 821 crossed isobaths. The greatest bathymetric range traversed by icebergs as observed from the mosaics and scour maps is 15 m, whilst the largest range from the scour tracks interpreted from the radar data was 45 m. Scours seen on the mosaics and scour maps are invariably shorter than those interpreted from radar because the seabed surveys are restricted in area. Thus only segments of scours are usually seen whereas the radar trajectories allow interpretation of longer scouring events.

Inventory data on the scours consists of orientation, length, shape, depth (where available), bathymetric range and width. For each survey area the salient scour statistics are presented followed by brief descriptions of seabed slope, geology and local oceanic current. A section on simplified theoretical modelling of upslope and downslope iceberg scouring is presented to give the reader some insight into the dynamics of the scouring process and to show how variations in seabed soil strength and in iceberg stability can affect scour length and depth. The inventory and its potential use as a database is discussed.

RESUME

Les données concernant les marques d'érosion glaciaire qui se retrouvent dans les régions comprises entre le sud de la Terre de Baffin et les Grands Bancs de Terre-Neuve, et qui traversent les lignes de niveau bathymétriques, ont été recueillies de dix mosaïques obtenues par sonar à balayage latéral ainsi que de deux cartes montrant les marques d'érosion en plus de renseignements relatifs aux trajectoires laissées par les icebergs, fournis d'après les observations faites par radar aux sites d'exploration de puits, et accumulés pendant dix saisons. On a analysé 5, 118 traces d'iceberg dont certaines ont été déduites à partir des observations faites par radar. Il faut remarquer que 821 traces traversent plusieurs lignes de niveau bathymétriques.

Lorsqu'elle est mesurée à partir des mosaïques et de cartes montrant l'érosion glaciaire, la différence maximum des niveaux traversés par un sillon est de 15 m alors qu'elle peut atteindre 45 m dans le cas des traces obtenues à partir d'observations faites au radar. Les traces mesurées dans le cas des mosaïques et de cartes montrant l'érosion glaciaire sont toujours plus courtes que celles obtenues à partir des lectures radar, ceci s'expliquant par la différence de surface couverte par chaque système.

Les données concernant les traces traversant des lignes bathymétriques fournissent des indications sur l'orientation, la longueur, la forme, la profondeur (lorsqu'elle est disponible) et la manière dont la trace varie en passant d'un niveau bathymétrique à un autre. Pour les traces les plus importantes, les données statistiques sont suivies d'une description rapide de la géologie et de la pente du fond marin ainsi que des courants locaux.

Une description des modèles théoriques utilisées pour représenter l'érosion causée par un iceberg dans le sens de la pente ou dans le sens contraire permet au lecteur de se familiariser avec les processus dynamiques qui interviennent lors de l'impact, et montre comment les variations des caractéristiques du sol et la stabilité de l'iceberg peuvent affecter ce processus.

Les possibilités offertes par une telle quantité de données, sont discutées.

INTRODUCTION

Icebergs are known to scour and ground on the continental shelf areas of Atlantic Canada. Numerous groundings have been documented from exploration drillsites in both the Labrador and Grand Banks shelf regions in the last decade. From these observations, knowledge of the behaviour of grounded and in particular scouring icebergs is expanding.

Scouring bergs on the continental shelf areas have the potential to damage or destroy seabed production facilities. An understanding of the ability of icebergs to scour upslope and downslope and of their physical responses is required. Charles Darwin theorized that current-driven icebergs could touch bottom and continue forward "scratching and grooving the undulatory surface in long, straight lines" (Darwin, 1855). The possibility that icebergs could scour up and down seabed slopes was not considered again until the mid-1970s when seabed sidescan mosaics from Labrador wellsites showed numerous scours crossing isobaths (e.g. Geomarine, 1976). Since then, work has been aimed at documenting the occurrence of scouring and grounded icebergs in this region (Barrie et al., 1982; Woodworth-Lynas et al., 1984a,b; 1985). Mathematical and physical modelling of upslope scouring has been carried out by the Ocean Engineering Group at Memorial University and recent models by Chari et al. (1980), Chari and Peters (1981), and Lopez et al. (1981) compute finite scour lengths and depths. Woodworth-Lynas et al. (1985) propose an upslope/downslope scouring model based on observations of scouring icebergs at Labrador wellsites which reintroduces the concept of berg rotation with upslope/downslope scouring ability and also of scour depth decrease and increase.

This study presents an inventory containing information on the range of bathymetry traversed by iceberg scours seen on sidescan mosaics, iceberg scour maps and from iceberg trajectory data from several wellsites on the Labrador shelf (Figure 1). Inventory results are presented and local seabed conditions, oceanic currents and theoretical upslope/downslope scour models are described and discussed.

Winds were not considered in this study because air movements are believed to be relatively unimportant in comparison with ocean currents, as the driving forces affecting berg trajectories. For instance, Sodhi and Dempster (1975), Mountain (1980) and Gaskill and Rochester (1984) note that iceberg motion is determined principally by ambient ocean currents, although Dempster (1974) and Sodhi and El-Tahan (1980) note that berg motion can be affected directly by strong winds during storms and also indirectly through wind-generated inertial currents.

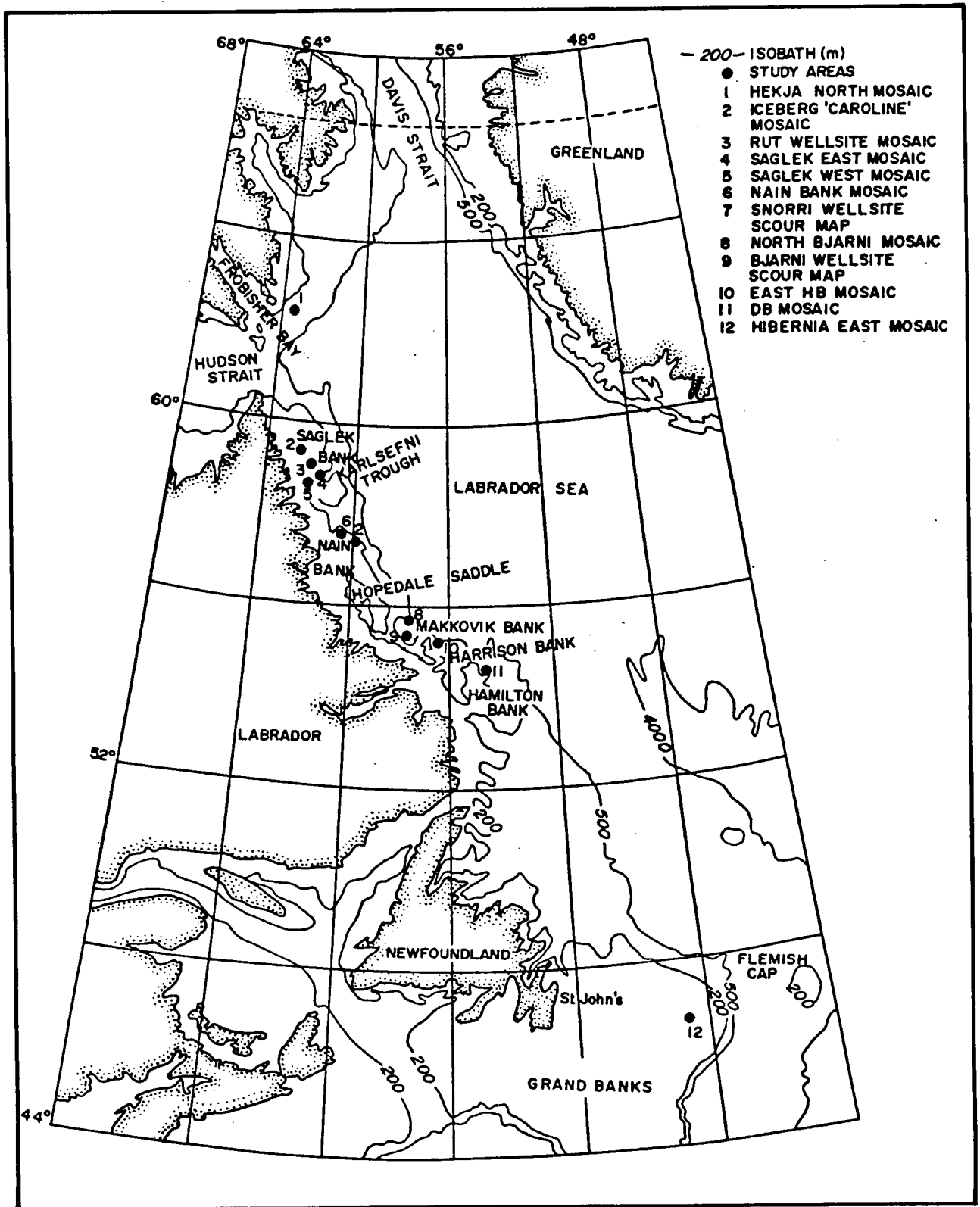


Figure 1. Location map of study areas.

A detailed statistical analysis of the inventory was not attempted because it is beyond the scope and intent of this work.

METHODS

Data used in compiling the upslope/downslope scour inventory were obtained from sidescan mosaics, seabed iceberg scour maps (which were drafted using information from sidescan sonographs) and from iceberg movement information derived from radar observations. Detailed bathymetric maps were required for all of the study areas to derive the bathymetric range of scours in each area. For all mosaics and scour maps detailed bathymetry with contour intervals of 2 m or 5 m were either already in existence or were constructed for each area. In all cases isobaths were extrapolated to 1 m intervals. In most cases the bathymetric range of individual scours was measured to accuracies of 0.5 m although in one case (the Rut mosaic) where the isobaths were consistently sub-parallel and widely spaced, the range was read to accuracies of 0.25 m. For the scours interpreted from iceberg radar observations bathymetric ranges are considered accurate to within 1-2 m.

DATA SOURCES

A total of twenty two different sidescan mosaics and scour maps were originally to be used in the study (Table 1). However, only twelve were studied. Of the original twenty-two, eight were discarded during the compilation. Five were not used because they contained information only on relict scours from areas or water depths no longer affected by scouring bergs. These data were deemed irrelevant to the study. One scour map (Gudrid wellsite) was discarded because detailed bathymetry was not available and the Makkovik Bank mosaic was not used because it contained duplicate information already available on the Bjarni wellsite scour map. The Greater Hibernia scour map was not used because it contains proprietary data.

Sidescan Mosaics

Of the ten mosaics used in this study four were collected by Geomarine Associates Ltd. The remaining six were collected jointly by the Centre for Cold Ocean Resources Engineering (C-CORE) and the Atlantic Geoscience Centre, Bedford Institute of Oceanography (AGC/BIO). All the mosaics had been assembled prior to commencement of this study. The four Geomarine surveys made in 1980 (Rut, East HB, DB and North Bjarni mosaics) were run using an ORE model

TABLE 1

Mosaics and Scour Maps Originally Targeted for Study

YEAR	AREA	WATER DEPTH (m)	COVERAGE	ORIGIN	BATHYMETRY
ICEBERG SCOUR MAPS (COMPILED FROM SIDESCAN DATA NOT IN MOSAIC FORM)					
*1975	Snorri J-90 wellsite Central Nain Bank	130-155	4.5 x 9 km	Geomarine	Yes
*1975	Bjarni H-81 wellsite Central Makkovik Bank	130-165	21 x 12.6 km	Geomarine	Yes
1975	Gudrid H-55 wellsite outer Cartwright Saddle	300	8 x 13 km	Geomarine	No
1985	Greater Hibernia	70-110	70 x 70 km	Mobil Oil (Proprietary)	?
WIDESWATH SIDESCAN DATA					
1980 July	Edge of Grand Banks	400-700	400 x 5 km	IOS	No
1983 June	Laurentian Channel	400	50 x 5 km	BIO	Yes
1984 July	West of Verrill Canyon, Scotian Shelf	400+	----	BIO	No
1984 Sept.	Hudson Strait	650-700	80 x 10 km	BIO	Yes
SIDESCAN MOSAICS (LABRADOR)					
*1979 1982	Iceberg Caroline Saglek Bank	120	4 x 2 km	C-CORE	Yes
*1979 1982	Nain Bank	140	4.5 x 2 km	C-CORE	Yes
*1977 1978 1979 1981	Saglek East	160-180	13 x 4 km	C-CORE	Yes
*1977 1978 1979 1981	Saglek West	155-180	13 x 2.5 km	C-CORE	Yes
1976 1979	Makkovik Bank	130-140	11 x 4 km	Eastcan('76) C-CORE ('79)	No
1980 1981	Hekja Wellsite	350-400	4 x 7.5 km	Geonautics('80) C-CORE ('81)	No
*1981	Hekja North	280	7 x 2.5 km	C-CORE	Yes
*1980	Rut Wellsite	120	4 x 2.5 km	Geomarine	Yes
*1980	North Bjarni	140-150	5 x 2.5 km	Geomarine	Yes
*1980	East HB	155	5.5 x 2 km	Geomarine	Yes
*1980	DB	215	5.5 x 3 km	Geomarine	Yes
SIDESCAN MOSAICS (GRAND BANKS)					
*1980	Hibernia East	84-99	3 x 7 km	C-CORE	Yes
1980 April & Oct.	Hebron North	88-95	9 x 4.5 km	BIO (Apr.) C-CORE(Oct.)	Yes

*indicates data sets used in this study.

160 sidescan system with a total swath of about 750 m. Analog tape records of the surveys were subsequently replayed, reduced, and distortion corrected copies at 1:2,000 scale were produced using an ORE Model 158 Graphic Processor (Geomarine Associates Ltd., 1980a,b,c,d). The mosaics were photographically reduced to 1:10,000 scale for analysis.

The C-CORE/BIO surveys were made using the BIO 70 kHz medium-range sidescan system operating with a total swath of 1500 m (Jollymore, 1974). The system is considered capable of resolving seabed features as small as 1 m (A. Boyce, AGC/BIO, pers. comm., 1985). The analog data tapes were replayed through a Honeywell 1856a fibre-optic visicorder and were reproduced on 152 mm dry-silver paper. In this way distortion-corrected copies of the original data were produced at a reduced scale of 1:10,000. The strips of dry-silver paper with the corrected data were then assembled on top of detailed ship's track plots also at the same scale. Corrections were made for layback, the lag effect introduced because the sidescan fish is towed some distance (up to 400 m) behind the ship. Small adjustments were made to match up scours that traversed survey lines and the assembled mosaics were photographed at scale and printed on resin-coated photographic paper. These prints were used as working copies.

Scour Maps

The two scour maps analysed in this study were compiled by Geomarine in 1976 as part of contract reports for industry. They were drafted using the original sidescan and depth profiler records. A modified ORE 1036-10980 sidescan system was used operating at 200 kHz. The total swath was about 600 m (Geomarine Associates Ltd., 1975).

During this study scour maps were drafted from all of the sidescan mosaics by tracing all definable scour features and assigning each an identification number. Oblate to circular scours, referred to as pits (NORDCO, 1983), with lengths less than three times the width were not included because they did not cross isobaths. Pits were probably not formed by continuously scouring icebergs.

Radar Iceberg Trajectories

Radar observations made from exploration well sites on the Labrador shelf between 1973 and 1981 have been used to delineate areas of active scouring (Woodworth-Lynas et al., 1985). The drift tracks of over 1,500 icebergs were analysed and more than fifty grounded and scouring bergs were identified (refer to page for description of how grounded and scouring icebergs were interpreted). Several

of the scouring bergs were tracked over horizontal distances in excess of 60 km and traversed often significant (up to 45 m) ranges in bathymetry.

The trajectory data were collected by ice observers on the drilling ships. The observers monitored berg movements for the entire drilling period (usually between three to ten weeks) twenty four hours a day. Data were collected by noting berg positions using standard x- or s-band marine radars on the bridges of the drilling vessels. Berg positions were noted nominally on an hourly basis, entering the time, range and bearing for each berg in a logbook.

INVENTORY COMPILATION

Using the scour morphology description scheme (Appendix A) up to six different types of measurement were made on each iceberg scour (or scour track interpreted from the radar data). These are, orientation, length, shape, depth, bathymetric range and change in width.

Orientation

The orientation of each partial or complete scour was measured using a protractor and was recorded as a three digit number in degrees from true north. Scour orientations beyond 180°, for example of 189°, are entered as 009°. The orientation is measured along a straight line joining the two termini of a scour.

Two other ESRF studies measure orientation differently. Geonautics (in preparation), in their Iceberg Scour Study 1 (ESRF Study #011-19-05 [S]) enter several orientations for one scour if it is curved, measuring the chords of several arbitrary segments (R. Gillespie, Geonautics, pers. comm., 1985). Geoterrex (in preparation), during their compilation of data on Beaufort Sea pressure ridge ice scours (ESRF Study #022-14-05), digitized their entire database allowing the derivation of a weighted averaged orientation for each scour together with standard deviation. We deemed these more sophisticated approaches unnecessary for this study.

Our simple method, although ignoring changes in orientation along the lengths of curved scours, provides a single non-weighted measurement which was used to compile rose diagrams of scour orientation for each study area. Scour orientations were not measured from the radar iceberg trajectory data because, in nearly all cases, the scouring bergs underwent very large changes in direction (more than 180° and in several instances 360°).

Length

Scour length is the distance, in metres, measured along the axis of the trough, between the two termini. Where incomplete scours were recorded the partial lengths are indicated by a "+" sign (e.g. 650+ indicates the scour is greater than 650 m long). Complete scours are rarely identified on mosaics and scour maps for several reasons. First, one or both ends of a scour may lie outside the mosaic or map area. Secondly, one or both ends may have been partially or totally obliterated by infilling sediment. Thirdly, scours often cannot be correlated between sidescan survey lines, a problem readily observed on some of the mosaics where scouring is intense. Lastly, there may be partial obliteration of older scours by younger scours. Scour tracks of great length (commonly in excess of 5 km) can be identified from the iceberg radar trajectory data.

In all cases, scour length was measured using an ALVIN 1112 mechanical map scale, to an accuracy of ± 20 m for scour maps at 1:10,000 scale and ± 1000 m for iceberg radar scour tracks at 1:250,000 scale. The decrease in measurement accuracy at increased scale is simply because inaccuracies during measurement are naturally amplified.

Shape

Shape refers to the straightness of the iceberg scour. Five different shape categories were developed to describe normal curvilinear scours together with four categories to describe craters and crater chains and a notation for scours that show evidence of having been formed by multikeeled icebergs. The scour morphology descriptions are given in Appendix A.

Depth

Iceberg scour depth measurements were available for two of the scour maps (Snorri and Bjarni wellsites) and in some cases if the survey pattern crossed the same scour more than once, measurements were made at different points along the scour. Scour depth information was read from ORE sub-bottom profile records. In all cases where scour depth was measured, the water depth at the measurement point was also recorded. Scour depth was measured from the sonar profiles as the vertical distance in metres from the deepest part of the scour trough to the level of the undisturbed seabed. Scour depth information, though available from three of the mosaics (Hekja North, Saglek East and Saglek West) could not be used because correlation of scours between the sonar profiles and sidescan records could not be made with any certainty. However, Geonautics (in preparation) (ESRF study #011-19-05[s]) after making a detailed study of the Saglek

East mosaic, believed they could make some correlations (pers. comm., R. Gillespie and E. King, Geonautics, 1985) and these results are reproduced in Table 2.

Bathymetric Range

The bathymetric range of an iceberg scour is the vertical range through which it passes. Where a scour traverses both upslope and downslope this is noted in the inventory, but the direction of scouring cannot be inferred from any but the radar trajectory data.

Change in Width

It was originally thought that scour width would normally increase upslope as the scouring keel became more entrenched in the seabed. However, unpublished work carried out at C-CORE indicates that this is not the case and scours may increase or decrease in width. A suitable theory to explain this phenomenon has yet to be developed and for that reason measurements of changes in width were made so that detailed analysis can be attempted in the future. A note is made whether the scour increases or decreases in width upslope or downslope together with the minimum and maximum scour width in metres. Scour width measurements are considered accurate to ± 5 m in all cases. Scour width measurements are, of course, not available from the radar trajectory data. An example of how a scour may be completely defined by using the descriptive system is given in Appendix A.

RESULTS

In this section each of the study areas are discussed separately beginning with the most northerly site and ending with the most southerly. For each area the inventory results are briefly discussed and the seabed slope, surficial geology and ocean currents are described.

HEKJA NORTH MOSAIC

Inventory Results (Appendix B)

This mosaic was compiled by C-CORE in 1981 as part of a study on iceberg scours for Canterra Energy Ltd. (Barrie et al., 1982). Water depths range between 280 m and 290 m. Of 775 scours on the scour map (Figure 2), 48 had bathymetric ranges equal to or in excess of 1.0 m. The maximum bathymetric range observed was 4.5 m (scour number 4).

TABLE 2
Range in Scour Depth Along Length of Scour
Saglek East

SCOUR NUMBER*	DEPTH (m)		WIDTH (m)		DEPTH DIFFERENCE (m)
	Line 1	Line 2	Line 1	Line 2	
506 (273)	1.0	1.5	35	20	0.5
461 (260)	3.5	3.5	25	25	0
424/346 (204)	2.5	0.5	40	20	2.0
300 (154)	0.5	0.2	20	15	0.3
306/423 (150)	1.2	1.5	25	20	0.3
262 (135)	5.0	5.0	60	22	0
258/297/305 (134)	1.0	1.0	60	60	0
253 (131)	2.0	1.5	60	17	0.5
209 (90)	0.5	2.5	22	25	2.0
137(63)	4.0	5.0	40	22	1.0
60 (60)	2.5	2.0	30	30	0.5
124 (50)	1.5	2.0	65	35	0.5
60 (31)	0.2	0.5	60	27	0.3
38 (20)	1.0	1.5	35	45	0.5
20/21/22 (7)	1.0	0.3	30	30	0.7
18 (6)	0.4	0.1	26	26	0.3
55 (3)	0.2	0.6	25	40	0.4
15/51 (2)	4.0	2.0	70	52	2.0
23 (1)	1.0	1.0	40	30	0

* Numbers without brackets refer to scour identification numbers given in this study. Numbers in brackets are those given to the same scours in the study by Geonautics (in preparation) ESRF study #011-19-05[S].

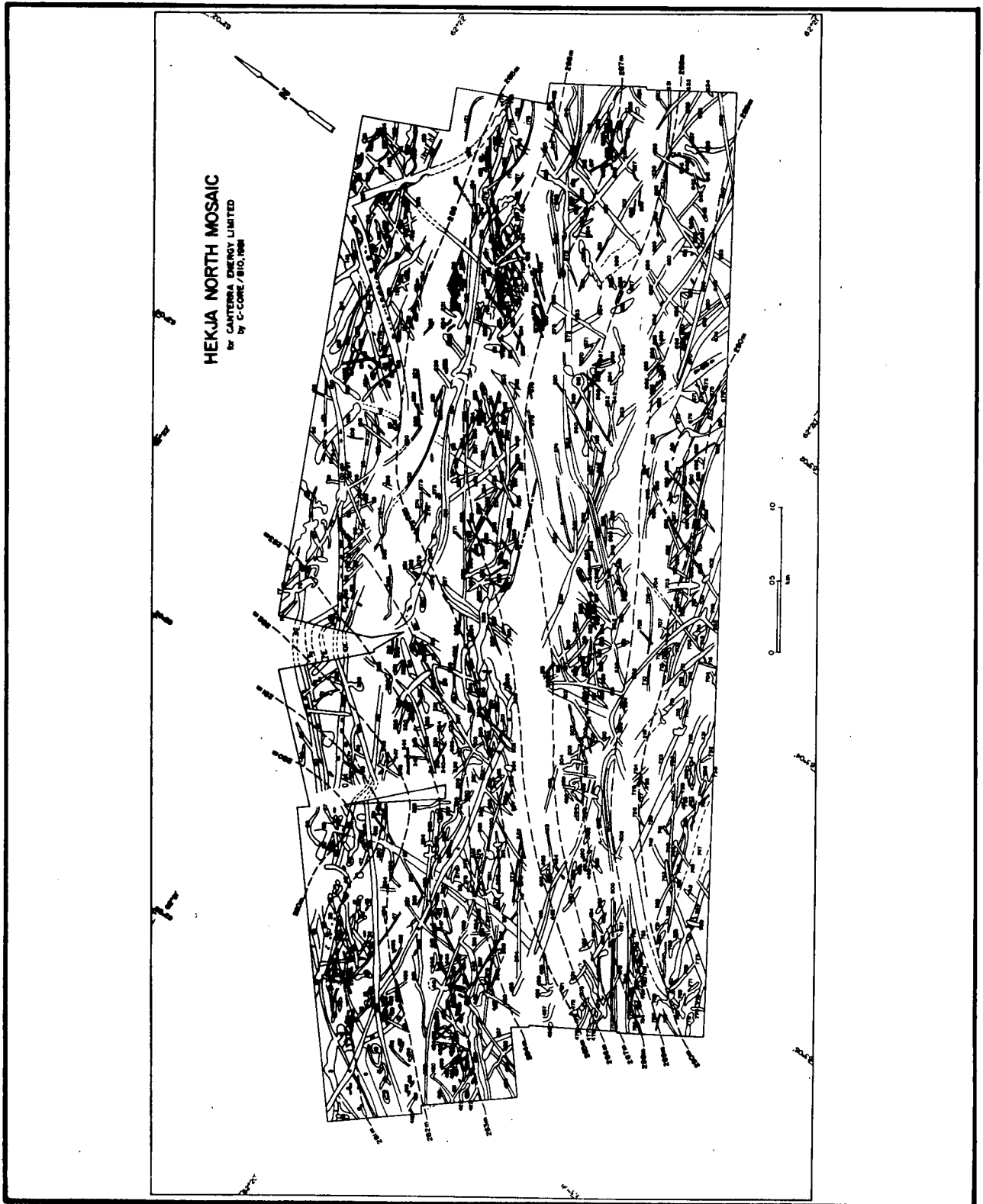


Figure 2. Hekja North mosaic scour map.

Twenty-one scours were observed to change in width with a maximum change of 180 m (scour number 186, width ranging between 15 m and 195 m). Eight scours increased in width upslope, six increased in width downslope and the remaining seven showed increases and decreases in width across the isobaths.

Seabed Slope and Surficial Geology

The regional seabed slope in the area is about 1 in 260 towards the southeast. The maximum gradient within the mosaic area is 1 in 200 to the southwest and a minimum gradient of 1 in 440 occurs in the northeastern sector.

No sediment samples were collected within the area of the mosaic. The nearest sample collection sites are between 10 km and 20 km away. Praeg et al. (in press) have defined the Quaternary geology of the region containing the mosaic as comprising of Davis Strait Silt, which consists of acoustically unstratified grey to black, sandy and/or gravelly silts and clays. In the mosaic area the Davis Strait Silt unconformably overlies what is interpreted to be Tertiary strata.

The morphology of the scours suggests that the sediments are easily scoured since fine structures are seen, such as the rake-like marks in one or two scour troughs, indicating formation by multikeeled icebergs, and also very narrow (5-10 m wide) scours can be easily discerned because of acoustically sharply defined berm crests. Mean scour depth in the mosaic area is 1.2 m with a maximum observed scour depth of 4.4 m and a minimum observed depth of 0.4 m (Pereira et al., in prep).

Overburden depths of up to 4.0 m of Davis Strait Silt occur in the mosaic area and several scours contain 'blocky' reflectors in their troughs which may represent large pieces of Tertiary bedrock that have been disrupted and exposed by the scouring action (Pereira et al., in prep). Woodworth-Lynas (1983) defined the relative ages of the Hekja North scours using cross-cutting relationships. From this work, he found that maximum scour width decreased through time suggesting that iceberg size has also decreased through time.

Currents

The currents at Hekja North are similar to those at Ralegh N-18 (62°18'N, 62°33'W), 28 km northeast of Hekja, where current measurements were collected by Canterra Energy in 1982, and reported by Seaconsult Marine Research (1982). These measurements show that the currents result mainly from the semi-diurnal tide and are in the order of 34 cm/sec, 28 cm/sec, 29 cm/sec and 10 cm/sec at depths of 68 m, 145 m,

317 m, and 344 m respectively. The semi-diurnal currents are aligned along directions 60° and 240° , with the higher currents in the 240° direction. The maximum current at each depth was 83 cm/sec, 69 cm/sec, and 37 cm/sec. The mean currents were 28 cm/sec, 23 cm/sec, 22 cm/sec, and 13 cm/sec.

Internal waves were reported at the Hekja site giving speeds up to 1.03 m/sec for short periods of time (Hodgins and Westergard, 1981). These waves have periods of 10 to 12 minutes, and therefore are not likely to have much effect on iceberg motions.

The rose diagram of scour orientations (Figure 3) shows only those 48 which cross isobaths. Clearly there is a fairly strong concentration in the 70° - 89° and in the 50° - 59° orientation, agreeing closely with the observed orientation of the semi-diurnal currents.

RUT MOSAIC

Inventory Results (Appendix C)

This mosaic on Saglek Bank (Figure 4) was compiled by Geomarine Associates for Petro-Canada Exploration as part of the pre-drilling survey at the Rut H-11 wellsite (Geomarine Associates Ltd., 1980a). From the map (Figure 5) 327 scours were identified, compared with a total of 238 interpreted by Geomarine Associates Ltd. (1980a), in a water depth range of 123-130 m. Forty-eight scours had bathymetric ranges equal to or in excess of 0.5 m. Because isobaths were widely and evenly spaced ranges were read to 0.25 m. The maximum bathymetric range observed was 3.25 m (scour number 116). Two scours increased in width downslope, one increased in width upslope and one displayed both increases and decreases in width with slope.

Seabed Slope and Surficial Geology

Gentle regional slopes of 1 in 750 towards the northeast and east are found on this northerly part of Saglek Bank. Slopes within the mosaic area are fairly consistent ranging between 1 in 400 and 1 in 540 towards the north in the western part, and 1 in 430 in the eastern part. Geologically, the mosaic covers an area of glacial till overlain by a thin (10 cm) veneer consisting of more than 60-75% sand, some silt and minor amounts of gravel and clay and poorly sorted silts (Geomarine Associates Ltd., 1980a; Gilbert and Barrie, 1985). Two seabed photographs from within the mosaic area confirm the presence of silty sand (Geomarine Associates Ltd., 1980a). Fillon and Harmes (1982) in defining acoustic/morphologic units for Saglek Bank describe an extensive area of the bank top, in which

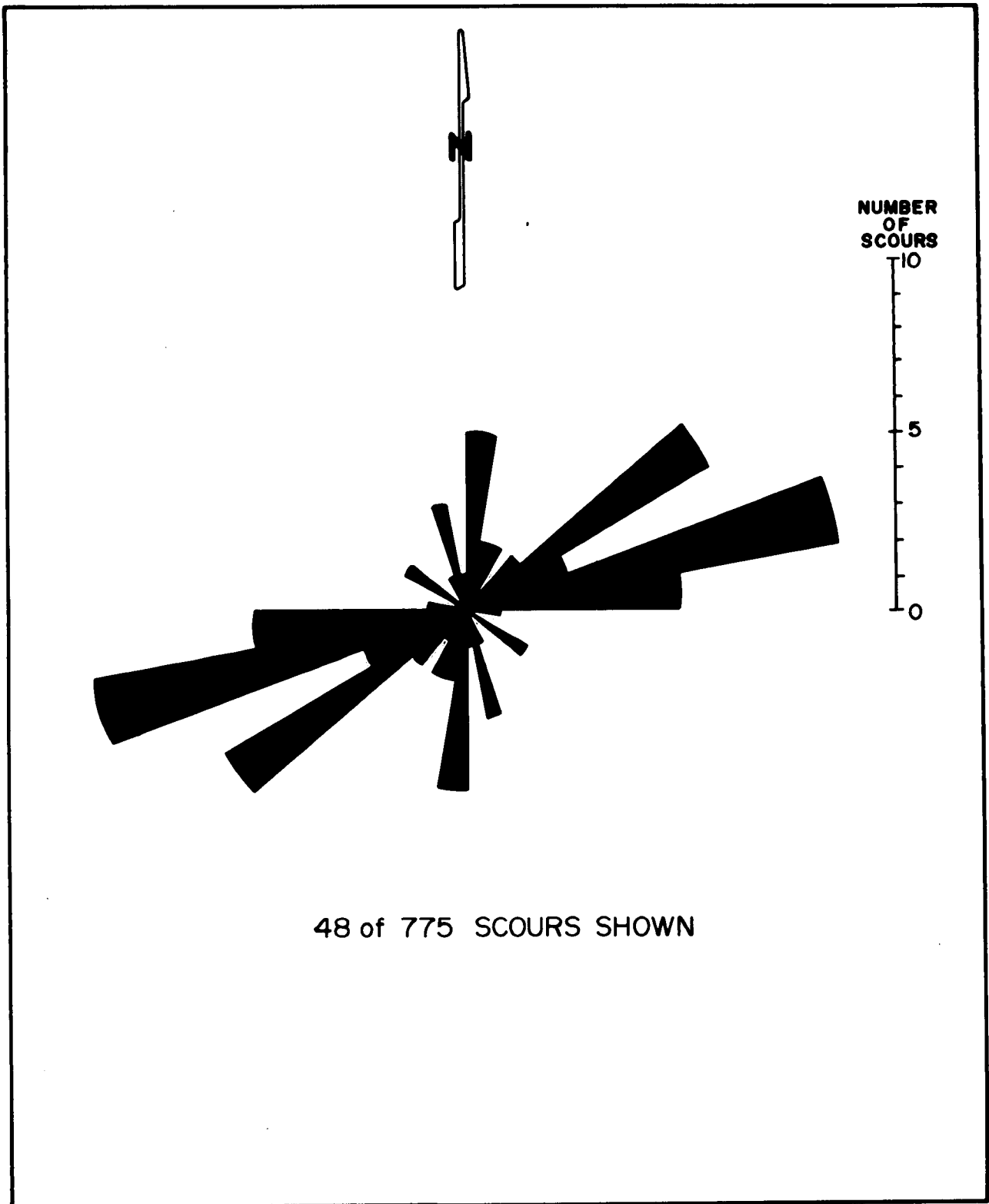


Figure 3. Hekja North mosaic orientations of isobath-traversing scours.

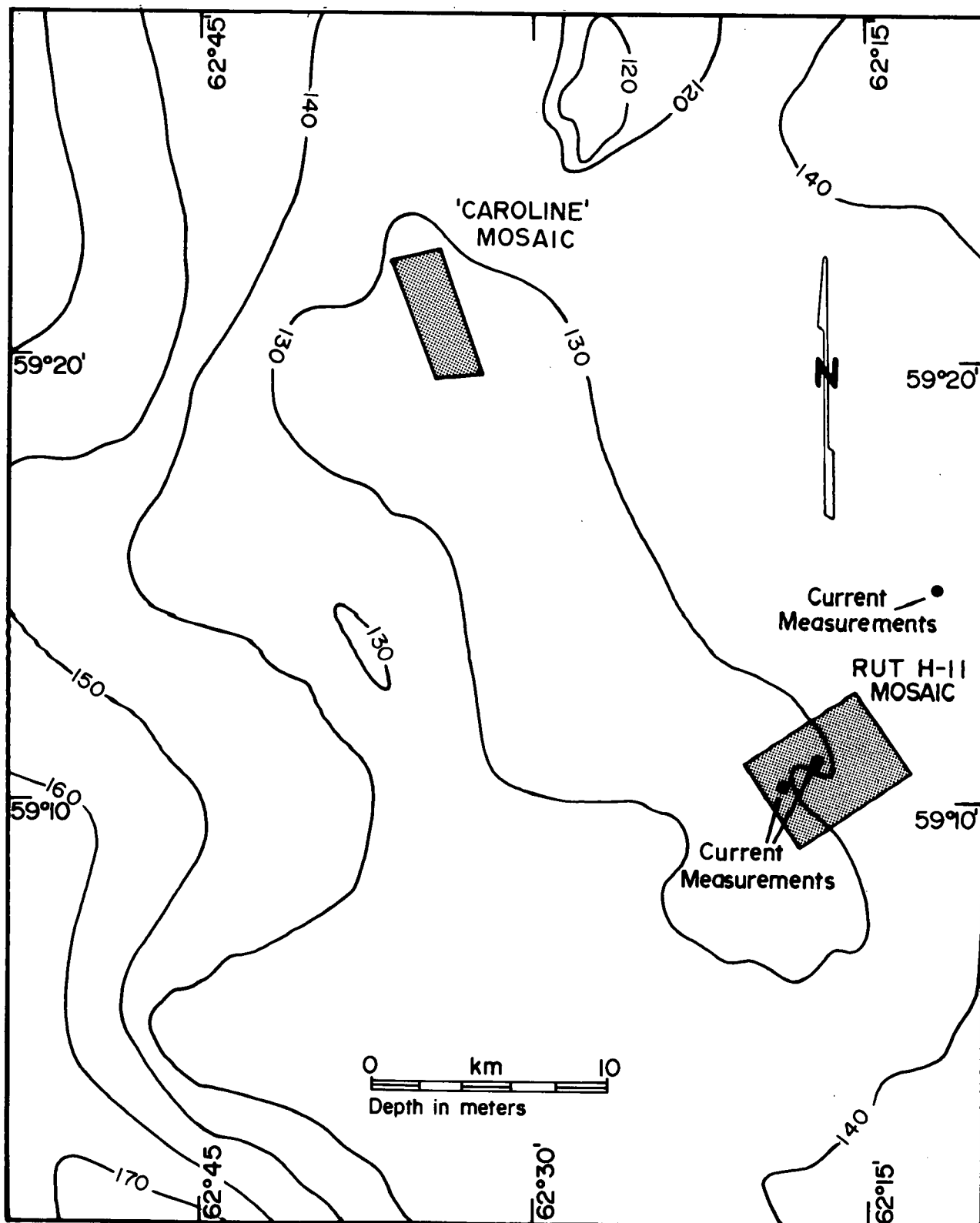


Figure 4. Location map of the Rut and Caroline mosaics.

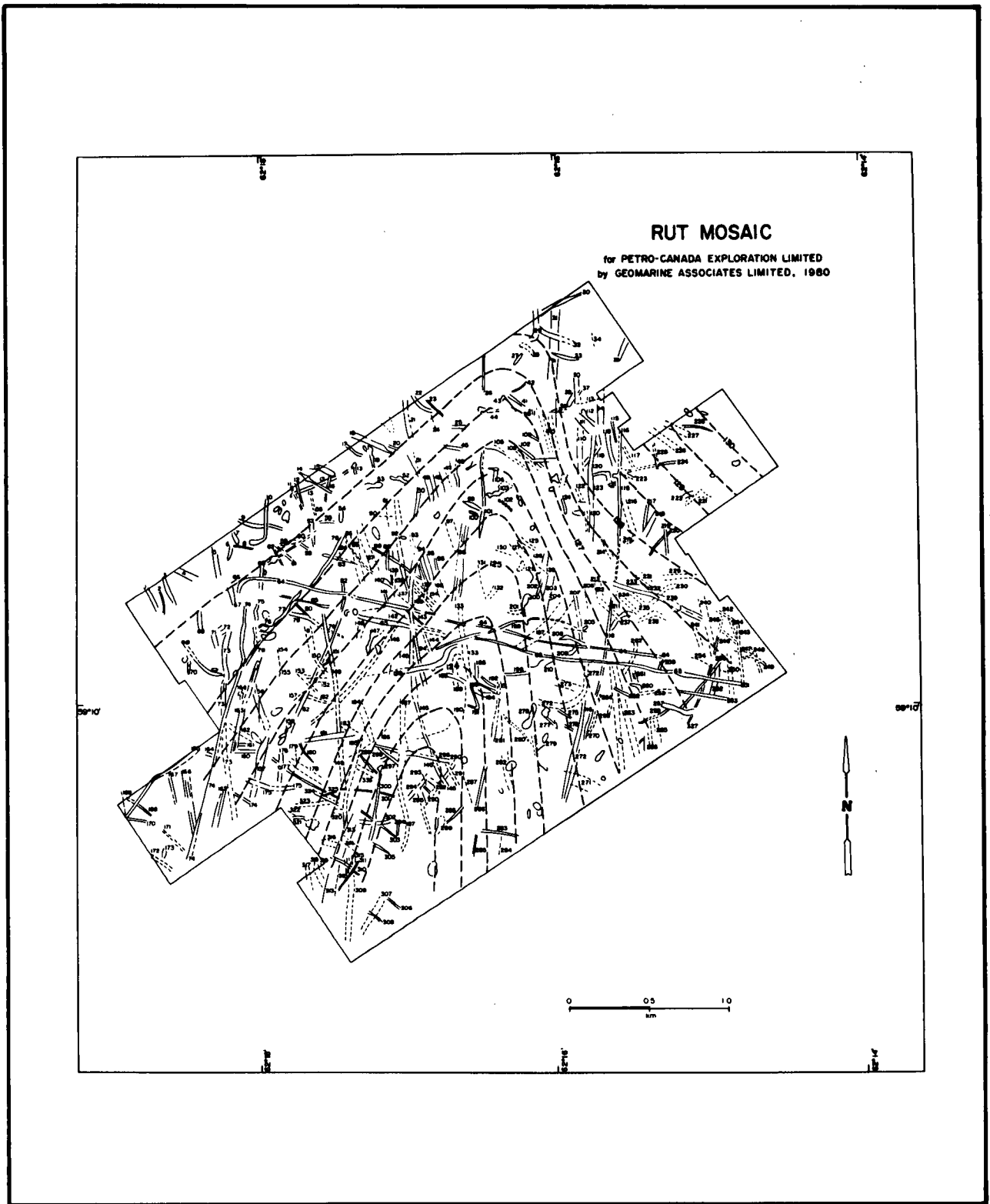


Figure 5. Rut mosaic scour map.

the mosaic area falls, as consisting of flat surfaces with fine microrelief (iceberg scours). Sub-bottom records show little apparent penetration and only occasional reflectors are evident (Fillon and Harmes, 1982).

Scour depth information is not available from this survey, however Geomarine Associates Ltd. (1980a) noted that scour depths were mostly less than 1-2 m with several scours 2-3 m in depth. They attribute this lack of relief to infilling of the scour troughs. This observation is confirmed from the mosaic on which most scours appear as double curvilinear berms (dark reflectors) bounding otherwise featureless non-reflective troughs and seabed.

Currents

With no steep bathymetric gradients to steer the flow in this region (Figure 6) the currents are characteristic of the general flow pattern found over the other banks on the Labrador Shelf.

The dominating current force on Saglek Bank is the semi-diurnal tide. Thus the direction of flow corresponds to that of the semi-diurnal tide. The tidal flow on Saglek Bank has a semi-diurnal component in the order of 13 cm/sec and a diurnal component in the order of 4 cm/sec.

Moored current meter data for this area are available for two locations (59°10.1'N, 62°18.7'W and 59°14.7'N, 62°12.0'W) collected by Dobrocky Seatech (Nfld.) Ltd. (1981; 1983). The 1981 data show that dominant currents are in the northwest and southeast directions. The peak currents also occur along these directions. The mean speed at 50 m is about 20 cm/sec whereas the maximum speed reaches 55 cm/sec in a northwesterly direction. At 117 m, just above bottom, the mean speed is 15 cm/sec and the maximum current is 40 cm/sec also in a northwesterly direction.

Figure 6 shows the pattern of the semi-diurnal tidal loops which are oriented in a northwest-southeast direction and are superimposed on larger fluctuations. The rotation of the tidal loops is in a clockwise direction. The 1983 data set gives similar results. The maximum speeds at depths of 20 m, 47 m, and 123 m, were 62 cm/sec (SSE), 45 cm/sec (SE), and 33 cm/sec (NW), respectively. The mean speeds were 22 cm/sec, 15 cm/sec, and 12 cm/sec, respectively. It would be expected that the strong semi-diurnal component for the general region encompassing the mosaic would drive scouring bergs in a predominantly northwesterly and southeasterly direction during ebb and flow cycles. However, the rose diagram (Figure 7) shows a strongly preferred north-south (0°-90°) scour orientation with a lesser northwest-southeast (100°-129°) concentration, the latter perhaps reflecting the semi-diurnal currents. It

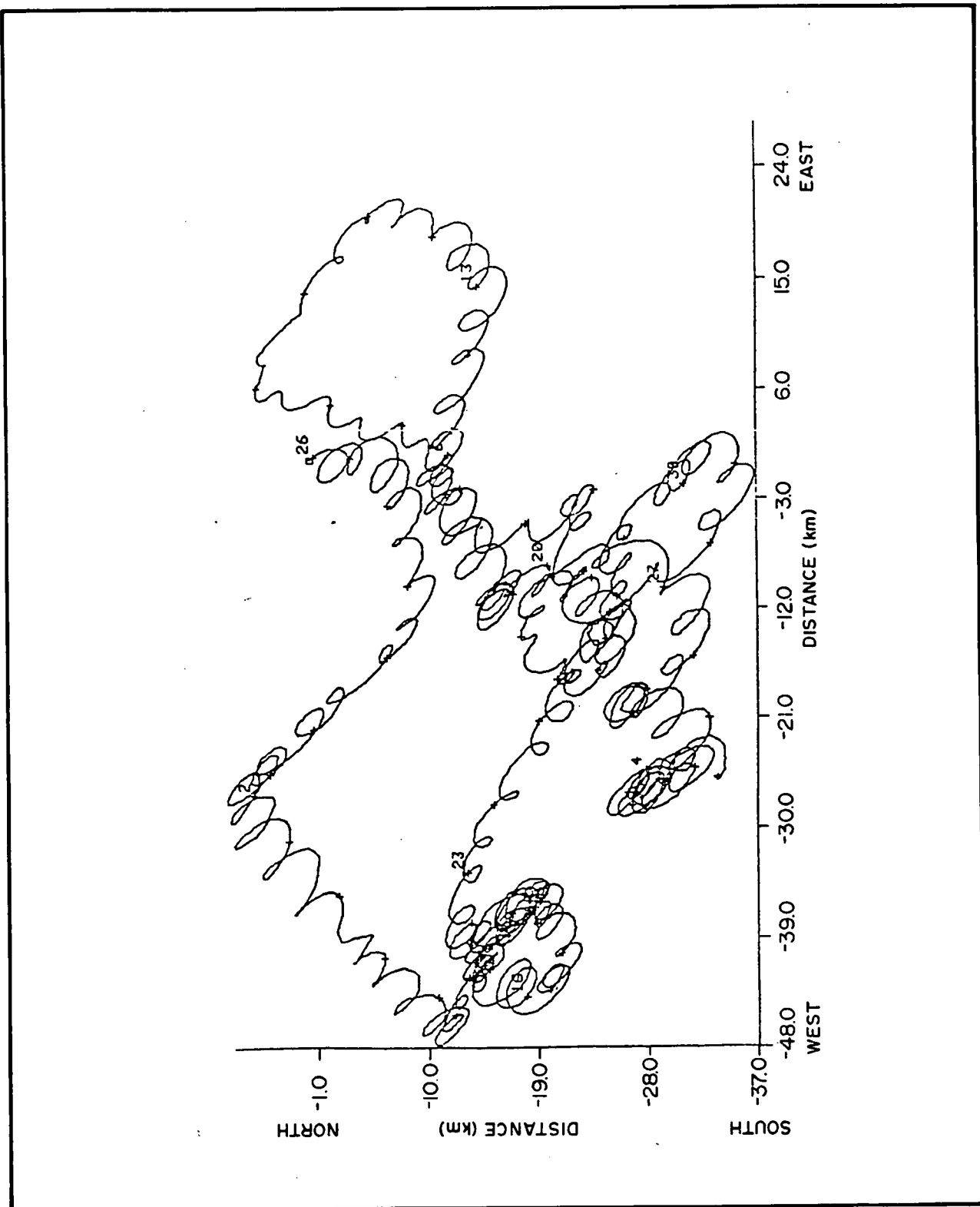


Figure 6. Progressive current vector diagram illustrating looping motion of semi-diurnal tides, Saglek Bank.

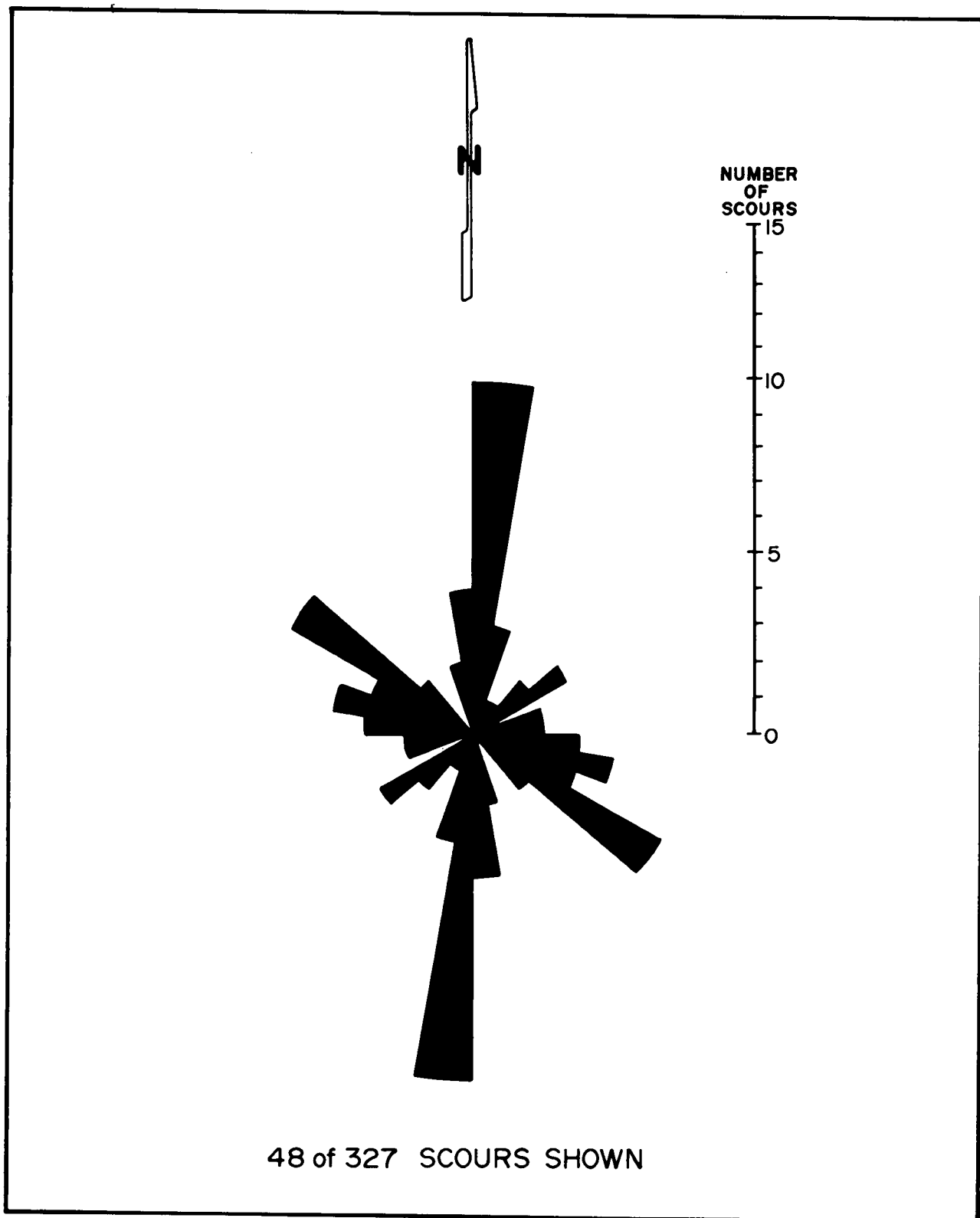


Figure 7. Rut mosaic orientations of isobath-traversing scours.

is apparent from the mosaic that the strong north-south orientation is brought about by older, possibly relict, morphologically subdued scours which are clearly cross-cut by those oriented northwest-southeast. This latter population is morphologically more sharply defined and may represent modern scouring.

SAGLEK EAST MOSAIC

Inventory Results (Appendix D)

This mosaic (Figure 8), together with the Saglek West mosaic has been resurveyed on four separate occasions in 1977, 1978, 1979 and 1981 as part of a joint C-CORE and BIO project to assess the rate of scouring and scour degradation processes (Woodworth-Lynas and Barrie, 1985). The 1979 mosaics are used in the present study since these are of best quality and resolution and also because the Saglek East 1979 mosaic was analysed in detail by Geonautics (in preparation) in their Regional Ice Scour Update No. 2 (ESRF Study # 377-22-05) so that direct comparisons may be made.

From the scour map (Figure 9) 532 scours were identified of which 101 had bathymetric ranges equal to or in excess of 1.0 m. The maximum bathymetric range observed was 13.5 m (scours 23 and 209), the greatest range in all of the mosaics. Water depths in the area range between 150-175 m.

Twenty-two scours had changes in width of which nine increased in width upslope, eight increased in width downslope, three had variable widths as they traversed bathymetry and two had width changes in portions of their tracks which ran parallel to contours.

Seabed Slope and Surficial Geology

Regional seabed slopes range between 1 in 110 to 1 in 250 on this the northern flank of Karlsefni Trough. Slopes are as steep as 1 in 120 in the southeastern part of the mosaic and as gentle as 1 in 300 in the central area with a general gradient of about 1 in 200.

The acoustic/morphologic units III and VI described by Fillon and Harmes (1982), occur within the mosaic area. Unit III, in the northeastern part has a very rough micro- and mesorelief (from <5-20 m). This grades into Unit VI to the southwest consisting of rough microrelief formed by numerous scours with numerous internal discontinuous sub-parallel reflectors. Two grab samples from within the mosaic area indicate the surficial sediments consists of

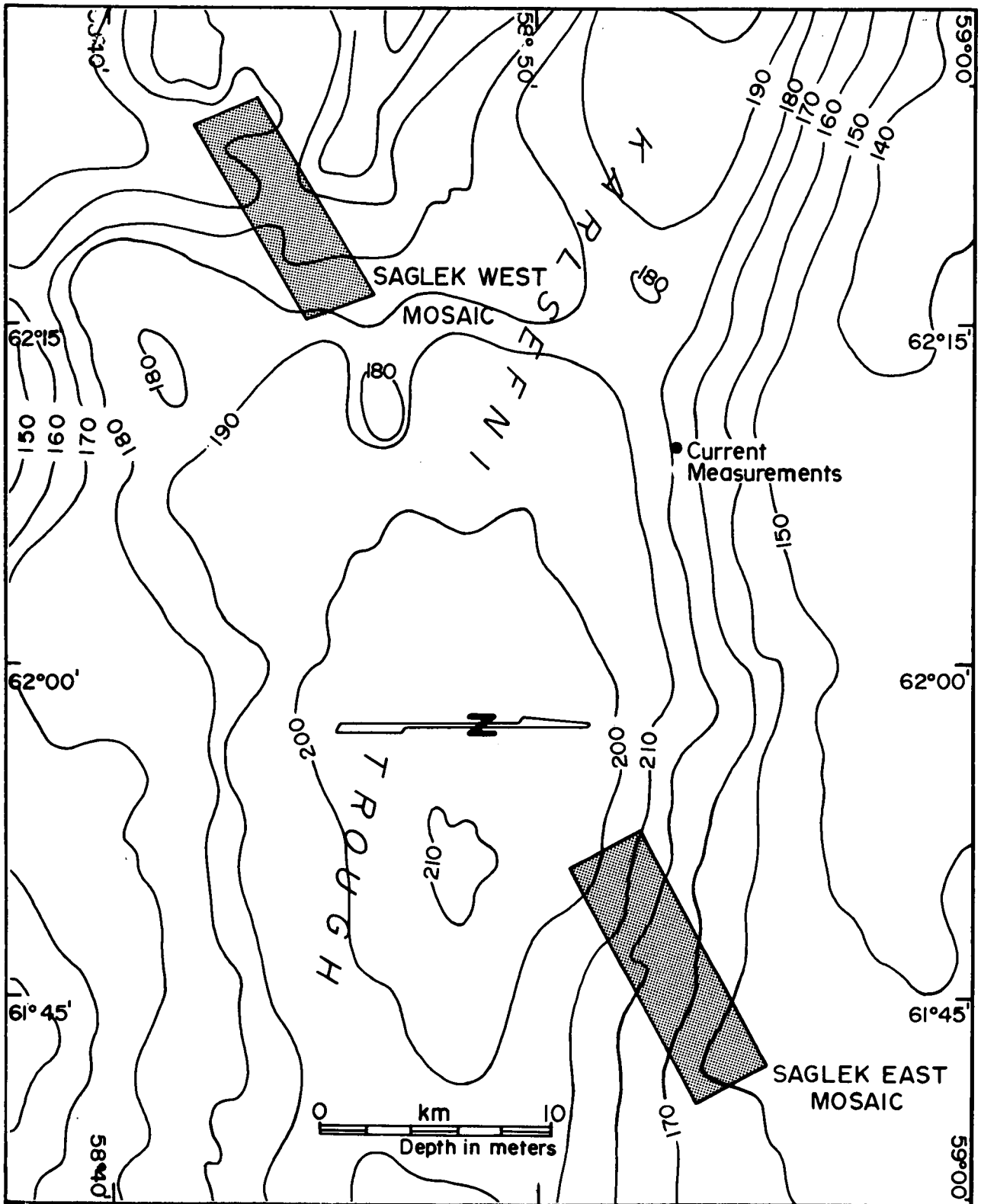


Figure 8. Location map of the Saglek East and Saglek West mosaics.

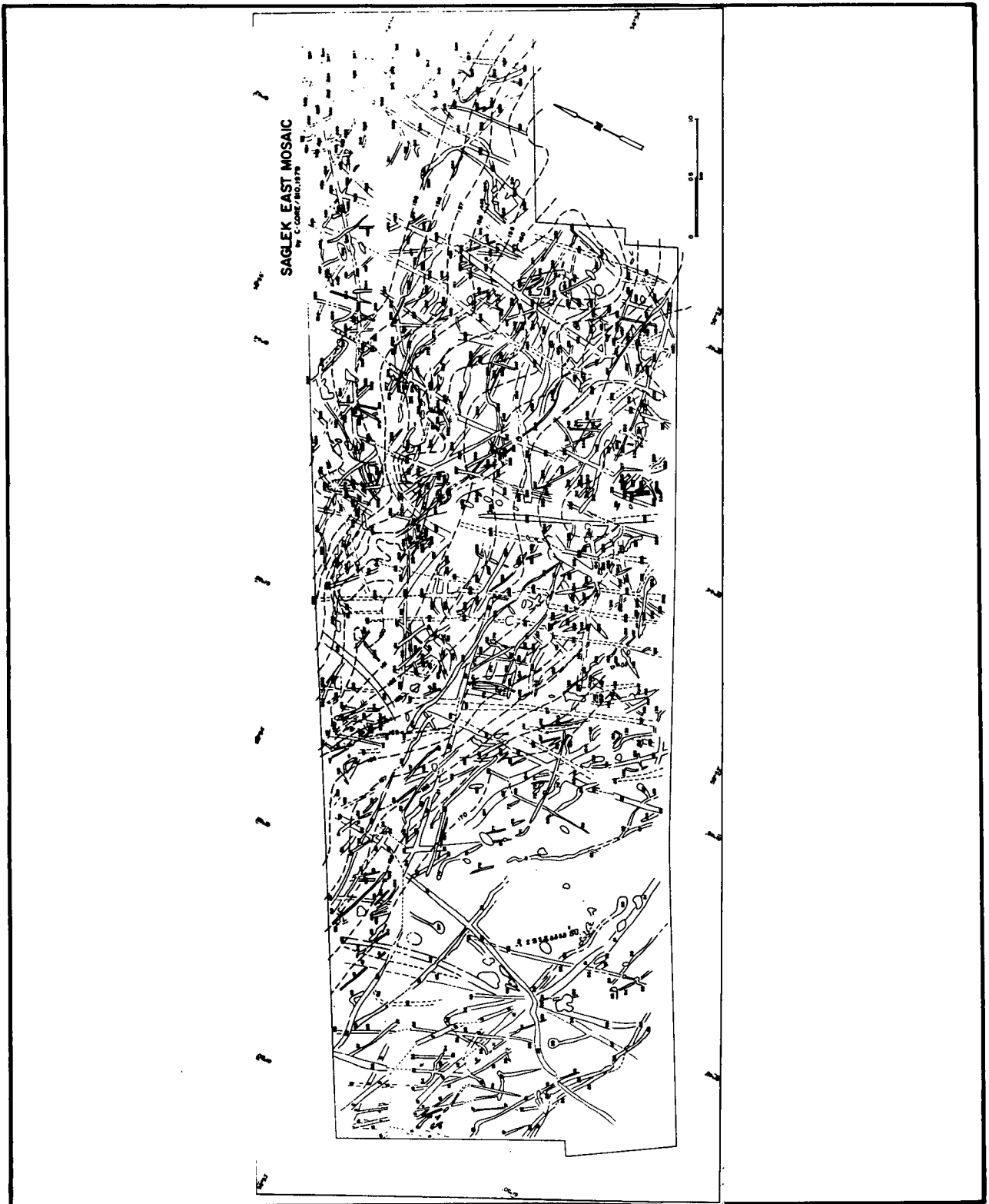


Figure 9. Saglek East mosaic scour map.

about 60% silt, 30% sand and 10% clay with no gravel (NORDCO, 1984).

Currents

The local bathymetric contours in this area run in an east-west direction due to the east-west oriented Karlsefni Trough located south of the study area (Figure 9). The semi-diurnal tide is the dominant force at this location with a semi-diurnal component in the order of 13 cm/sec and the diurnal component in the order of 4 cm/sec. Fissel and Lemon (1982) found a measurable inertial frequency of 14 hours on Saglek Bank.

Moored current meter data for this area are available from one location (58°53.3'N, 62°10.3'W) (NORDCO, 1981). The data show a strong semi-diurnal tidal component rotating in a clockwise direction. The peak directions of the tidal current are centred around 165° and 300° at depths of 62 m and 170 m respectively (Figure 10). The dominant currents at 62 m are in a westerly direction with a mean speed of 18 cm/sec. At this depth the maximum speed was 47 cm/sec in an east northeast direction. Near bottom, the maximum speed was 34 cm/sec in the same direction. Over the complete record the mean speeds were 14 cm/sec at 62 m and 12 cm/sec at 170 m. The mean velocity was 5.4 cm/sec towards 160° at both depths. The currents at this site are much more steady than characteristic of the bank areas.

The rose diagram of scour orientations (Figure 11) indicates a dominant north-northwest and south-southeast trend between 120°-139°. The current information suggesting a strong east-west component is reflected in the secondary east-west scour trend but does not explain the dominant trend. However, cross-cutting analysis of the scours (Woodworth-Lynas, 1982) indicates that the dominant set is relict, and thus the east-west trending scours are more recent and may indicate the orientations of modern scouring icebergs.

SAGLEK WEST MOSAIC

Inventory Results (Appendix E)

This mosaic, together with the Saglek East mosaic, was resurveyed four times, and as before, the 1979 mosaic has been used in this study. The water depth in the survey area is 155-170 m on the southern flank of Karlsefni Trough (see Figure 8). Of 265 scours shown on the scour map (Figure 12), 71 had bathymetric ranges equal to or in excess of 1.0 m. The maximum bathymetric range observed was 7.5 m (scour number 89).

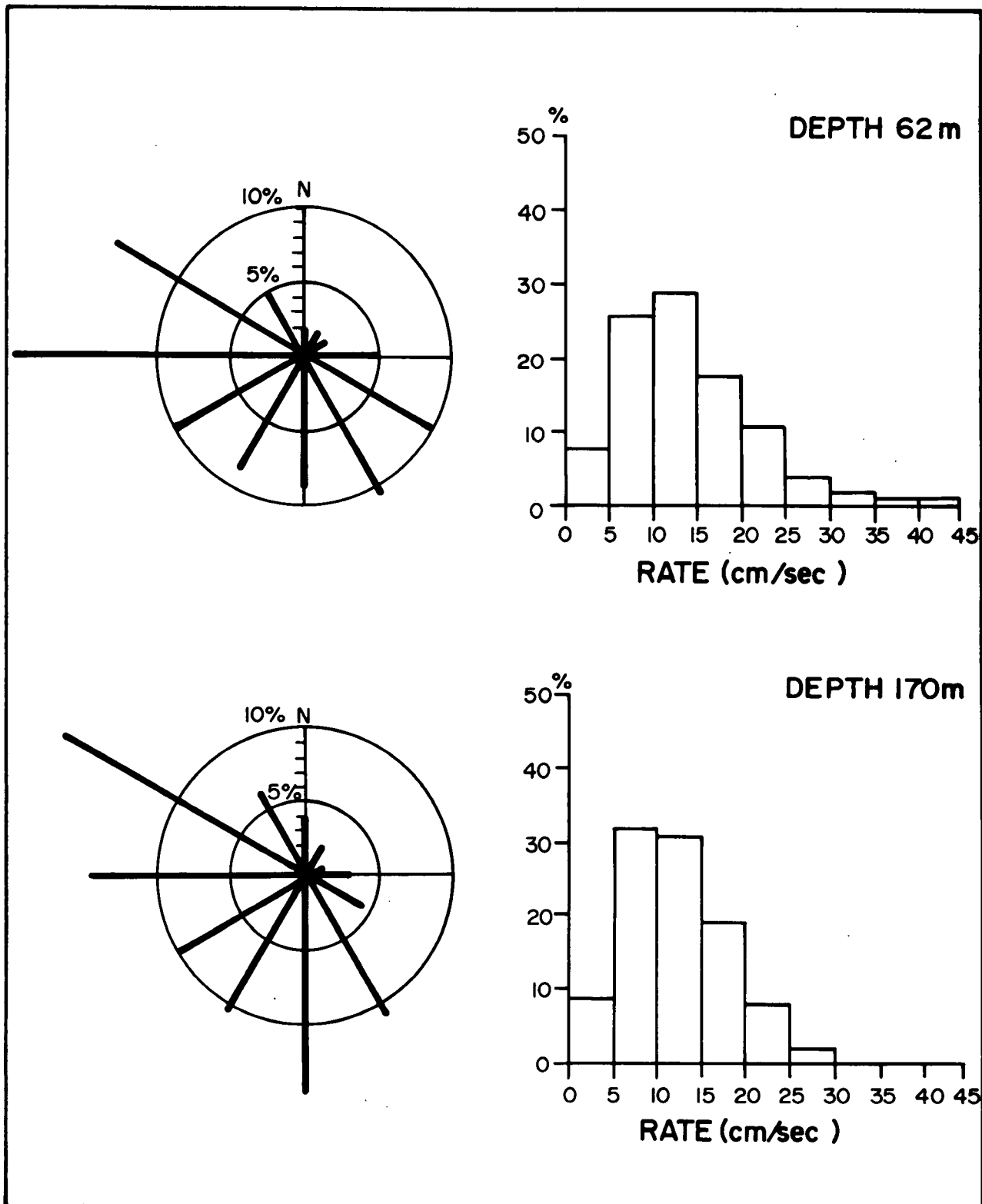


Figure 10. Current directions and speeds on Saglek Bank.

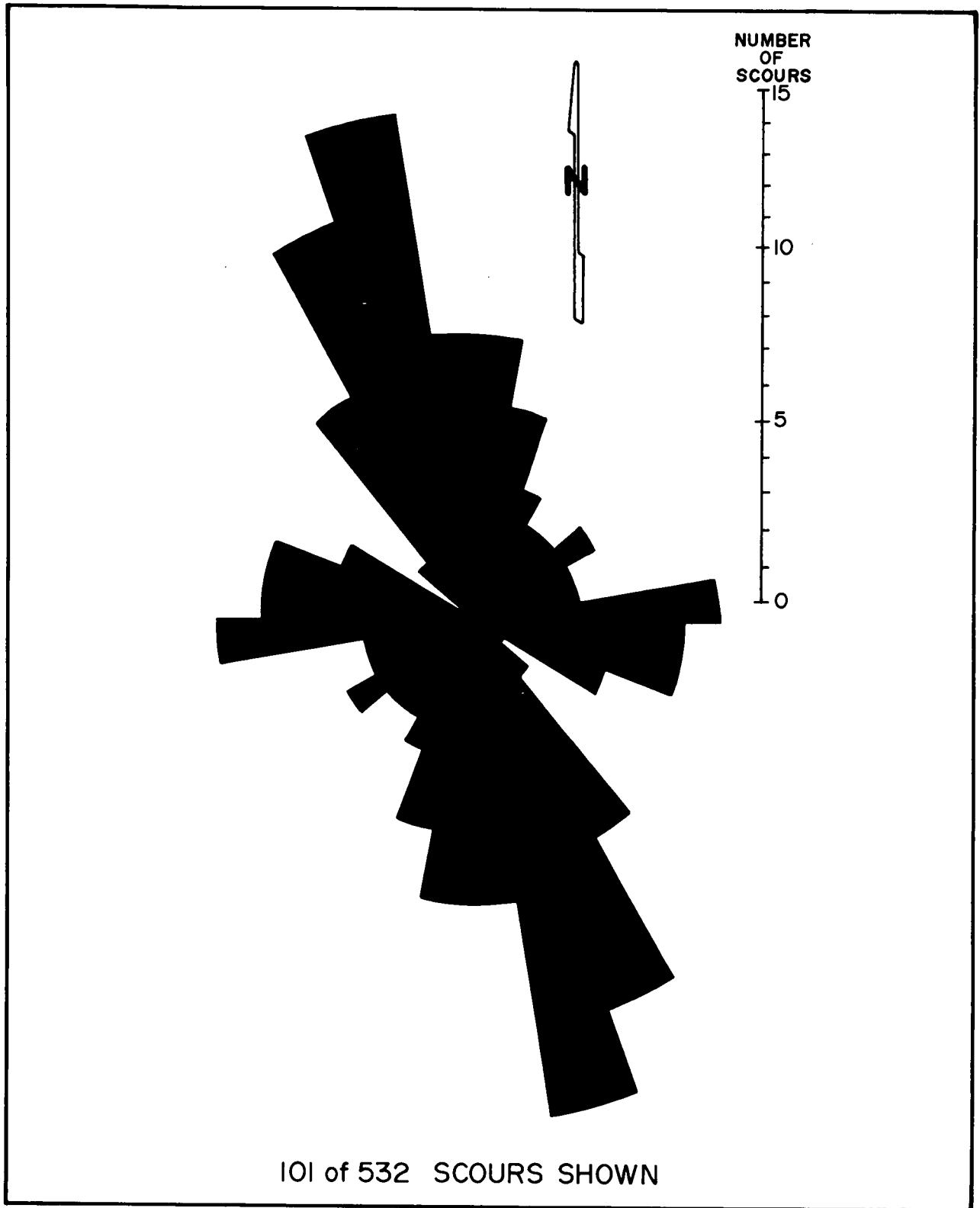


Figure 11. Saglek East mosaic orientations of isobath-traversing scours.

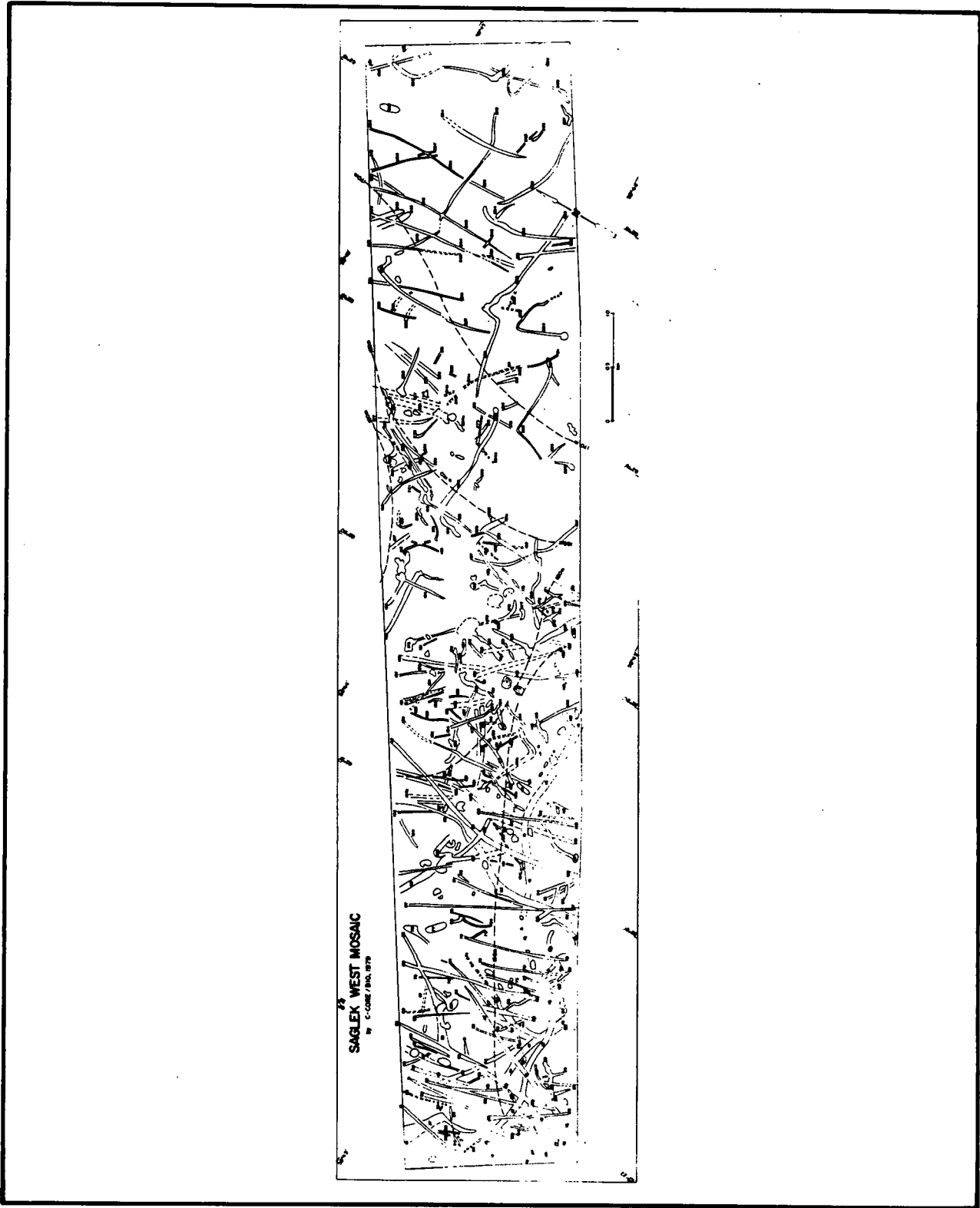


Figure 12. Saglek West mosaic scour map.

Of 19 scours that changed width 12 increased and 5 decreased in width upslope. Two scours had variable widths as they crossed isobaths. The greatest change in width was 55 m (scour number 82).

Seabed Slope and Surficial Geology

Regional seabed slope varies considerably from 1 in 85 to 1 in 360 within a few kilometres of the mosaic area. Steep slopes reflect the rather rugged relief of the Precambrian erosion surface which comes close to the seabed immediately west of the mosaic area. Local slopes within the mosaic area are also highly variable ranging from as steep as 1 in 20 and 1 in 40 in the central and northwestern portions respectively, to less than 1 in 540 in the central and southwestern areas.

The surficial geology within the mosaic area consists of a veneer, 5-6 m thick, predominantly of reworked sands and glacial till which is exposed in the central part of the mosaic (NORDCO, 1984). Fillon and Harmes (1982) define two acoustic/morphologic units within the mosaic area. Unit II is acoustically transparent with numerous sub-parallel draped reflectors at the top and bottom, and has a smooth gently undulating surface with occasional scours. This unit occurs at the northwest end of the mosaic area and corresponds to a decrease in scour density. Fillon and Harmes (1982) dated the uppermost part of Unit II at about 8380 years before present (B.P.). Unit VI (Fillon and Harmes, 1982) occurs in the southwest part and consists of numerous discontinuous sub-parallel reflectors bracketing an acoustically transparent section. The surface is roughened by the presence of numerous scours. Unit II was supposedly rapidly deposited from sediment-laden supraglacial runoff. Later, intense scouring by locally calved bergs from a collapsing ice sheet located on Saglek Bank modified much of Unit II, now recognized as Unit VI. Unfortunately, no seabed samples have been retrieved from the mosaic area and the closest sampling points are 30 km distant. However, from the clarity of scour preservation it is likely that the sediments are relatively cohesive because little degradation of scours has occurred since their formation.

Currents

The regional isobaths (see Figure 8) are aligned northwest/southeast with some irregularities in the study area. The average water depth is about 170 m.

The semi-diurnal tide should be dominant, but there is a geostrophic current component not present at the other three locations on Saglek Bank which, together with the alignment of the isobaths causes the current to be directed

southward. The geostrophic current is caused by a density gradient between the low salinity coastal water formed by river run-off and higher salinity water over the bank area. The study area in consideration is at the outside edge of the water density gradient.

The semi-diurnal current component should be similar to that at the other locations, 13 cm/sec and 4 cm/sec, respectively. There should still be energy in the low frequency band with periods of 5 and 28 days.

There are no direct current measurements at the Saglek West location. The nearest current meter measurements are those made by Memorial University in August 1972 at one location (58°28'N, 61°57'W), 15 km to the southeast. These measurements gave maximum speeds of 38 cm/sec and 37 cm/sec at depths of 13 m and 136 m respectively, and mean speeds of 20 cm/sec and 15 cm/sec. The mean velocities were 4.1 cm/sec and 6.3 cm/sec in directions 205° and 200°, respectively.

The Saglek West study area should have similar currents with a projected increase of about 10 cm/sec in the mean current speed resulting from the geostrophic component. The rose diagram (Figure 13) indicates a fairly wide spread in scour orientation between 110° and 200° with dominance between 160°-200° which correlates with the surmised orientation of the geostrophic current.

Barrie (1980) presented a rose diagram (Figure 14) for all scours in the Saglek West survey using the rather poor quality data from the 1978 mosaic. Although the orientation data in Figure 13 represent only isobath-traversing scours, the dominant trends are very similar.

ICEBERG CAROLINE MOSAIC

Inventory Results (Appendix F)

This mosaic, located northwest of the Rut mosaic (see Figure 4) in water depths of between 117-121 m is one of two repetitive mosaic surveys conducted at this site. The first in 1979, was made during the generation of a scour by an iceberg, code-named "Caroline." A subsequent survey, in 1982, was made over the Caroline scour to determine if the berg had continued scouring from its position in 1979 and to observe any degradation that might have taken place, from bottom current activity, since the scouring event. A detailed analysis of this particular scour has been made by Comfort and Graham (in press).

Of 305 scours identified from the scour map (Figure 15), 50 had bathymetric ranges in excess of 0.5 m. The

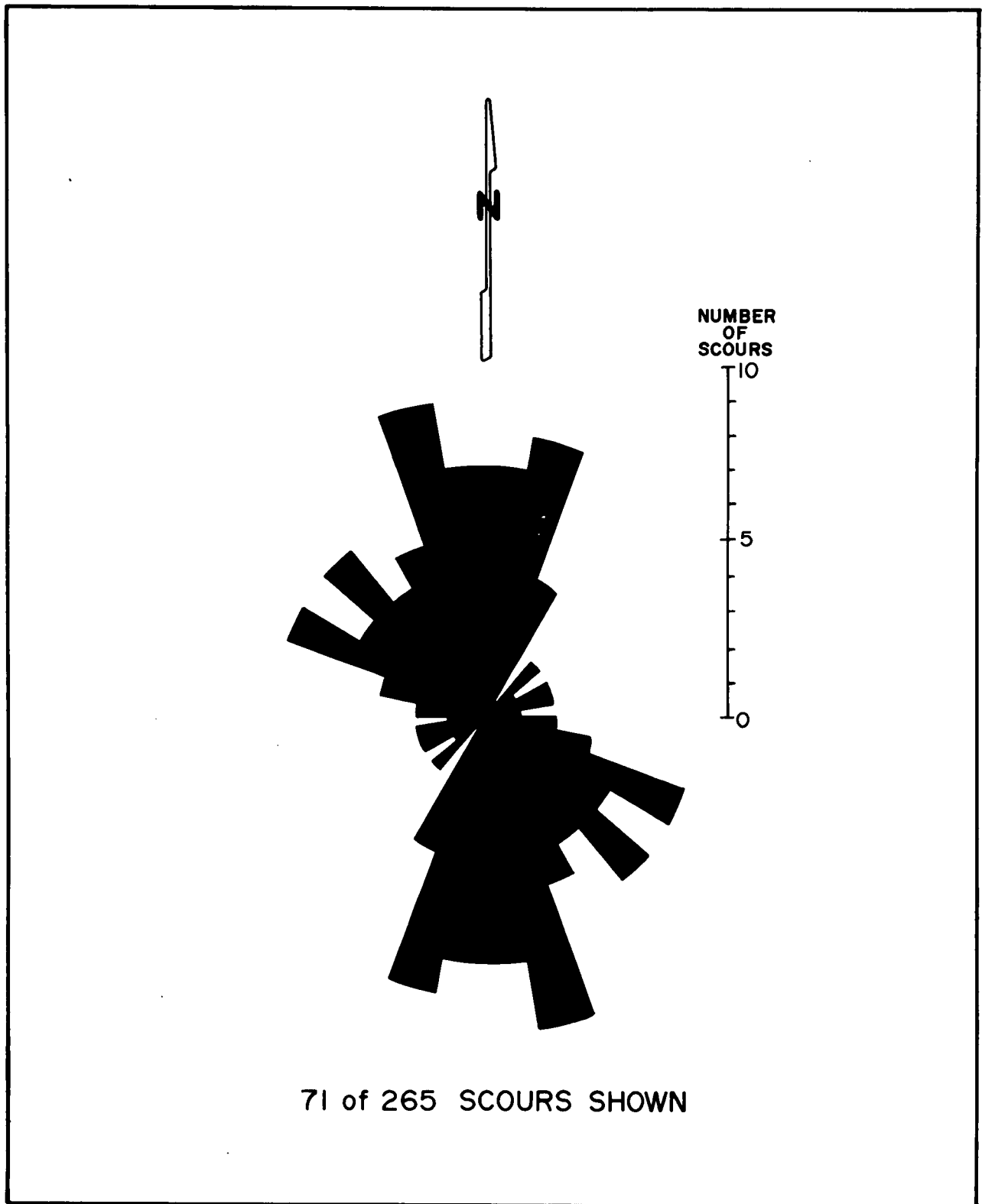


Figure 13. Saglek West mosaic orientations of isobath-traversing scours.

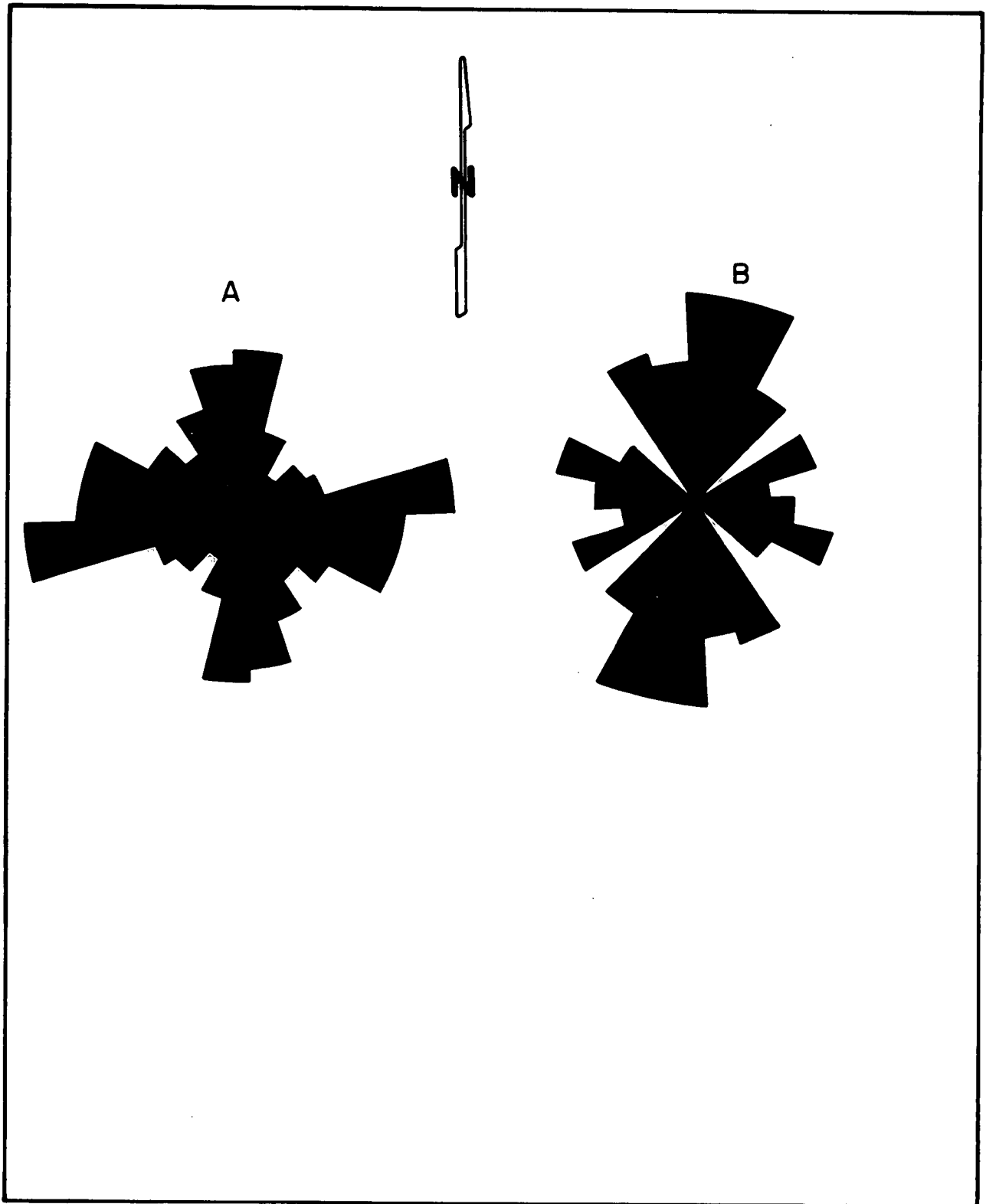


Figure 14. Orientations of all scours from the 1978 Saglek East (a) and Saglek West (b) mosaics.

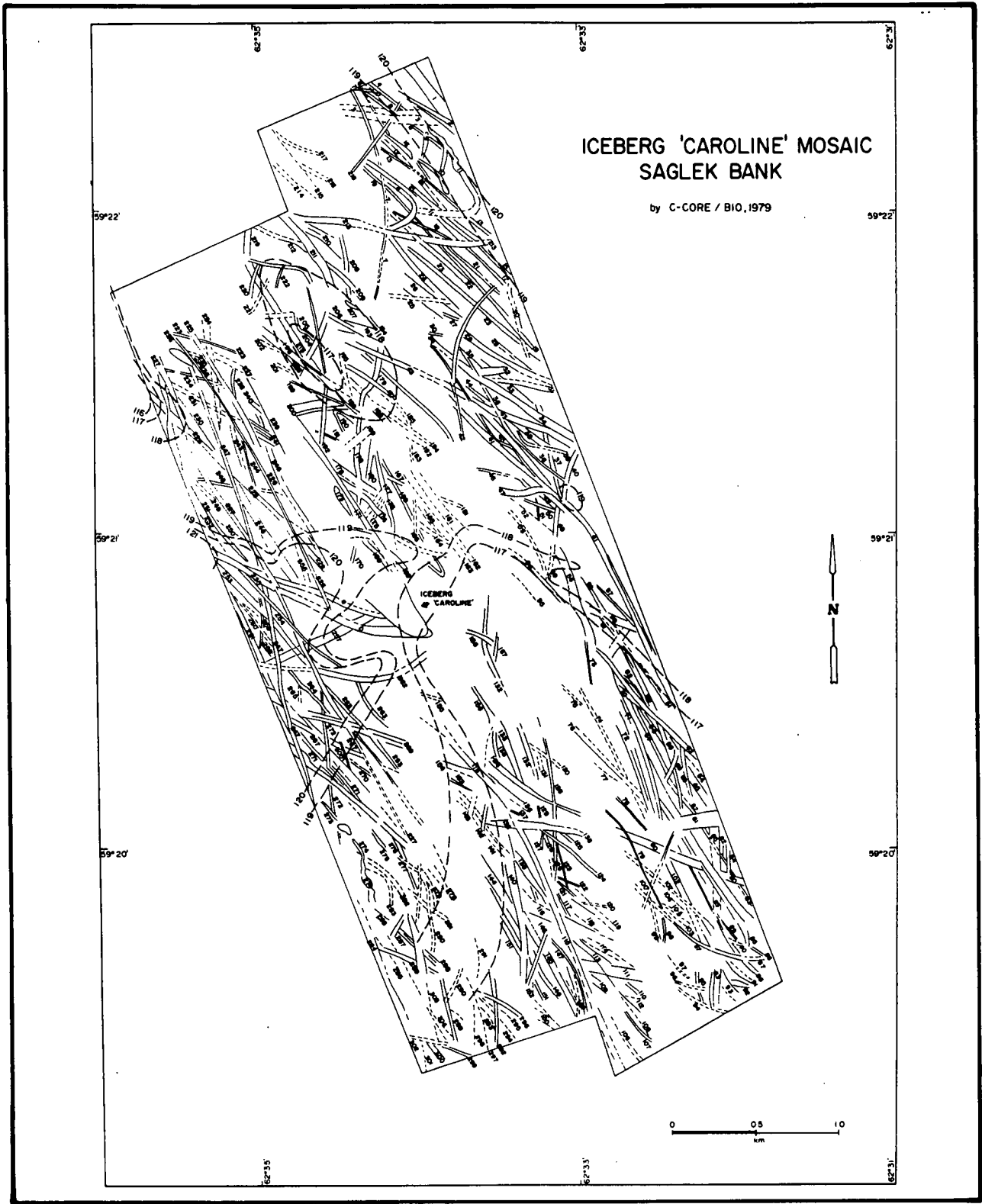


Figure 15. Iceberg Caroline mosaic scour map.

maximum bathymetric range was 4.0 m (Caroline scour and scour number 228). Four scours had width changes of which two increased in width downslope (two of these are the scours A and B of iceberg Caroline which generated two separate tracks from two scouring keels) and one increased in width upslope. Maximum width change was 25 m (scour number 252).

Seabed Slope and Surficial Geology

Regional seabed slopes range between 1 in 2500 and 1 in 250. Slopes within the mosaic area range from almost horizontal in many places to between 1 in 430 in the western part and 1 in 375 in the northwest.

The mosaic falls within a large region of post-glacial reworked sands 0-2 m thick (NORDCO, 1984) and within Fillon and Harmes' (1982) acoustic/morphologic unit VI (described previously). A grab sample from the eastern fringe of the mosaic area indicates that the constituents of the surficial sediments are generally 50% sand, 25% silt and equal remaining parts of gravel and clay (NORDCO, 1984). Scours are strikingly linear and mostly sub-parallel, making definition of individual scours difficult in such a heavily scoured region.

Currents

Current meter data used to extrapolate the current regime for the mosaic area are the same as those used for the Rut mosaic, consequently the section on currents for the Rut mosaic should be consulted. Briefly, the dominant current at this site is from the semi-diurnal tides which flow predominantly in northwesterly and southeasterly directions (see Figure 6). This trend is strongly reflected in the rose diagram (Figure 16) which shows a very narrow spread of about 15°-20° about the dominant scour orientation of 140°-149°.

SAGLEK BANK ICEBERG SCOURS FROM RADAR OBSERVATIONS

Inventory Results (Appendix G)

Icebergs were tracked from a number of well sites on Saglek Bank between 1975 and 1981 (Figure 17). Of 604 bergs tracked during this time, 26 (4.3%) were interpreted to ground and/or scour (Woodworth-Lynas et al. 1985) in water depths of 115-220 m. Of these, 5 were interpreted to ground only without scouring and 21 were interpreted to scour.

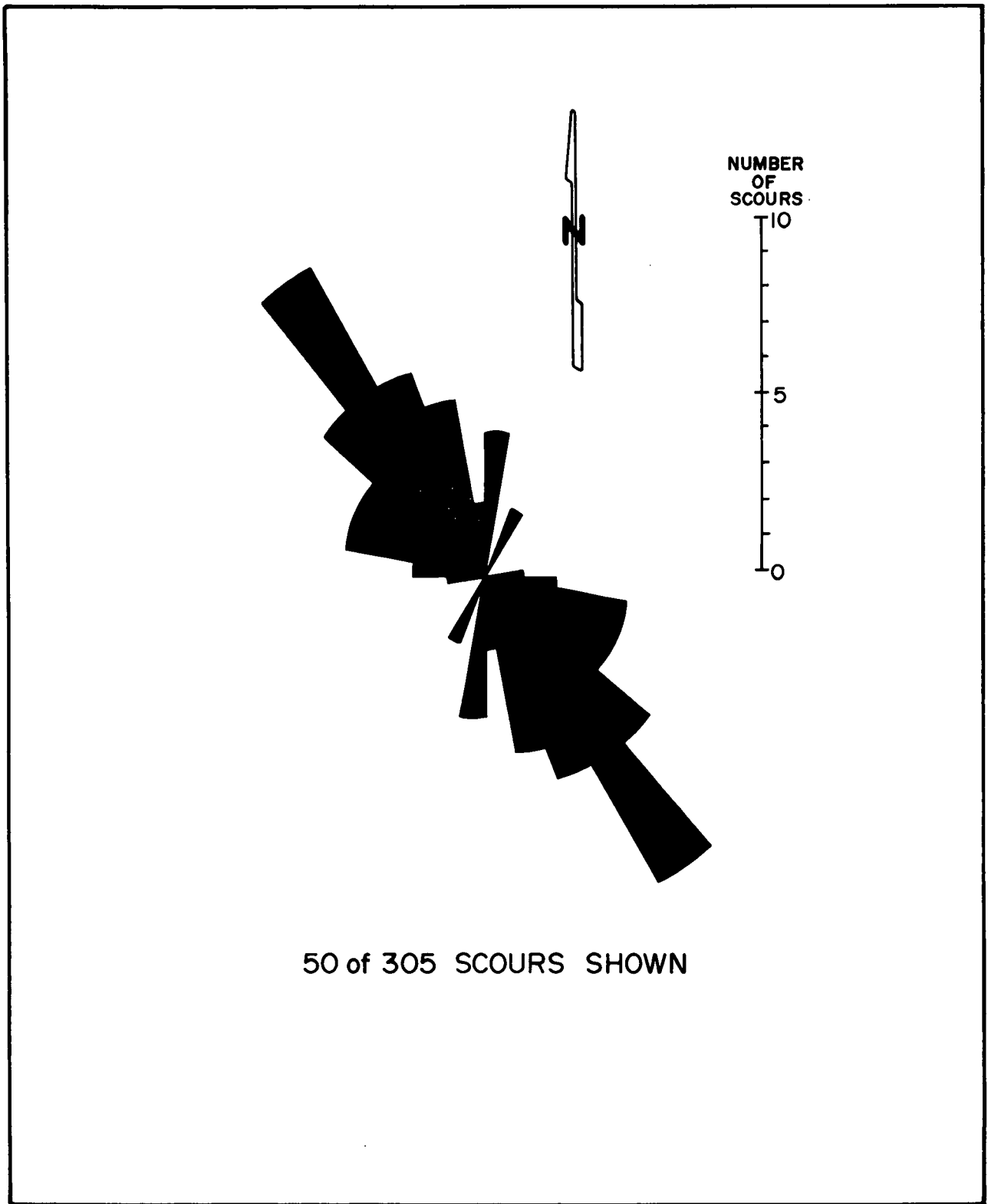


Figure 16. Iceberg Caroline mosaic orientations of isobath-traversing scours.

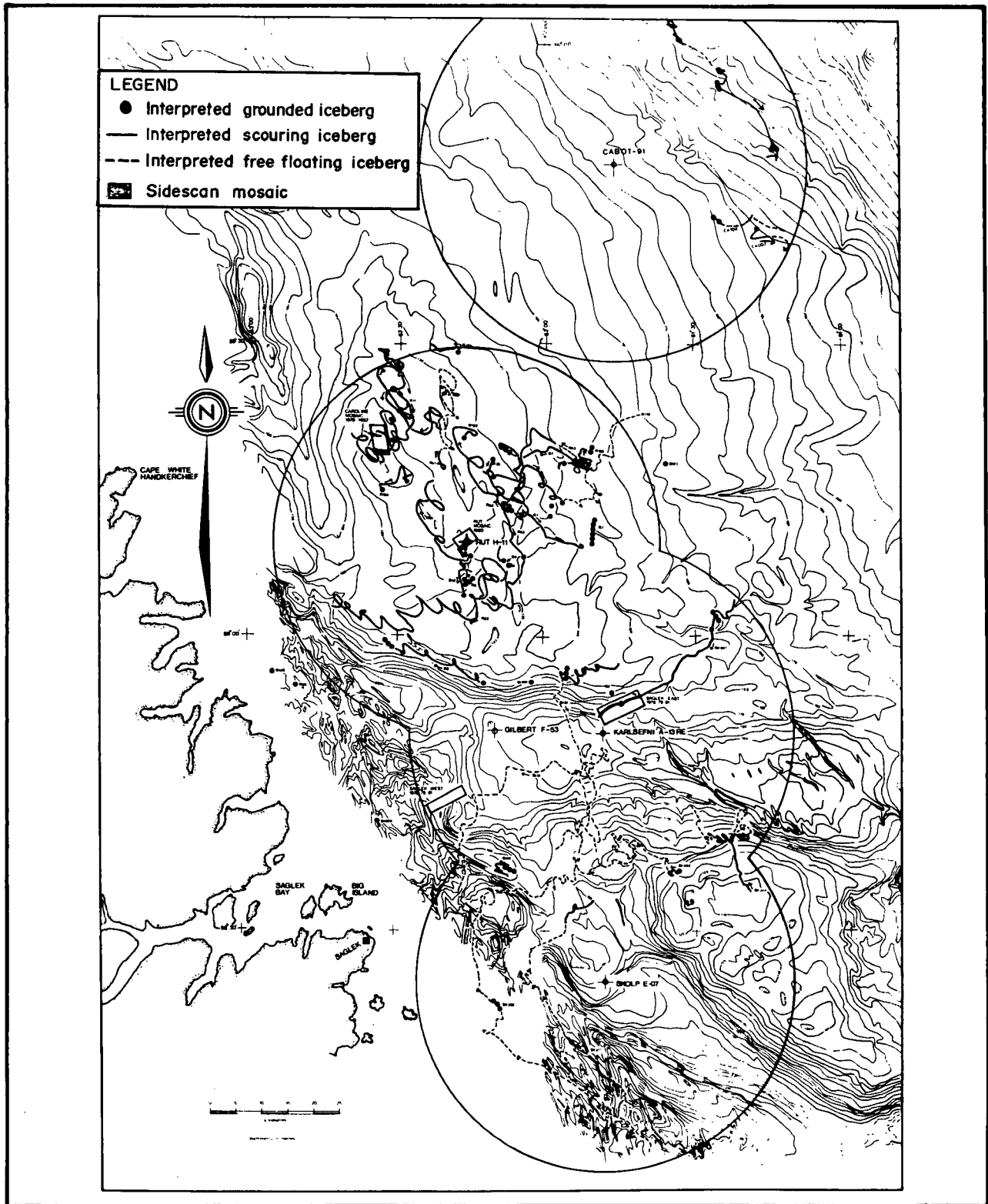


Figure 17. Radar tracks of icebergs on Saglek Bank interpreted as grounded or scouring.

In their model for identifying scouring icebergs Woodworth-Lynas et al. (1985) first distinguish bergs that remain stationary for more than 12 hours interpreting these to be grounded. Such bergs were cross-checked with reference to the motions of other bergs in the vicinity to see if all bergs became stationary at the same time. In all cases, the other bergs were moving which verified the grounded status of motionless bergs. Acoustically measured drafts (where available) were also checked against the water depths of the grounded bergs to further verify interpreted groundings. Once a grounded berg began moving again if its course took it into shallower water it was interpreted to be scouring (Woodworth-Lynas et al. 1985).

The 21 scouring bergs interpreted from the data set traversed bathymetric ranges in excess of 1 m. The maximum traverse was 35 m (Rut H-11 wellsite iceberg number 3, 1981). Because the actual scour marks were not observed, scour depth and changes in width could not be determined. However, scour lengths could be inferred. The shortest interpreted scour track was 2,500 m long and the longest (Rut H-11 wellsite, iceberg number 53, 1981) was 220,000 m. Orientations of the interpreted scour tracks were not measured because all the bergs changed direction commonly in excess of 180° and often through 360°.

Seabed Slope and Surficial Geology

Regional slopes north of Karlsefni Trough on Saglek Bank vary from as little as 1 in 1500 to 1 in 1170 for the bank top and edge respectively. Steeper slopes of 1 in 62 are found on the western flanks of the bank where it drops into the Labrador Marginal Trough whereas regional slopes of 1 in 145 and 1 in 260 for the north and south flanks are found on the bank top south of Karlsefni Trough east of the Skolp E-07 wellsite. Regional slopes of 1 in 500 are more common.

Geologically, surficial sediments consist dominantly of glacial till (of which an upper, middle and lower member can be distinguished) the surface of which has been reworked to form a veneer, predominantly of sand (NORDCO, 1984). Gilbert and Barrie (1985) in their detailed study of surficial sediments from Saglek Bank, found predominantly fine sands and poorly sorted coarse silts. They also found that mean grain size increased with increasing water depth and that sediments around the 210 m isobath along the southeast margin of the bank are coarser and better sorted than bank top sediments.

Fillon and Harmes (1982) describe the majority of bank top areas as consisting of acoustic/morphologic units III (described earlier) and VI whereas unit II is restricted to Karlsefni Trough. Unit 1 occurs in central Karlsefni Trough

and in patches along the southwestern margin of the bank area south of the trough. This unit is described as smooth with flat surfaces and contains numerous parallel reflectors and is interpreted by Fillon and Harmes (1982) as a late glacial deposit unaffected by iceberg scours.

Currents

Semi-diurnal tides are the dominant current force on Saglek Bank. Maximum surface currents are between 30 to 50 cm/sec, whereas the mean velocity of only a few centimetres per second reflects the variability and oscillatory nature of the flow. Current variability is well expressed in the pronounced clockwise looping trajectories of the scouring bergs (see Figure 17) and is reflected in the progressive vector diagram from the Rut H-11 wellsite (see Figure 6).

NAIN BANK MOSAIC

Inventory Results (Appendix H)

This mosaic (Figure 18) contained only 22 identifiable scours (Figure 19) of which 18 had bathymetric ranges in excess of 0.5 m in a water depth range of 129-136 m. The greatest bathymetric range was of the scour made by iceberg Frances (4.5 m) observed during the scouring event in 1979. Three scours showed evidence of width variation and all increased in width downslope, the maximum change being 35 m (scour number 11).

Seabed Slope and Surficial Geology

This mosaic covers a shoal area of Nain Bank immediately south of the southern flank of Okak Trough (see Figure 19) which has a regional north-facing slope of 1 in 77. The shoal top has regional slopes of between 1 in 625 and 1 in 1750. Slopes within the mosaic area range from a maximum of 1 in 25 to a minimum of 1 in 400, the general slope being towards the east at about 1 in 300.

The surficial sediments on this part of Nain Bank consist of glacial till overlain by large areas of reworked sediment from 1-3 m thick (NORDCO, 1984). Two grab samples from within the mosaic area indicate that the seabed is composed of 60-75% sand and equal parts each of gravel, silt and clay. The paucity and poor acoustic definition of the scours in the mosaic may indicate the 'hard' nature of the seabed.

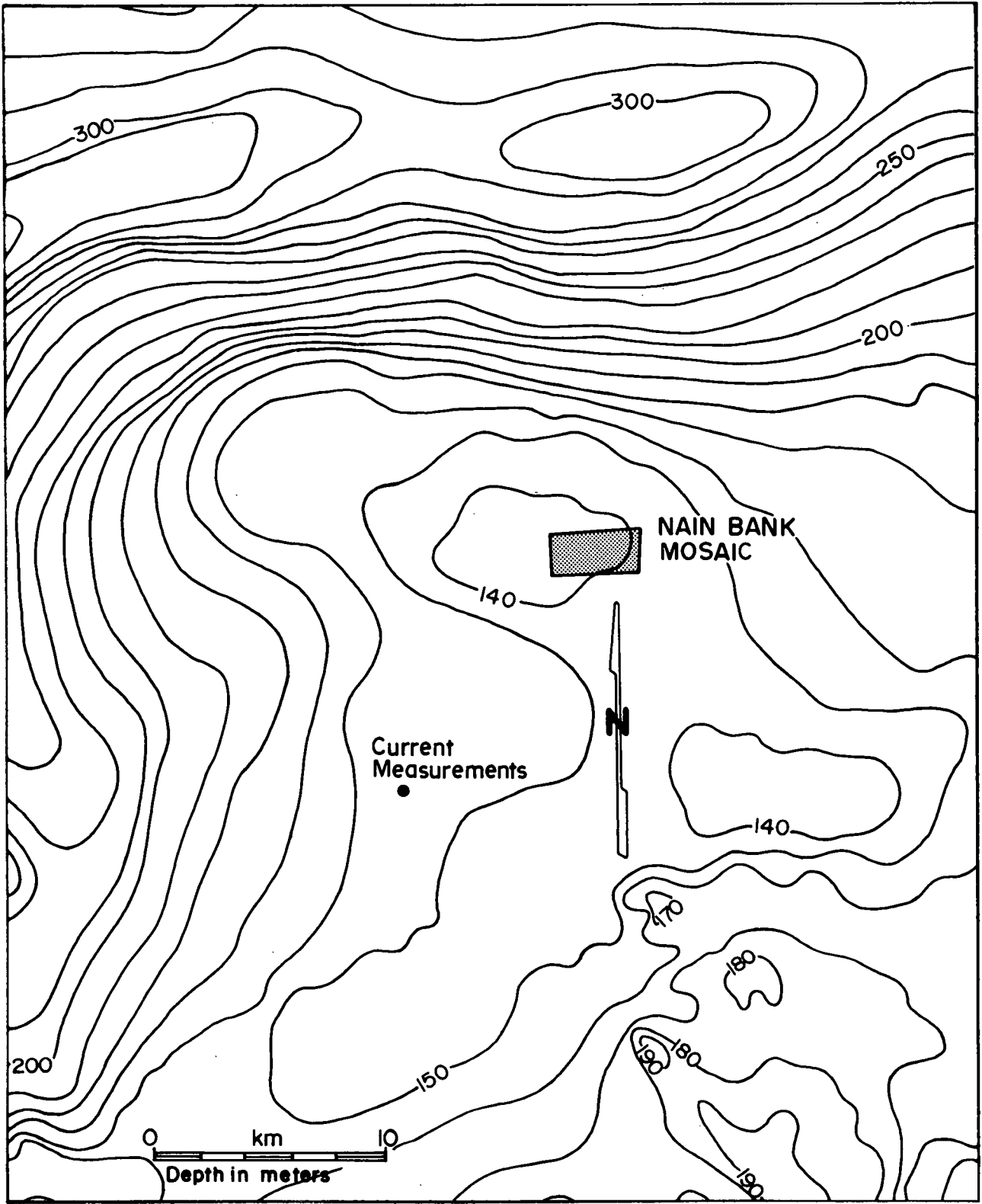


Figure 18. Location map of the Nain Bank mosaic.

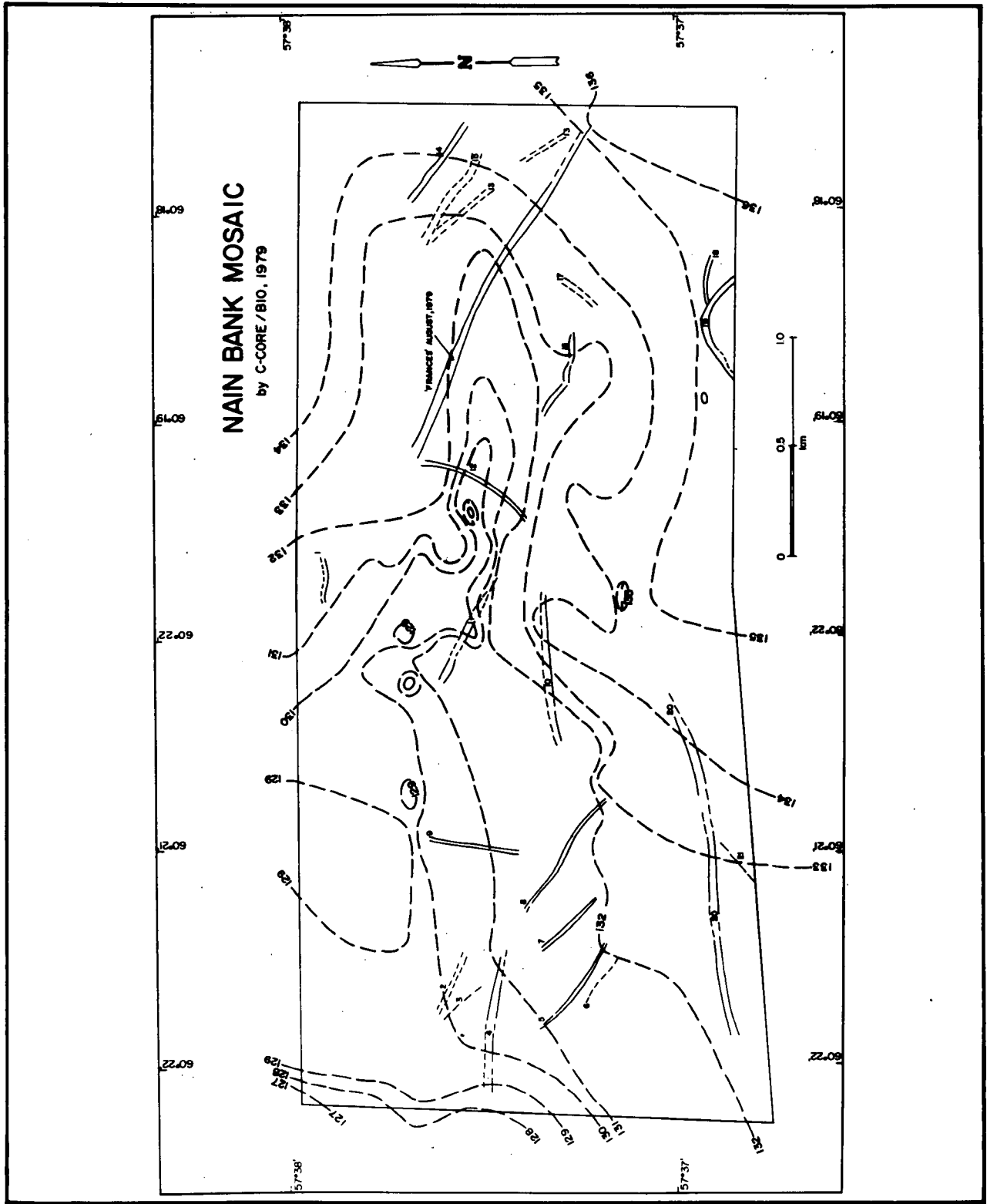


Figure 19. Nain Bank mosaic scour map.

Currents

About 5 km north of the study area the isobaths are aligned in an east-west direction (see Figure 18) and the bathymetric gradient is sufficient to influence the current flow. Direct current measurements were collected by NORDCO Ltd. for Petro-Canada Exploration Inc. in 1980 from one location (57°32'N, 60°29'W) about 10 km southwest of the study site in a water depth of 155 m. These currents were relatively weak with a maximum speed of 34 cm/sec in direction 120° at a depth of 56 m. The mean speed was 11 cm/sec. The mean velocity was directed southeast at 150° with a magnitude of 5 cm/sec. A histogram showing the distribution of speeds and directions is shown in Figure 20.

The current measurements show that the semi-diurnal current is of the order of 4 cm/sec and the diurnal current about 3 cm/sec. Even though the tidal currents are weak, their influence is quite obvious in the time series plots because the total current velocity is low. The semi-diurnal tidal currents are aligned along directions 130° and 310°. This site also has a low-frequency current component with a period of 14 days. All the major oscillatory components have a clockwise rotation.

The mosaic area should have a current regime similar to that at the current meter mooring site (57°32'N, 60°29'W). However, because the mosaic is closer to the bathymetric gradient, the currents are likely to be flowing more often in an eastward direction and at slightly higher speeds.

The dominant scour orientation falls between 110° and 129° (Figure 21) correlating with the observed alignment of the semi-diurnal tidal component from the current meter site. Scour orientation deviates from the observed mean velocity direction agreeing with the extrapolation of a more easterly-directed flow at the mosaic site.

BJARNI WELLSITE SCOUR MAP

Inventory Results (Appendix I)

Three hundred scours are represented on this scour map (Figure 22) in water depths between 130-165 m. Of these, 88 scours had a bathymetric range in excess of 1 m with the maximum traverse being 15 m (scour number 167). Available scour depths have been included in the inventory, and range between 0.5 m and 3.3 m. There is no information on changes in width because most scours are seen only as short segments generally less than 400 m long (width variation is usually only seen in relatively long [1000 m] scours). Geomarine (1976) interpreted depressions identified on some of the acoustic profiles as kettle features directly related to the

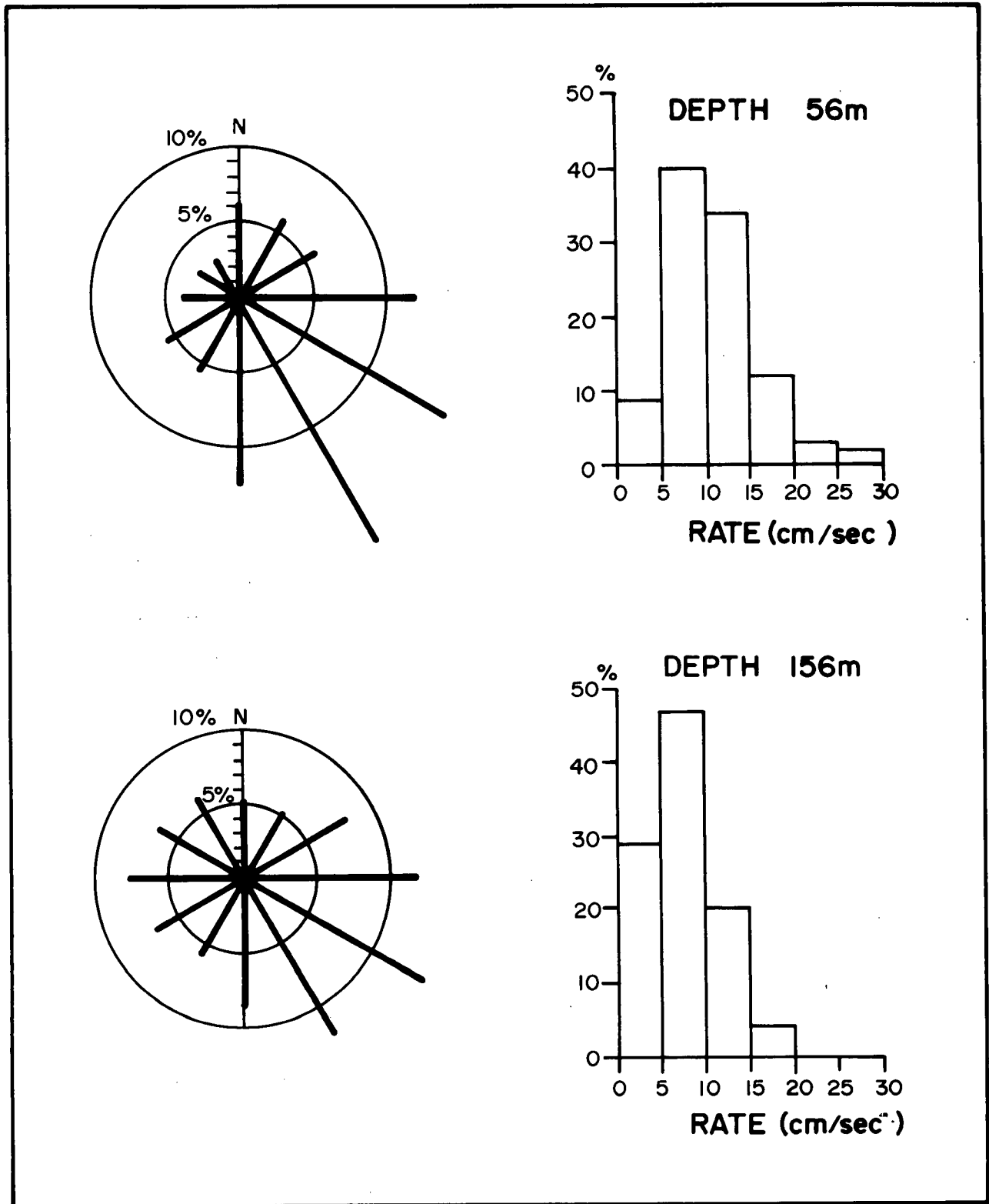


Figure 20. Current directions and speeds on Nain Bank.

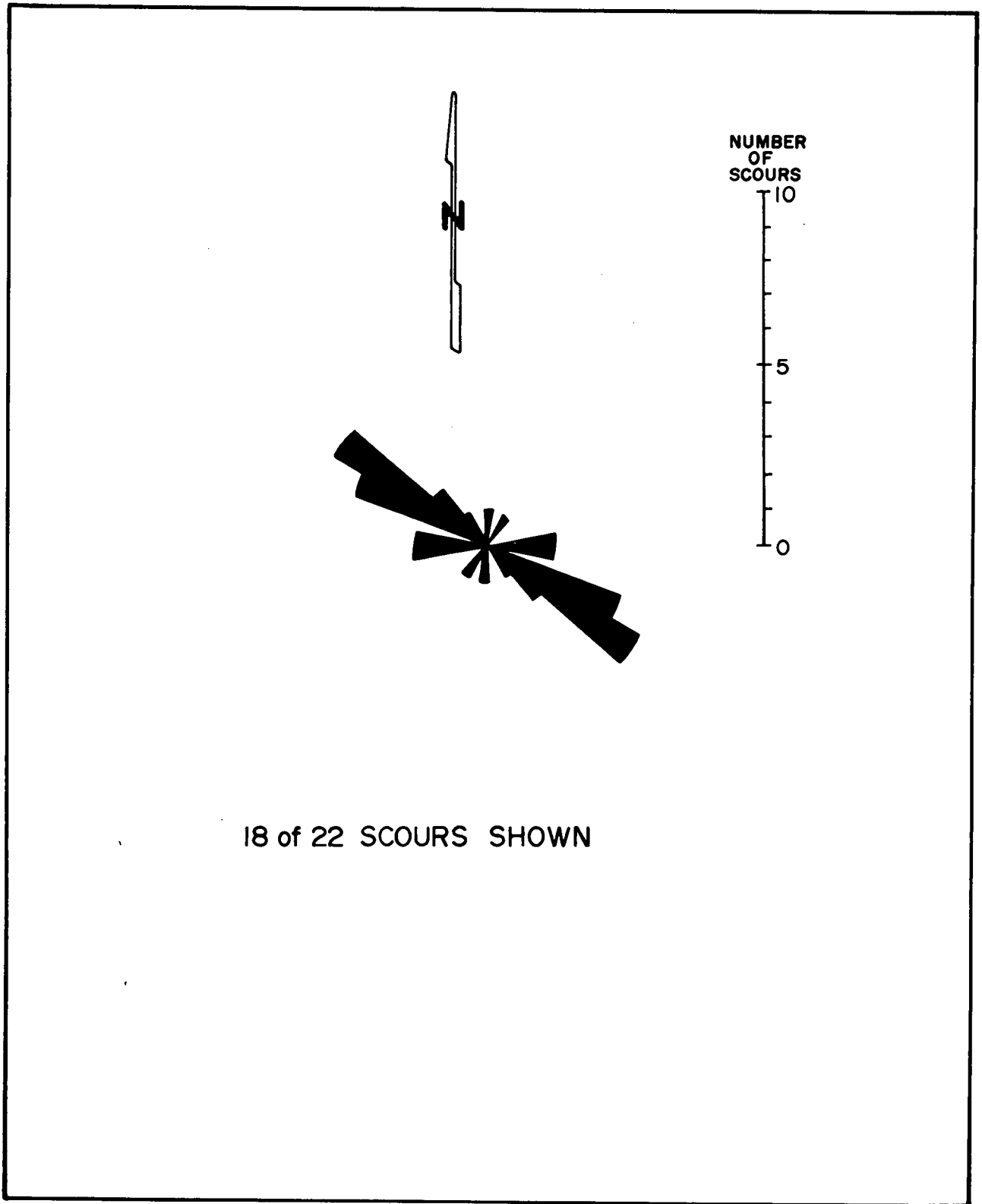


Figure 21. Nain Bank mosaic orientations of isobath - traversing scours.

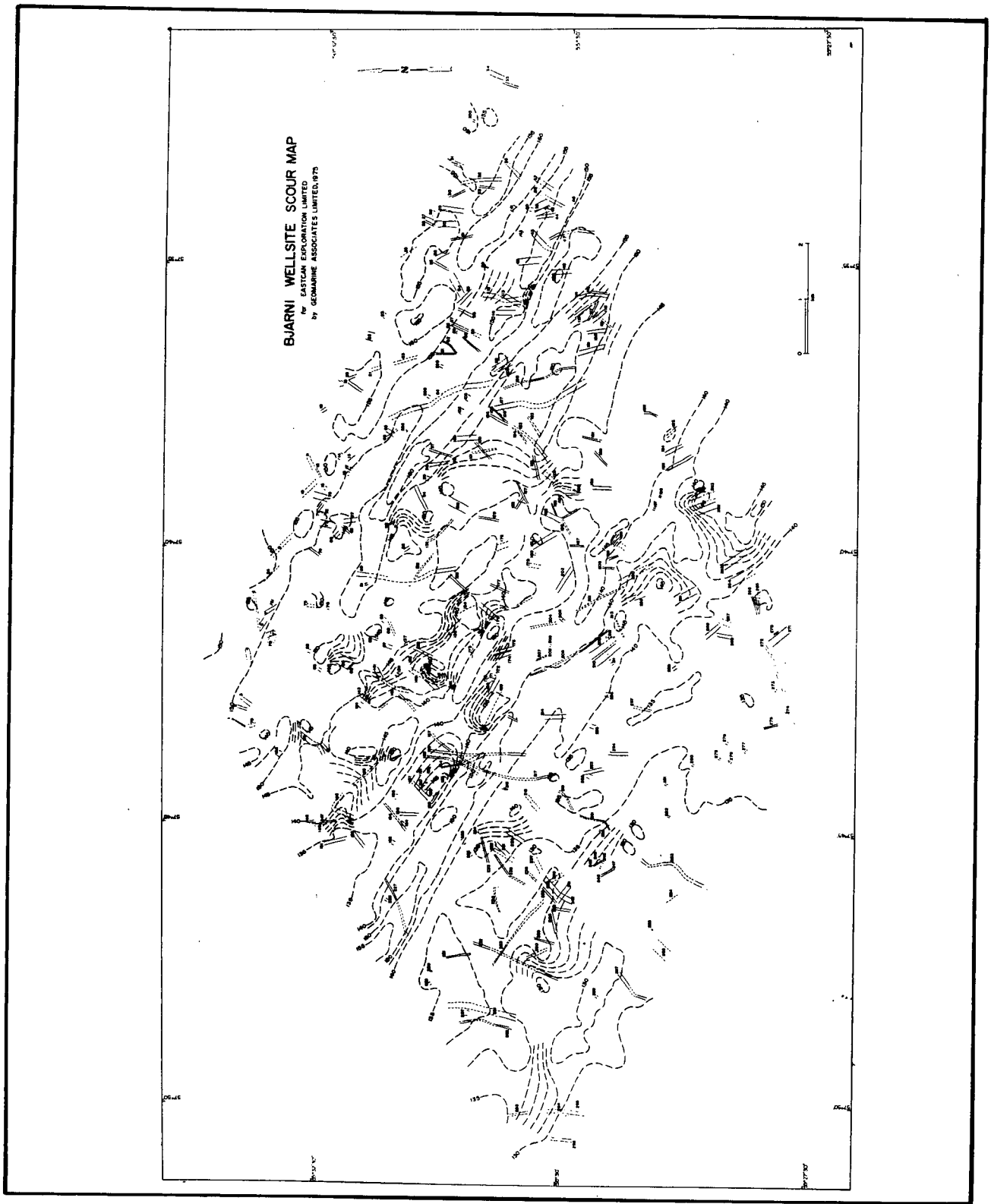


Figure 22. Bjarni wellsite scour map.

collapse of surficial sediments into hollows left by melted ice. Some of these depressions are plotted on the Geomarine (1976) scour map and are included among the 300 scours in Figure 22. However, because the depressions have no linearity they do not cross isobaths and consequently have not been included in the upslope/downslope inventory.

Seabed Slope and Surficial Geology

Gentle northeasterly slopes of around 1 in 500 typify this area of Makkovik Bank (Figure 23). The topography within the map area consists of pronounced linear ridges and troughs trending northwest-southeast with maximum reliefs of 20 m and gradients as steep as 1 in 10. The general slope is about 1 in 400 to the northeast.

Throughout the region glacial till is overlain in some areas by reworked sediments generally less than 1 m in thickness (NORDCO, 1984). Bottom photographs from within the map area show a dominance of silt and sand with occasional cobbles (Geomarine, 1976).

Currents

Gentle bathymetric gradients in the area (see Figure 23), suggest that the currents are similar to those at the North Bjarni site because of three main components; the semi-diurnal tide, the diurnal tide, and a low frequency component of five days. There is also a weak geostrophic flow. The five day low frequency component is likely to have the most energy. The rotations of all oscillatory components are clockwise.

The dominant flow should be in a southeasterly direction. The mean current speeds are low and, for all practical purposes, can be taken as identical to those at the North Bjarni site. There exists 10 days of near-bottom data for one location (55°28'N, 57°41'W), collected by the Bedford Institute of Oceanography in 1979. The maximum current speed at 138 m in these measurements was 20 cm/sec, and the mean speed was 8 cm/sec. The mean velocity was 3 cm/sec in a southeasterly direction. Because of the short sampling period the current speeds from North Bjarni are more appropriate for practical application. Geomarine (1976), using all scour orientation data, found two distinct trends with azimuths of 40°-45° and 130°-135°. The plot of the 88 scours that cross isobaths (Figure 24) also indicates a bimodal distribution but with peaks between 20°-49° and 150°-179°. The latter orientation correlates with the observed southeasterly flow but does not explain the more dominant 20°-49° trend. Geomarine (1976) were also at a loss to explain the existence of two trends. Although the ages of scours are not known it is reasonable to suggest

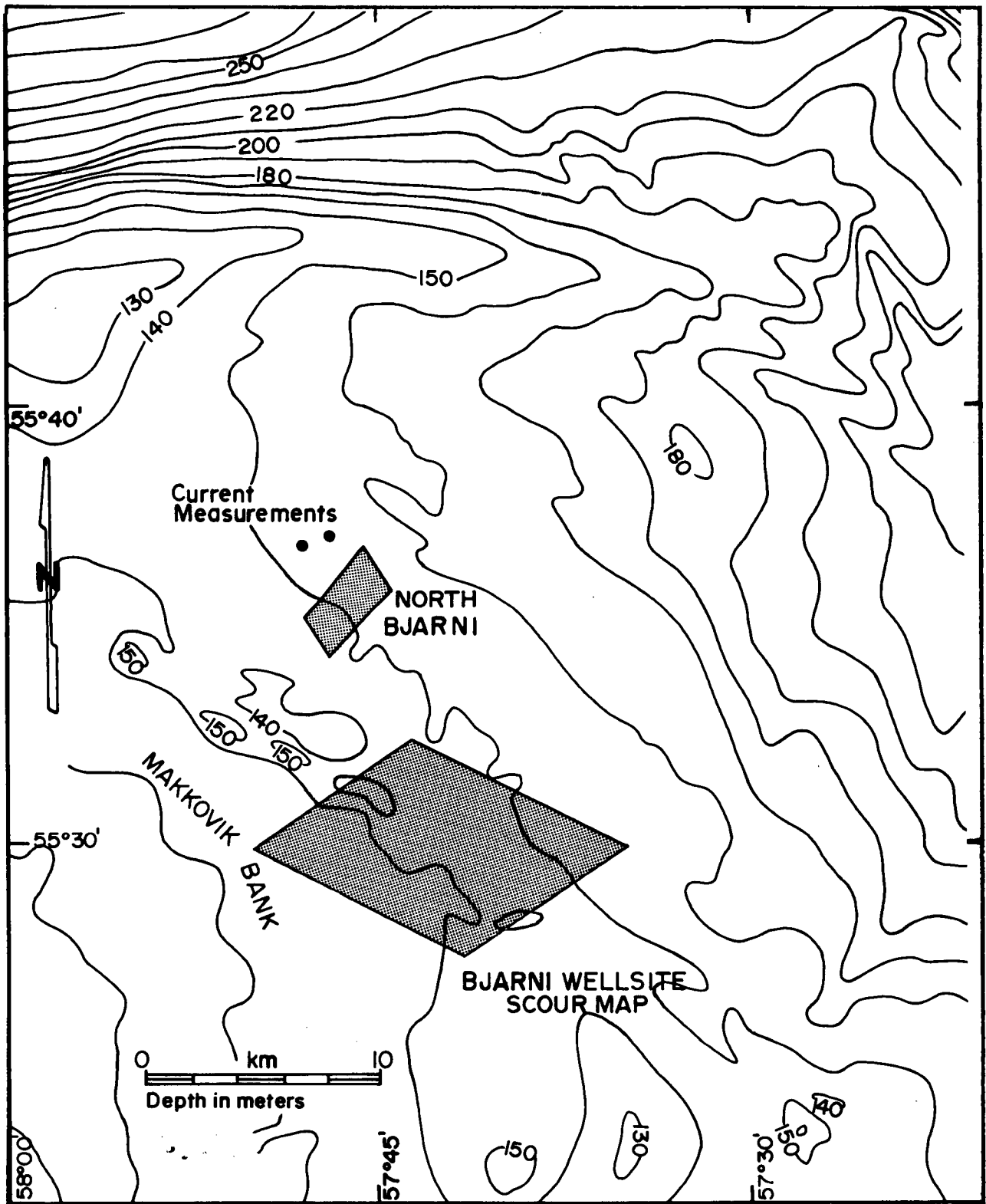


Figure 23. Location map of Bjarni wellsite scour map and North Bjarni mosaic.

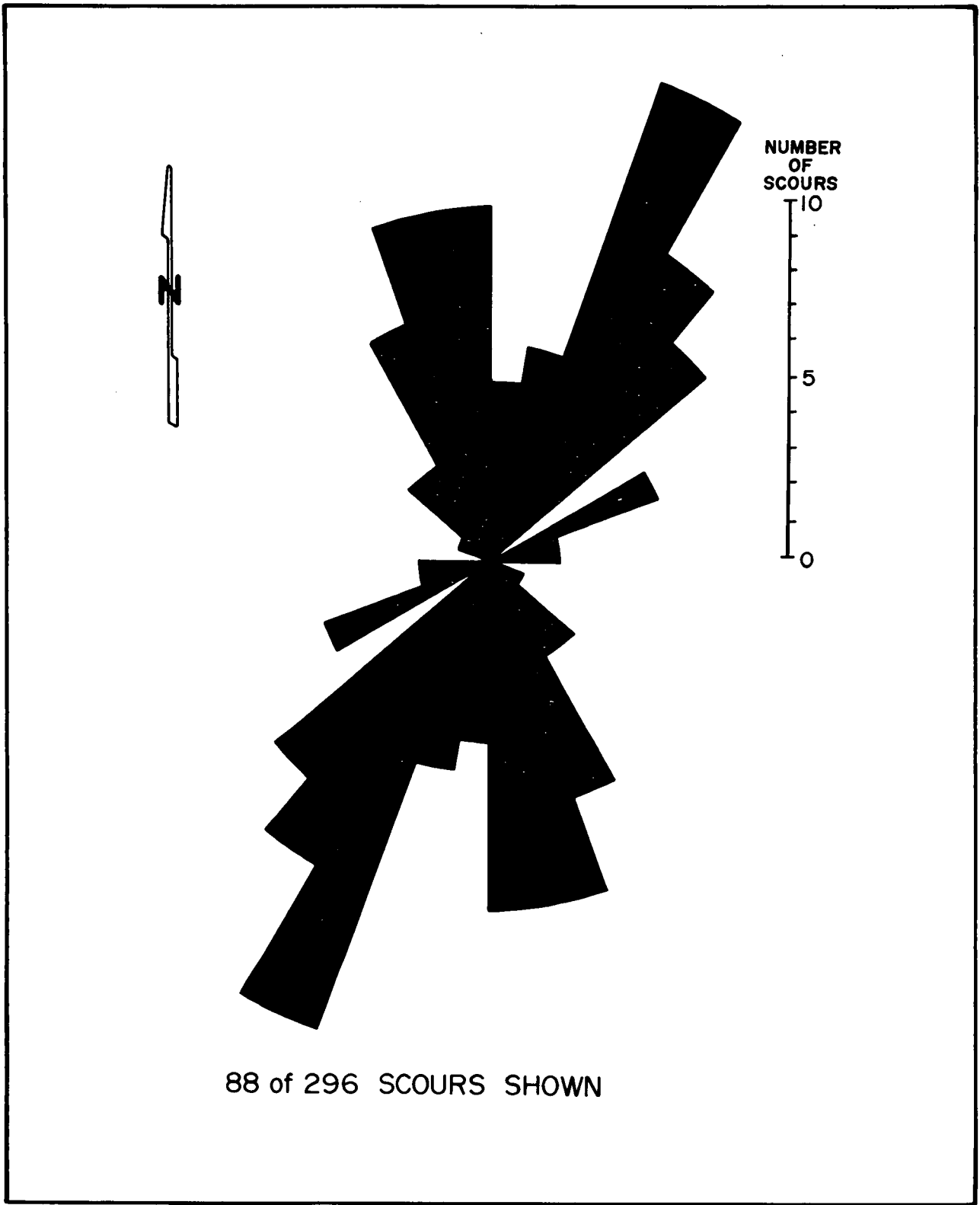


Figure 24. Bjarni wellsite scour map orientations of isobath-traversing scours.

that one of the two trends represents a relict scour population. Because the 150°-179° set appear to correlate with observed and expected current flow, then the 20°-49° set may represent ancient scours generated during times of different current regimes.

NORTH BJARNI MOSAIC

Inventory Results (Appendix J)

From this mosaic 219 scours were identified in a water depth range between 146-152 m (Figure 25). Twenty-two scours crossed isobaths; the greatest bathymetric range traversed was 3 m (scour number 136) and none of these exhibited variations in width.

Seabed Slope and Surficial Geology

This mosaic, like the Bjarni wellsite scour map area, is located on a gentle northeast-facing slope with a regional gradient of 1 in 470 (see Figure 23). Slopes reach a maximum of 1 in 250 in the southwest corner of the area with a general gentle northeast-facing gradient of 1 in 410.

The surficial geology is identical to that found within the Bjarni wellsite scour map area, namely, glacial till overlain by thin (<1m) veneers of reworked sediment. Grab and core samples from within the mosaic area indicate a varied seabed ranging in composition from 60% gravel, 30% sand and about 5% each of silt and clay to about 55% sand, 20% gravel and equal remaining parts of silt and clay (NORDCO, 1984). Josenhans and Barrie (1982), during submersible operations on Makkovik Bank, noted that old scour berms always consisted of boulders, cobbles and pebbles coarser than the surrounding seabed. This textural variation between scour berms and surrounding seabed may explain the variation in grain size between the samples described above.

Currents

The local isobaths (see Figure 23) trend northwest-south-east, without much influence on the currents at this location. With temporal variability they may be in any direction at any given time.

The currents have three main components; the semi-diurnal tide, the diurnal tide, and a low frequency component of five days. There is more spectral energy in the five day component than in either of the tidal frequencies. The five day frequency is sometimes apparent

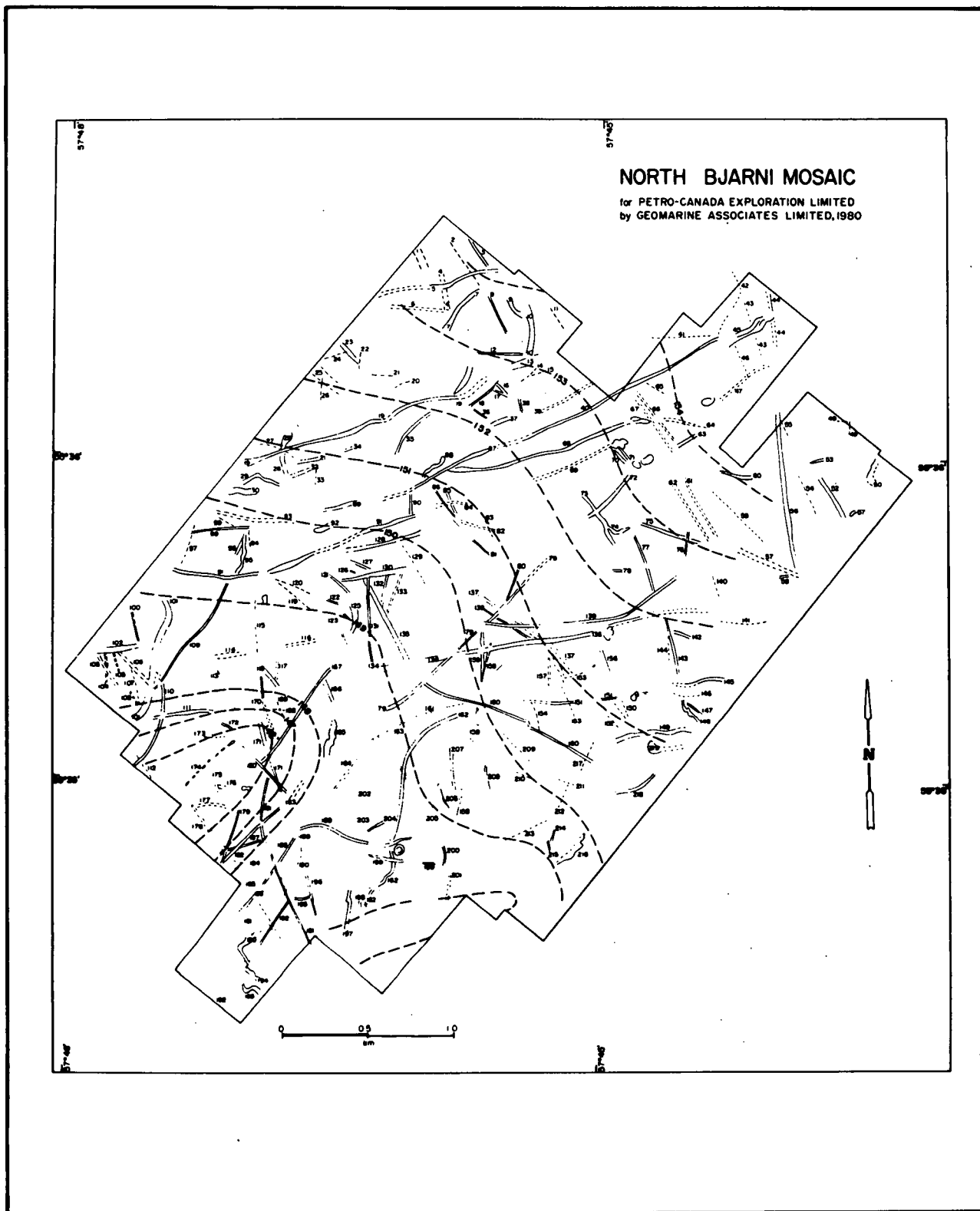


Figure 25. North Bjarni mosaic scour map.

in progressive vector diagrams by large looping motions, but these motions are not continuous. Both the tidal flows and the five day motions rotate clockwise. The dominant easterly and southeasterly flow is probably influenced by the isobaths, by a weak geostrophic current, and by the oceanographic conditions farther north in Hopedale Saddle.

Direct current measurements were collected at this site by NORDCO Ltd. for Petro-Canada Exploration in 1980 (NORDCO, 1981). The mean speeds were 17.4 cm/sec, 14.6 cm/sec and 11.0 cm/sec at depths 25 m, 55 m and 145 m, respectively. Maximum speeds at the same depths were 77.4 cm/sec, 47.4 cm/sec, and 33.4 cm/sec. The mean velocities at 25 m, 55 m and 145 m were 5.6 cm/sec at 140°, 4.5 cm/sec at 140°, and 5.5 cm/sec at 121°, respectively. Histograms showing the distribution of current speeds and directions are given in Figure 26.

The rose diagram (Figure 27) shows a dominant scour orientation between 70°-79° (only six scours however) which does not correlate with the observed southeasterly flow.

SNORRI WELLSITE SCOUR MAP

Inventory Results (Appendix K)

The water depths in this area on northern Nain Bank are between 130 m and 160 m. Although Geomarine (1976a) recorded 724 scours, only 697 scours were identified from the scour map (Figure 28) of which 285 crossed isobaths. The greatest bathymetric range was 12.5 (scour number 339). Changes in widths were observed in 51 scours of which 16 increased in width upslope, 25 increased in width downslope and 10 increased in width both upslope and downslope.

Seabed Slope and Surficial Geology

Slopes of between 1 in 250 and 1 in 415 to the northeast are typical of this region. There is considerable variation in the general northwest-southeasterly trend of isobaths within the map area with corresponding variations in gradient. The general northeasterly slope of 1 in 200 is locally as steep as 1 in 25 in the central region and as gentle as 1 in 700 in the western area. The regional surficial geology is rather poorly defined but consists of stratified reworked sandy sediments overlying glacial till (NORDCO, 1984). Two grab samples from the scour map area retrieved silty sand, although gravel patches and boulders were also observed on bottom photographs (Geomarine, 1976a).

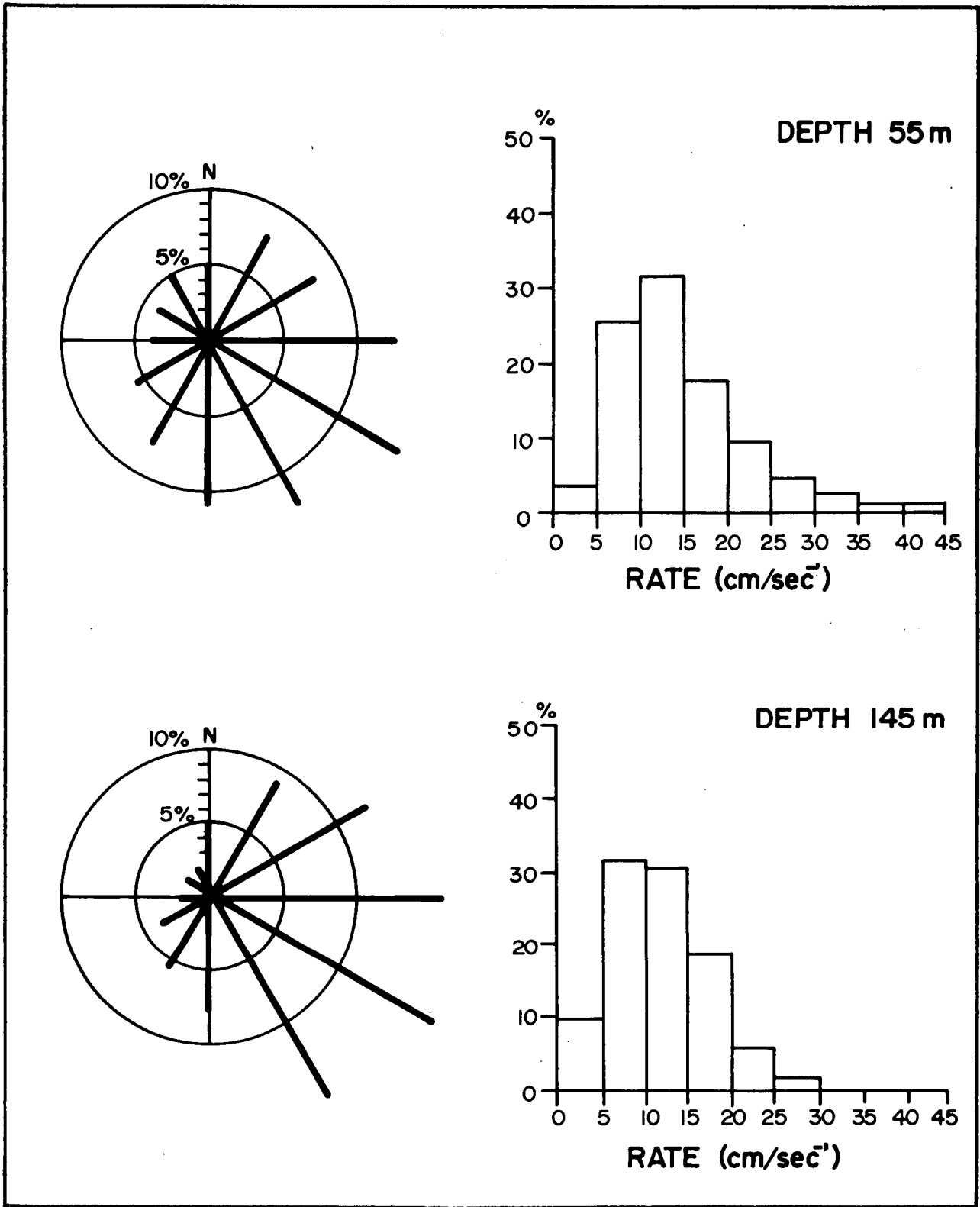


Figure 26. Current directions and speeds on Makkovik Bank.

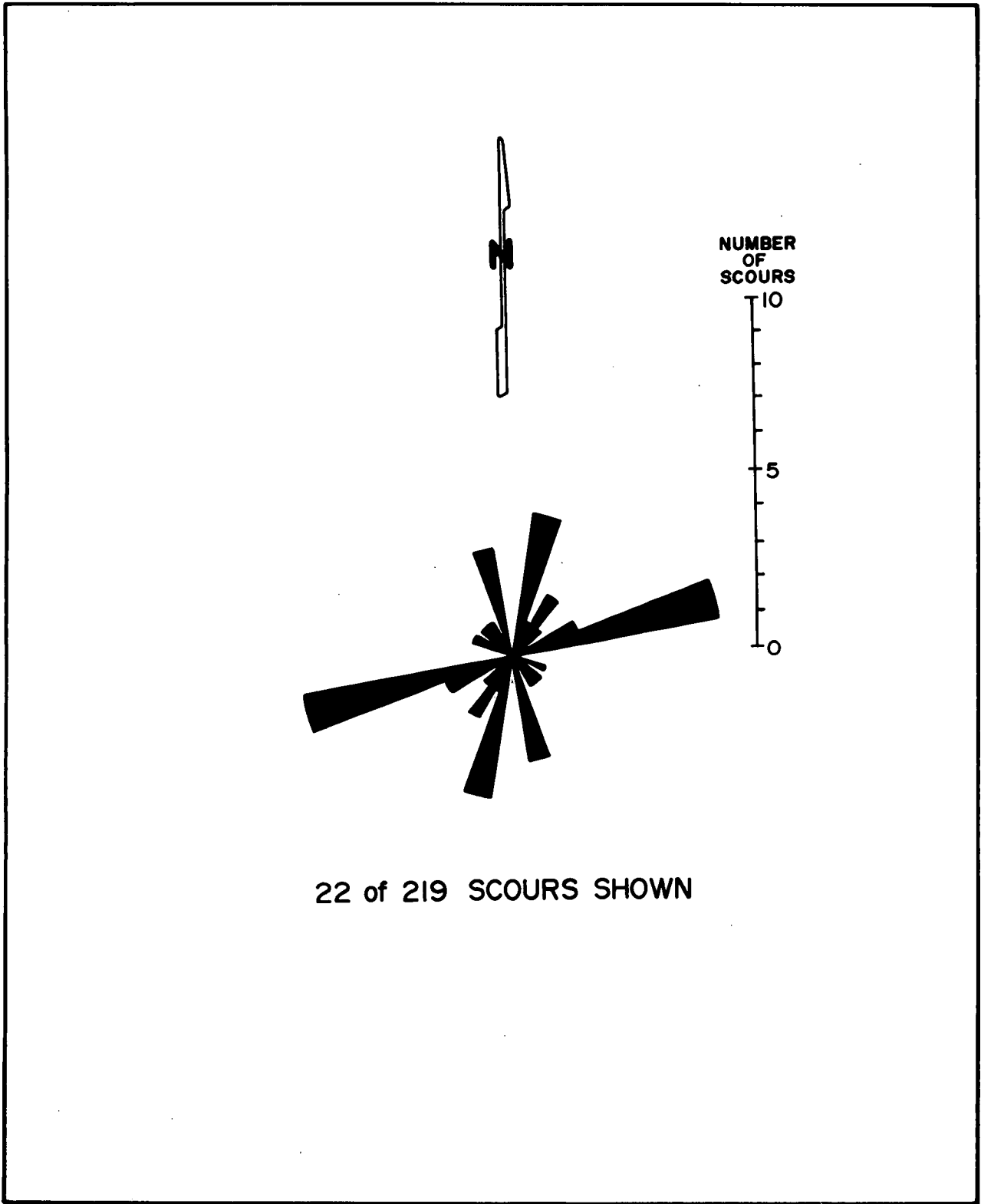


Figure 27. North Bjarni mosaic orientations of isobath-traversing scours.

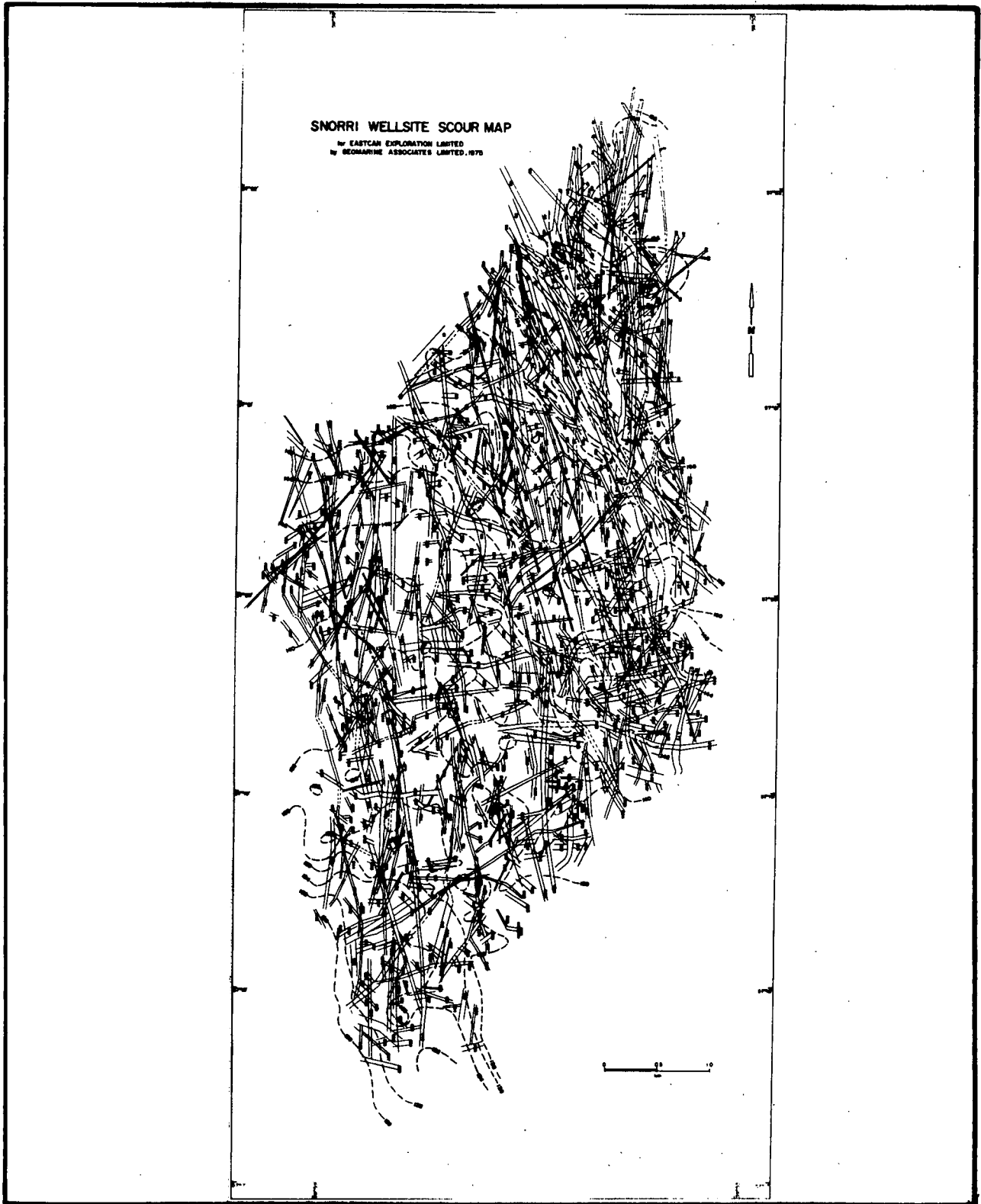


Figure 28. Snorri wellsite scour map.

Currents

At this site there are no steep bathymetric gradients to exhibit a steering effect on the current direction (Figure 29). The currents will have many of the flow characteristics found on the banks further south on the Labrador Shelf.

The only direct current measurements on Nain Bank are those from a location (57°32'N, 60°29'W) 38 km away which were collected in 1980 (NORDCO, 1981). The tidal currents are of the order of 4 cm/sec for the semi-diurnal constituent and 3 cm/sec for the diurnal constituent. The rotation is clockwise for these oscillatory flows. In general, the currents measured on Nain Bank were relatively weak with a residual southeasterly flow.

The maximum speed at the 56 m depth was 34 cm/sec in direction 120°. The mean speed was 11 cm/sec whereas the mean velocity was only 5 cm/sec in a southeasterly direction. Histograms showing the distribution of speeds and directions for Nain Bank are given in Figure 20. The dominant scour trend is between 160°-199° (Figure 30) with a minor trend between 060°-089° neither of which correlate well with observed current trends.

MAKKOVIK BANK ICEBERG SCOURS FROM RADAR OBSERVATIONS

Inventory Results (Appendix L)

Iceberg movement data were collected from several wellsites on Makkovik Bank between 1973 and 1981 (although in 1975 and 1977 there was no drilling activity and consequently no data were collected). During this time 915 bergs were observed of which 30 (3.3%) were interpreted to ground and/or scour (Woodworth-Lynas et al., 1985) (Figure 31). Criteria for identifying scouring icebergs are summarized earlier in the inventory results for Saglek Bank.

Twenty-five bergs were interpreted to scour of which 20 traversed more than 2 m in bathymetric range. The maximum bathymetric range traversed was 45 m (Bjarni H-81 wellsite, iceberg number 37, 1973). The shortest interpreted scour track was 2,500 m long and the longest was (96,250 m) (Bjarni H-81 wellsite, iceberg number 37).

Seabed Slope and Surficial Geology

Regional slopes of between 1 in 45 and 1 in 35 occur on the north and west flanks of Makkovik Bank where the seafloor descends into Hopedale Saddle and the Labrador Marginal Trough respectively. Gentler slopes of 1 in 310

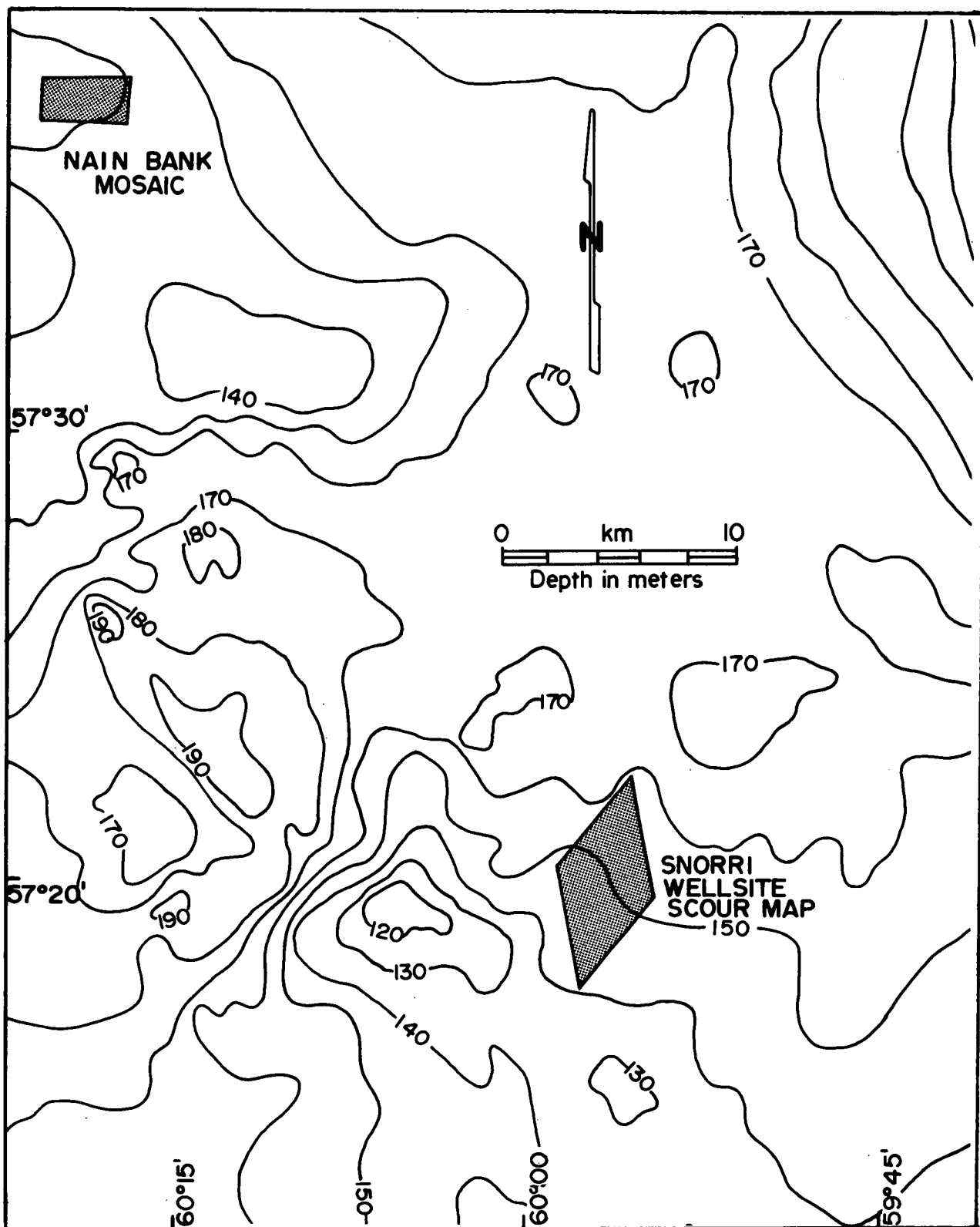


Figure 29. Location map of the Snorri wellsite scour map and also location of Nain Bank mosaic.

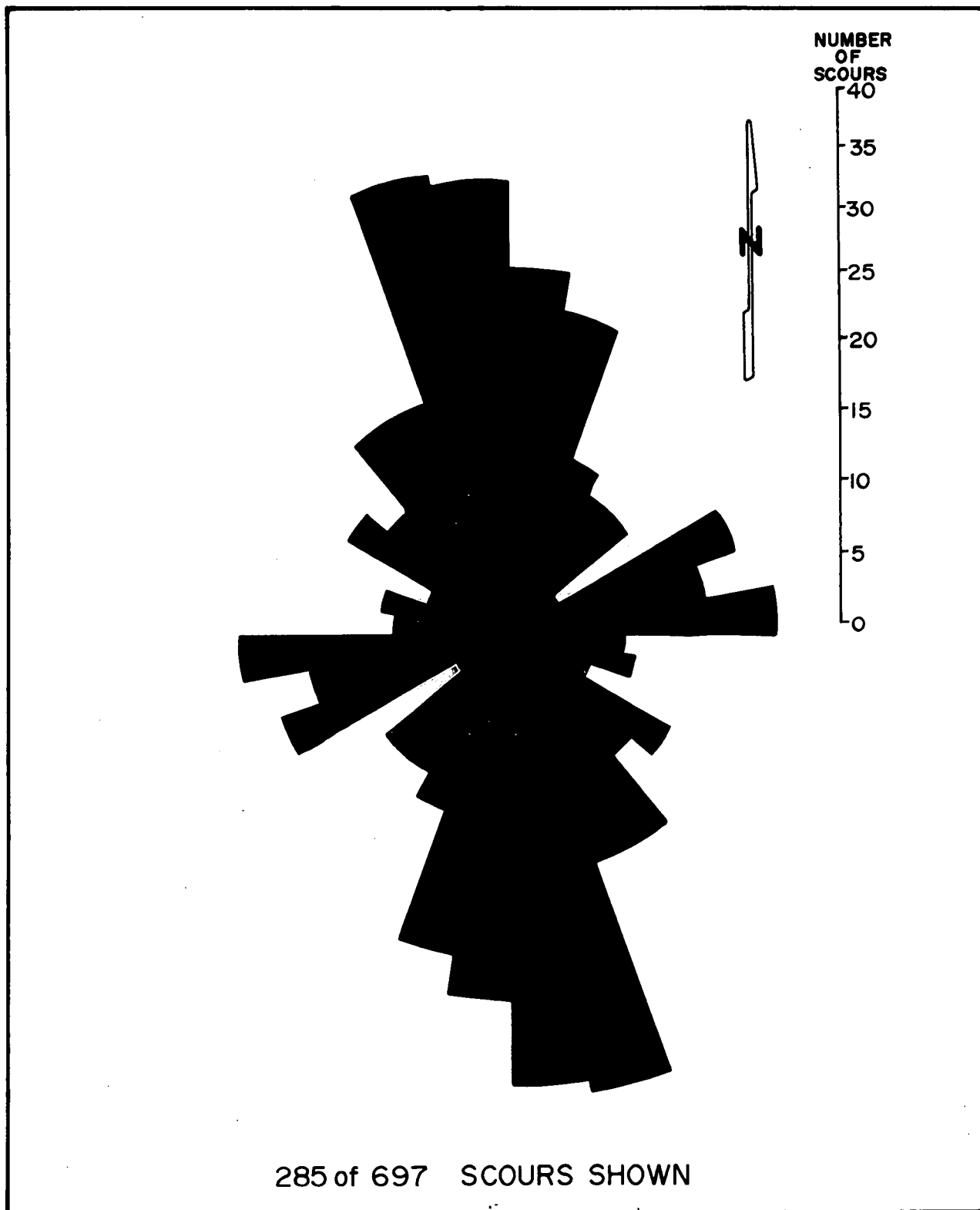


Figure 30. Snorri wellsite scour map orientations of isobath-traversing scours.

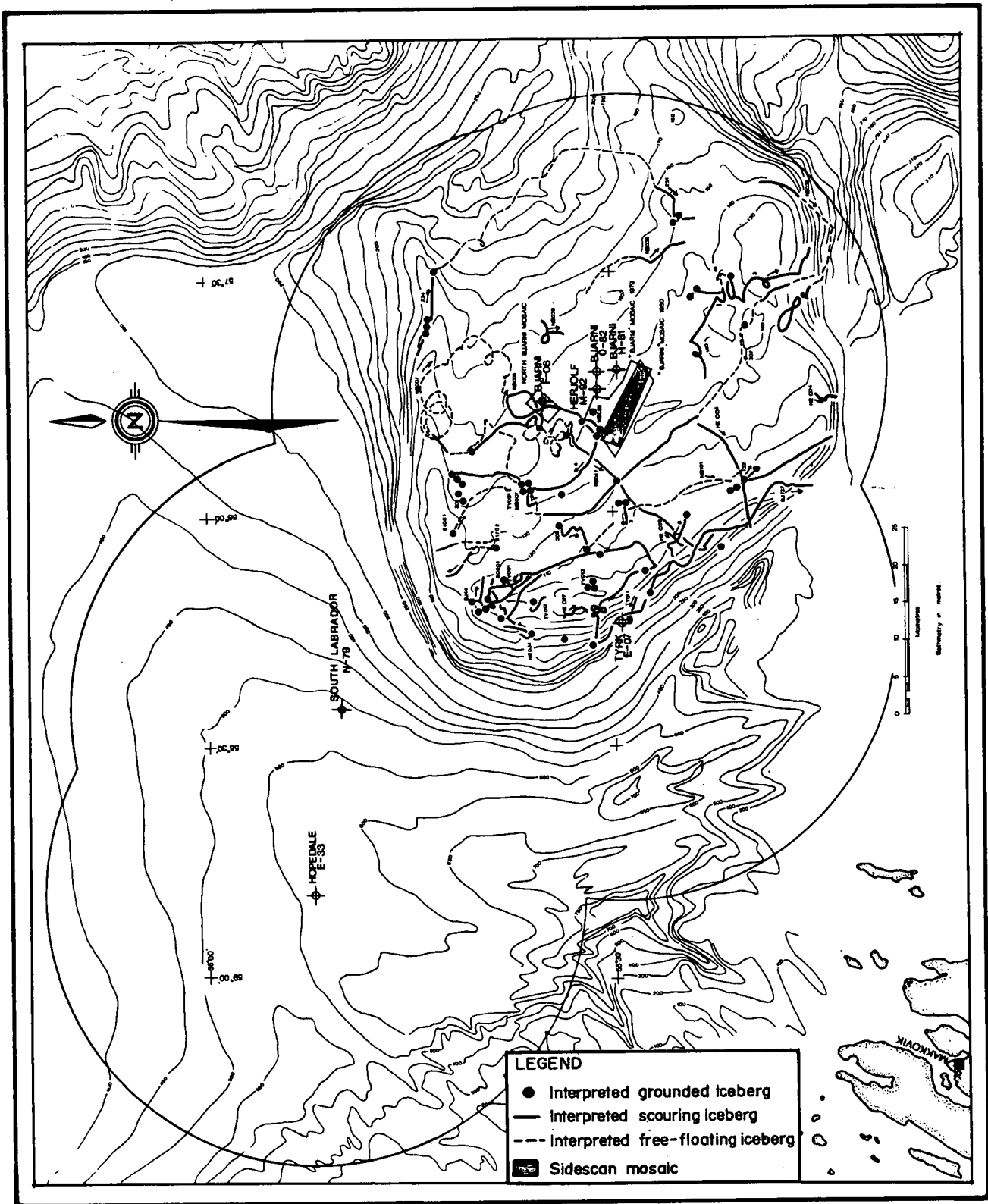


Figure 31. Radar tracks of icebergs interpreted as grounded or scouring on Makkovik Bank.

occur on the eastern edge of the bank and gradients of between 1 in 175 and 1 in 80 are found on the southern edge where the water depth increases into the northern part of the saddle separating Makkovik and Harrison banks. The entire top of Makkovik Bank has a gentle east-to-northeasterly gradient of about 1 in 385. Between about 300 m and 160 m the seabed consists of 1-2 m of unstratified post-glacial reworked sediments consisting mainly of sand (NORDCO, 1984). Gilbert and Barrie (1985) find that sediments from 120-140 m depth are exclusively fine sand (mean grain size diameter 0.177 mm). Above about 160 m, the bank top consists dominantly of exposed glacial till with thin (up to 3 m) local veneers of reworked sediments (NORDCO, 1984). Numerous grab samples from above 160 m indicate a consistent dominance of sand, generally never less than 75% with minor amounts of silt and clay and one or two areas of gravelly sands (NORDCO, 1984).

Currents

The current flow over the Labrador Shelf has a strong spatial variability dependant on bathymetry and different water masses. The paths followed by low-pressure systems also contribute to the variability, because the systems usually travel perpendicular to the coast with different wind directions on opposite sides of the low-pressure centre.

In general, the Labrador Current consists of two distinct southward transports, often referred to as the inshore and offshore streams. These are two geostrophic currents produced by density gradients at the boundaries between the distinctively different water masses in the area. The inshore stream is located inside the banks and follows the contours of the Labrador Marginal Trough. The offshore stream is located outside the banks along the Continental Slope. Makkovik Bank is located in the central region between the two southward flows. The southward residual flow on Makkovik Bank is hardly measurable and of the order of a few centimetres per second.

In Hopedale Saddle, a third, but weaker, density gradient contributes to a flow directed out of the saddle in its southern region, along the northern edge of Makkovik Bank. Current measurements by Chevron Standard in 1980, at their drilling site in the southwestern part of the Hopedale Saddle at the 500-m isobath, show that the dominant current flow is directed northeasterly along the contours of the saddle.

The currents around the perimeter of Makkovik Bank are much stronger than on the bank itself, where the currents are weak and variable. On the bank the current is mainly made up of tidal components, direct wind effects, inertial

effects, low-frequency oscillations, and internal density adjustments. Spectral analysis of the data show that the energy is concentrated mainly in two broad frequency ranges, a low frequency band and a tidal and inertial band. The low-frequency variations are the dominating factors.

On Makkovik Bank, the tidal current has a semi-diurnal and a diurnal component which are comparable in magnitude. The M_2 constituent is in the order of 7 to 10 cm/sec and the K_1 constituent is in the order of 6 cm/sec. The tidal ellipses are more circular than elsewhere on the Labrador Shelf showing that there is no preferred tidal current direction other than rotation in a clockwise direction. The tidal flows change relatively little with depth with respect to amplitude and degree of circular polarization.

The greatest low-frequency component on Makkovik Bank has a period between four and five days. The forcing agent responsible for this low frequency component has not been identified because of lack of research. Low-frequency oscillations may be a response to pressure systems moving through the area. The response of the ocean to synoptic-scale meteorological forcing by fluctuating wind fields are in the period range of two to ten days. At these time scales, waves are usually locally forced and are strongly dependant on bottom bathymetry.

The passage of weather systems over ocean areas induces changes in currents and in sea level, both by variations in atmospheric pressure and in the action of the associated wind stress. The surface is depressed about 1 cm for an increase of 1 mb in atmospheric pressure. In the presence of a coastline with winds directing water against the coast, the sea surface depression can be increased. The changes in sea level and a redistribution of the internal pressure gradient in stratified waters will force both barotropic and baroclinic oscillations.

The mean current speed on Makkovik Bank is about 14 cm/sec. From current measurements taken in 1979 by NORDCO, it was noted that the highest speeds at all depths occurred during times when the winds increased. From a longer data record in 1980, the maximum current speeds at depths of 25 m, 55 m, and near bottom were 77 cm/sec, 47 cm/sec and 33 cm/sec respectively. The increase in current speeds at all depths show that wind effects are not restricted to the wind-driven surface layer, but instead produce both barotropic and baroclinic components throughout the water column.

DB WELLSITE MOSAIC

Inventory Results (Appendix M)

This mosaic, located on the northern edge of Hamilton Bank covers water depths between 182 m and 200 m (Figure 32). Of 43 scours identified, 24 traversed more than 1 m of bathymetric range. Only one scour exhibited a width change (scour number 1) with an increase upslope of 40 m.

Seabed Slope and Surficial Geology

Regional slopes of 1 in 655 to the northeast are common in this region (Figure 33) steepening locally to 1 in 185, also to the northeast. Topography within the mosaic area consists of a single broad ridge and trough in the southwestern part with a maximum relief of 6 m. A southwest-facing slope characterizes the southwestern edge of the mosaic, forming one flank of the ridge, the gradient of 1 in 83 being the steepest in the mosaic area. The northeast-facing slope of the ridge has a gentler gradient of about 1 in 200. A gentle northeasterly slope of 1 in 153 characterizes the northeastern part of the mosaic. The regional surficial geology is characterized by extensive stratified post-glacial reworked sediments. Within the mosaic the north and northeastern area is composed of fine sand less than 1 m thick whereas the remaining area consists of gravel (NORDCO, 1984). These surficial sediments unconformably overlie glacial till about 65 m thick (NORDCO, 1984).

Currents

The isobaths (see Figure 33) are aligned in a northwest-southeasterly direction and tend to direct the currents in a southeasterly direction.

Current measurements collected by NORDCO (1981) from one location (54°39'N, 54°44'W) are representative of the currents at the DB site. The current has a measurable semi-diurnal tidal component of 6 cm/sec (Fissel and Lemon, 1982) and a negligible diurnal tidal component. A significant amount of spectral energy is found in the low-frequency band with a 14 day period. All rotational flows are clockwise. A southward geostrophic current is also present.

The dominant flow is directed southeast as shown in Figure 34. The maximum speeds are 49 cm/sec and 38 cm/sec and the mean speeds are 14 cm/sec and 10 cm/sec at depths 54 m and 153 m respectively. The mean current velocities are 6.6 cm/sec in direction 157° and 5.4 cm/sec in direction 146°, at depths 54 m and 153 m.

To the north of the study area the currents generally flow eastward because of the peculiarities of the flow in

DB MOSAIC

for PETRO-CANADA EXPLORATION LTD.
by GEOMARINE ASSOCIATES LTD., 1980

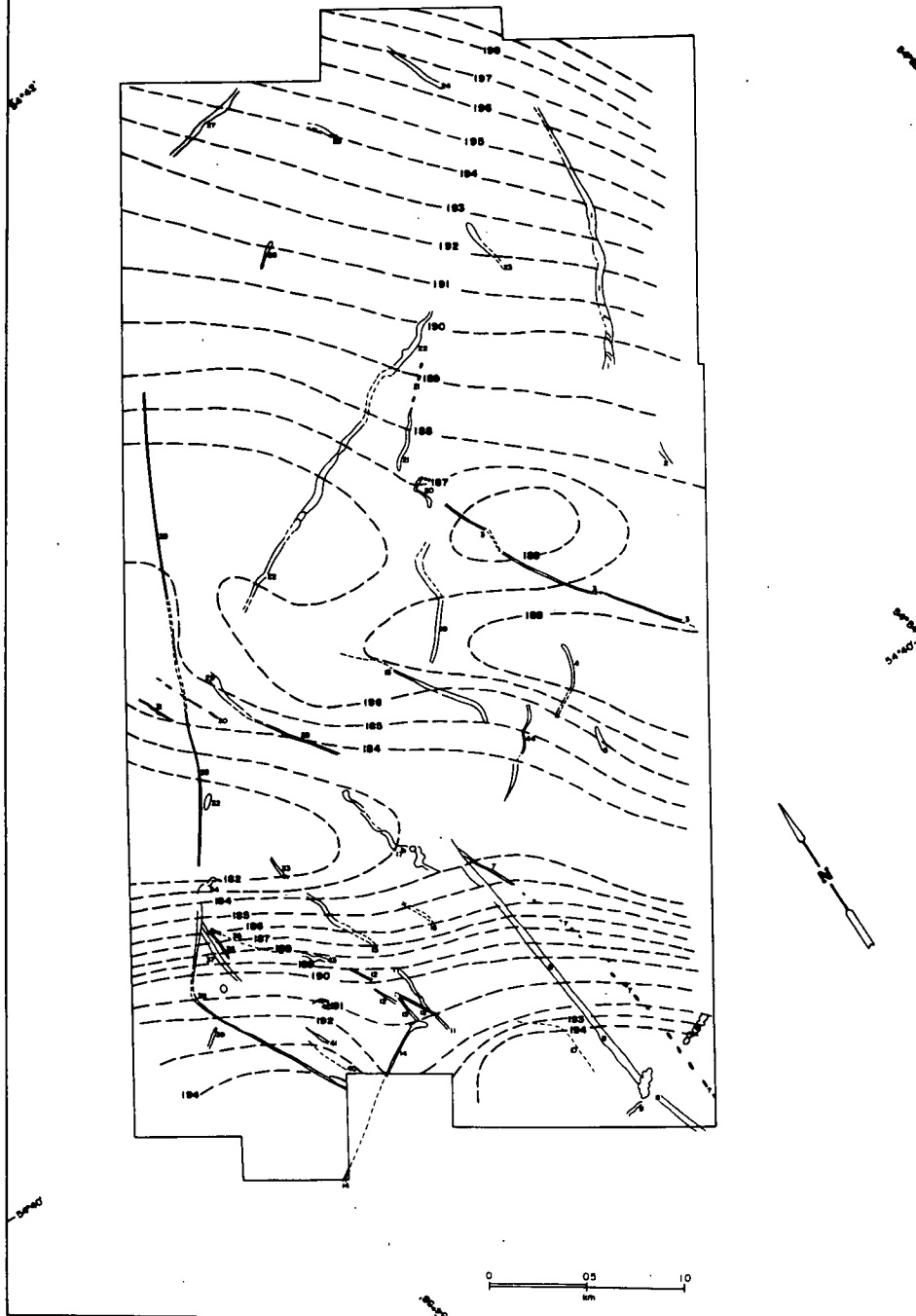


Figure 32. DB wellsite mosaic scour map.

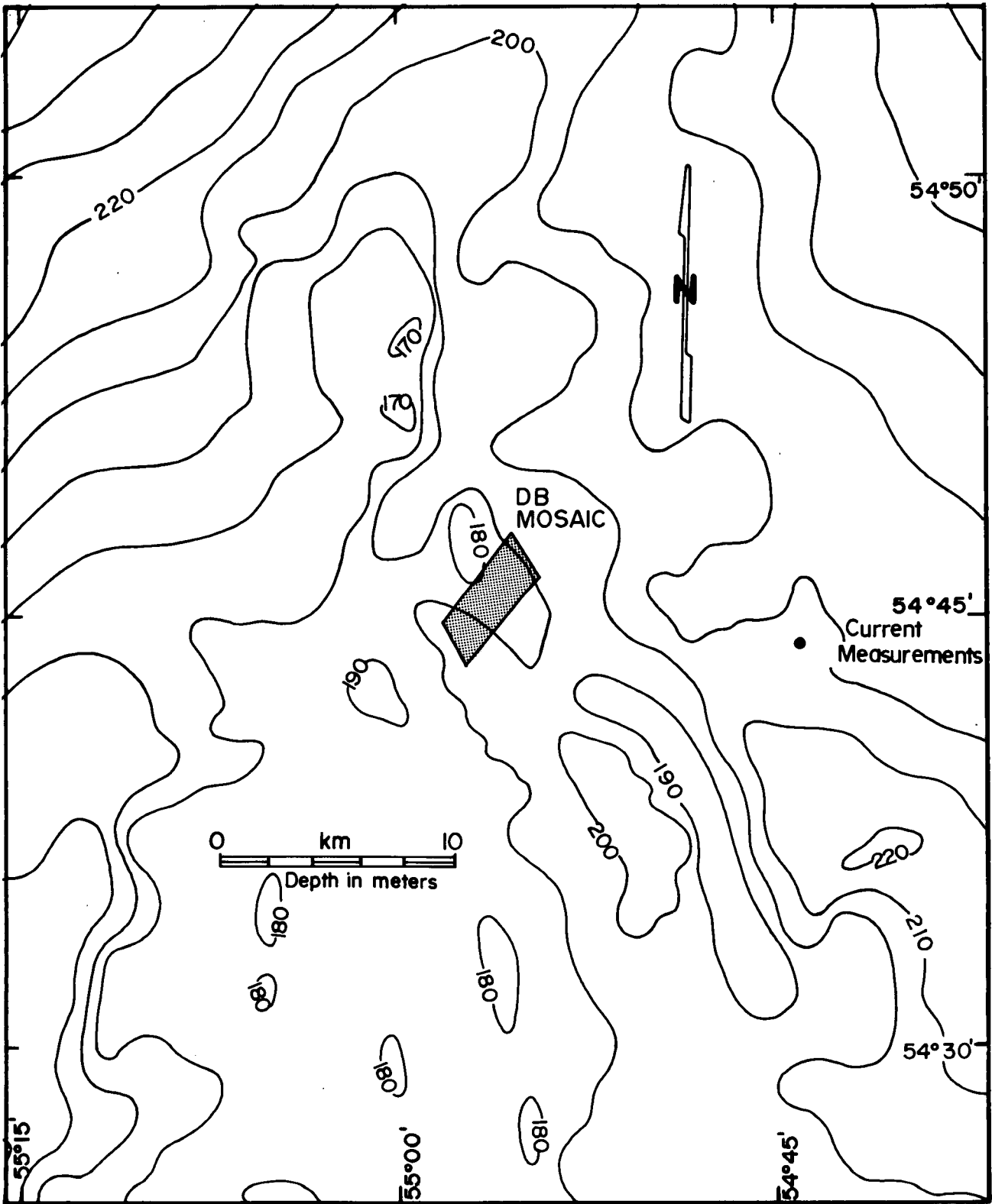


Figure 33. Location map of the DB wellsite mosaic.

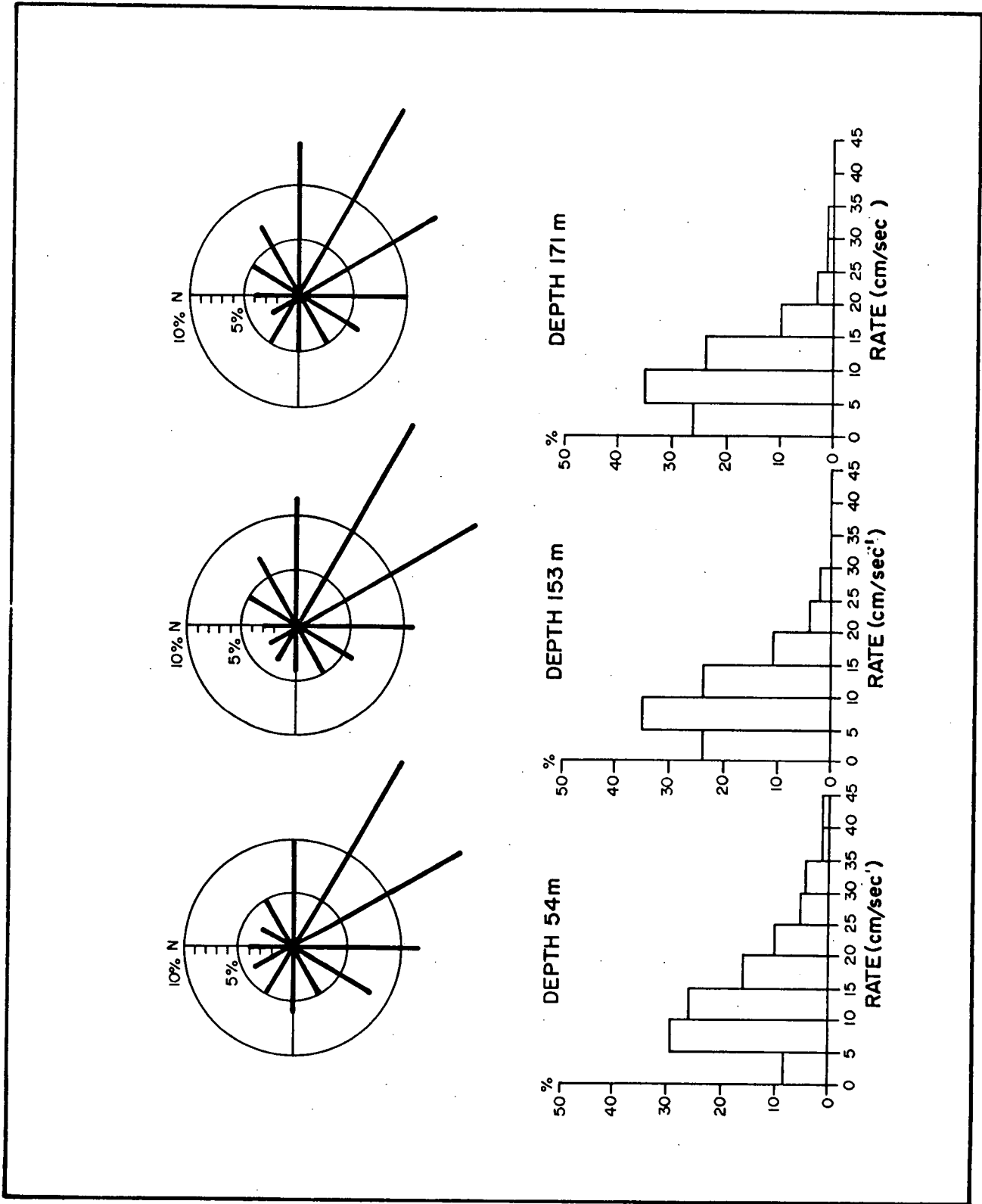


Figure 34. Current directions and speeds on Hamilton Bank.

Cartwright Saddle and may sometimes be present in the study area.

The mean southeasterly flow is not mirrored by the scour orientations (Figure 35) which have a net north-south orientation within a moderate spread between 160°-199°. Scours located northeast of the prominent southeast-northwest trending ridge (at 182 m) have a noticeably northeast-southwesterly orientation whereas southwest of the ridge, where most scours are seen, the dominant trend is almost north-south. This marked change in orientation may reflect localized current anomalies which do not conform to the interpretation of easterly and southeasterly flow.

EAST HARRISON BANK MOSAIC

Inventory Results (Appendix N)

This mosaic represents an area on northern Harrison Bank with water depths of 152-162 m. Of 108 scours identified (Figure 36), 23 traversed more than 1 m of bathymetric range; the maximum range was 7 m (scour number 67). Three scours had changes in width: one increased in width upslope and the other two increased in width both upslope and downslope. The greatest increase in width was 80 m (scour number 44).

Seabed Slope and Surficial Geology

Regional northeasterly seabed slopes of between 1 in 95 and 1 in 155 typify the bank edge (Figure 37), whereas the bank top is virtually flat. Slopes within the mosaic area are locally as steep as 1 in 35 in the west to less than 1 in 820 towards the north in the eastern part.

The regional surficial geology consists of a thin (2-3 m) veneer of reworked, stratified, post-glacial sediments above glacial till (NORDCO, 1984). A grab sample from within the area of the mosaic consists of about 75% sand, 20% gravel and minor silt and clay; the gravel has been interpreted as a lag deposit (NORDCO, 1984).

Currents

The local isobaths run in a northwest-southeasterly direction but are not steep enough to be of major influence (see Figure 37). There are no direct current measurements available for Harrison Bank but the currents in this area are expected to be similar in magnitude and variability to that at the North Bjarni site on Makkovik Bank. The current is expected to have three main components; the semi-diurnal

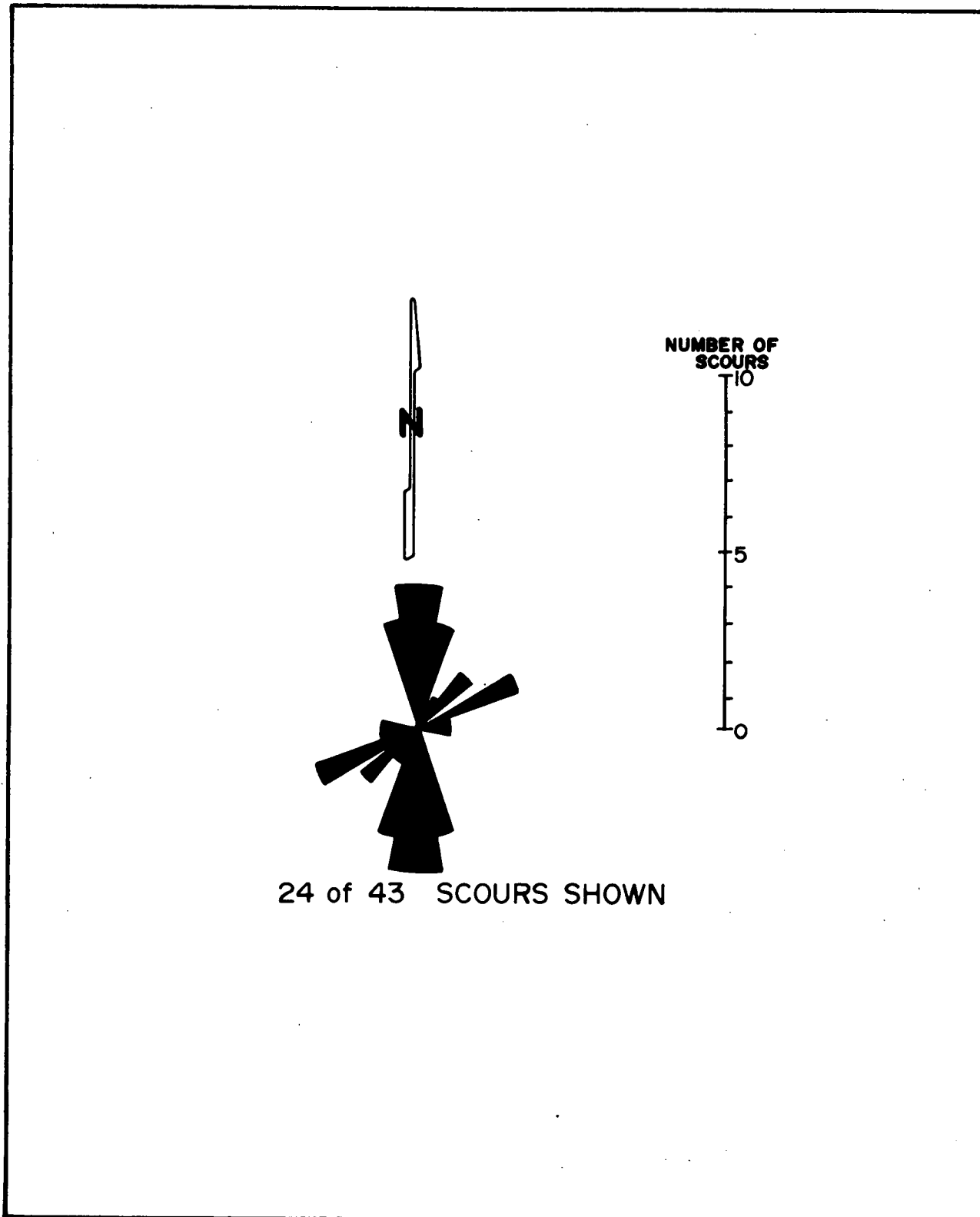


Figure 35. DB wellsite mosaic orientations of isobath-traversing scours.

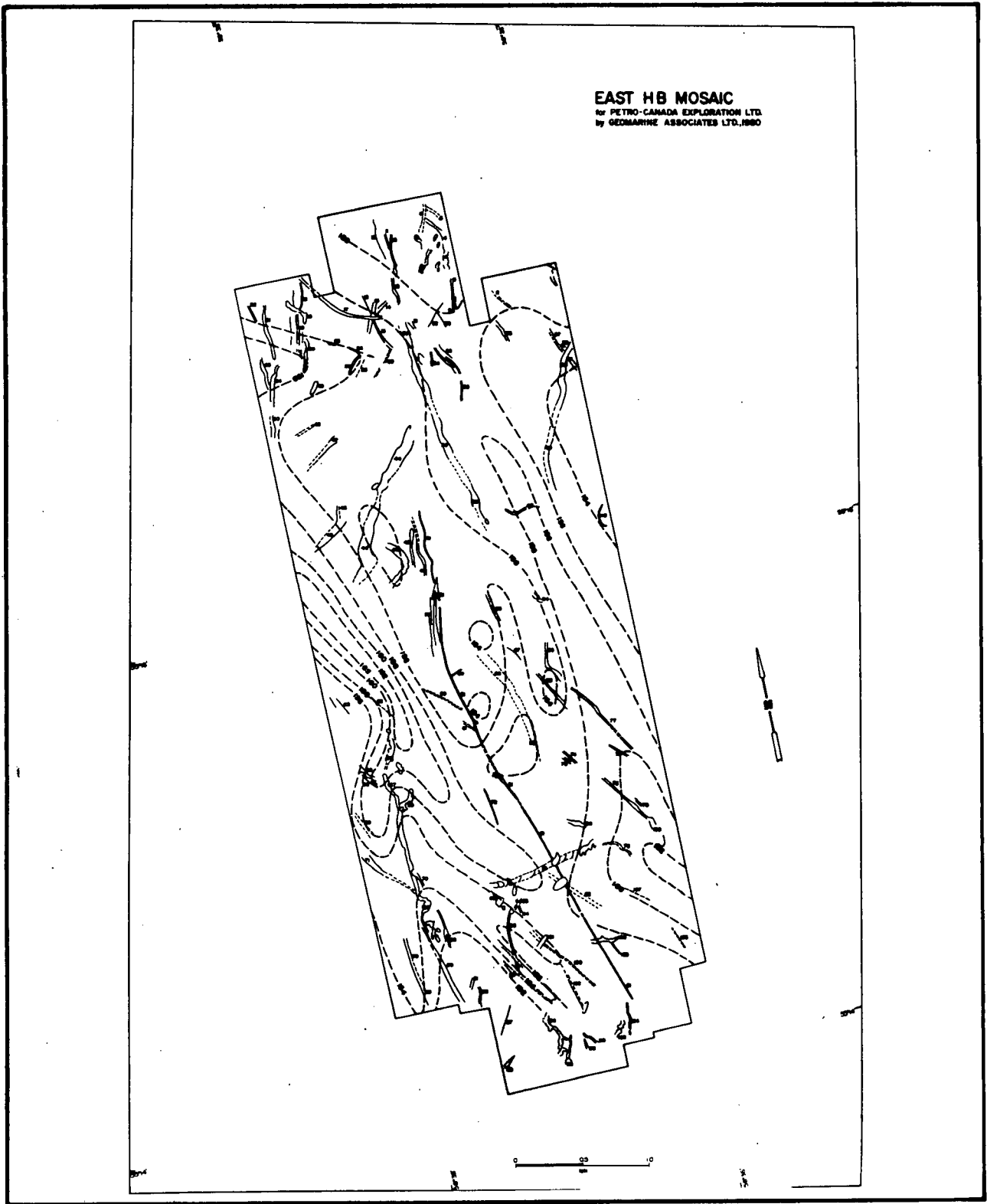


Figure 36. East HB mosaic scour map.

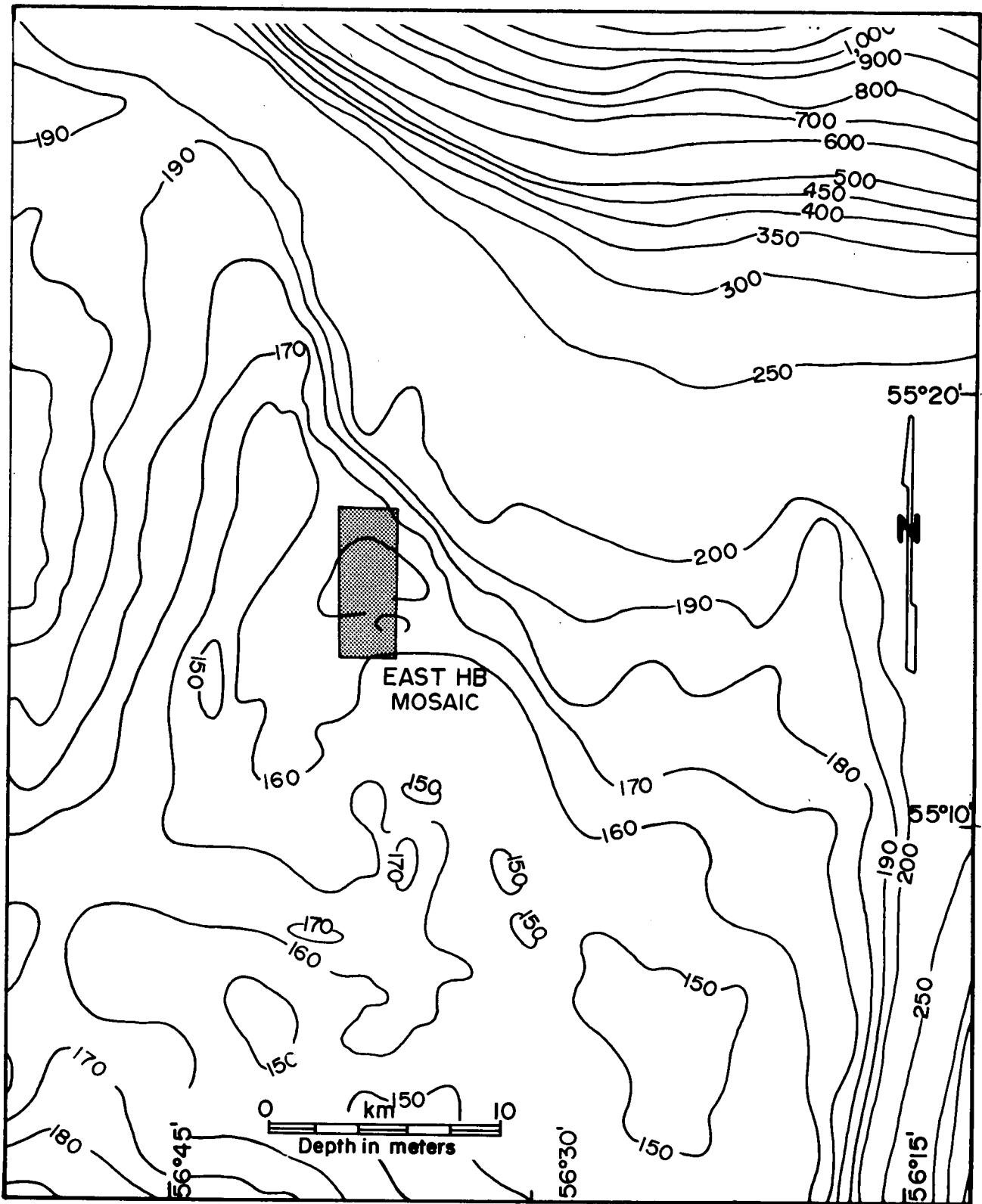


Figure 37. Location map of the East HB wellsite mosaic.

tide, the diurnal tide, and a low-frequency component.

The dominant current is expected to be southeasterly along the local isobaths. The temporal variability should be significant, such that the flow can be in any direction at a given time. There is good correlation between the expected current flow and scour trend (Figure 38) which has a dominant orientation of 130-149°.

HIBERNIA EAST MOSAIC

Inventory Results (Appendix O)

The most southerly area, represented by this mosaic, is located on the northeastern Grand Banks in water 85.4-96.4 m deep. Only ten scours were observed (Figure 39) on the mosaic of which two traversed bathymetric ranges of 1 m and at least 4 m. Neither scour showed changes in width.

Seabed Slope and Surficial Geology

Regional gradients of between 1 in 217 and 1 in 375 characterize the area separating a flat upper terrace at 80 m depth from a lower terrace at 100-110 m depth (Barrie et al., 1984). The mosaic straddles north-northwest to south-southeast trending sand ridges, each about 2-3 m thick. The ridge troughs represent exposures of the Grand Banks Gravel which rest unconformably above Tertiary strata, and within the ridge field the sediments coarsen progressively to the west from gravelly sands to sandy gravels (Barrie et al., 1984).

Currents

The seafloor in this area is relatively flat such that it has little effect on the current pattern. On the Grand Banks, the semi-diurnal tide is the major force driving the current. Spectral analysis ranked the inertial component next to the semi-diurnal component in spectral energy. These factors cause the current directions to be oscillatory in nature such that the flow can be in any direction at a given time. The other significant components are the diurnal tidal current and wind-driven current.

Available current measurements near this site were collected by MacLaren Plansearch Lavalin (1981; 1982). Measurements were collected at 46° 47'N, 48° 46'W, at depths of 25 m, 45 m, and 60 m. Harmonic analysis showed that the semi-diurnal tidal constituents had values of 14 cm/sec, 13 cm/sec and 10 cm/sec and the diurnal constituent has values of 6 cm/sec, 5 cm/sec and 5 cm/sec. Both the semi-

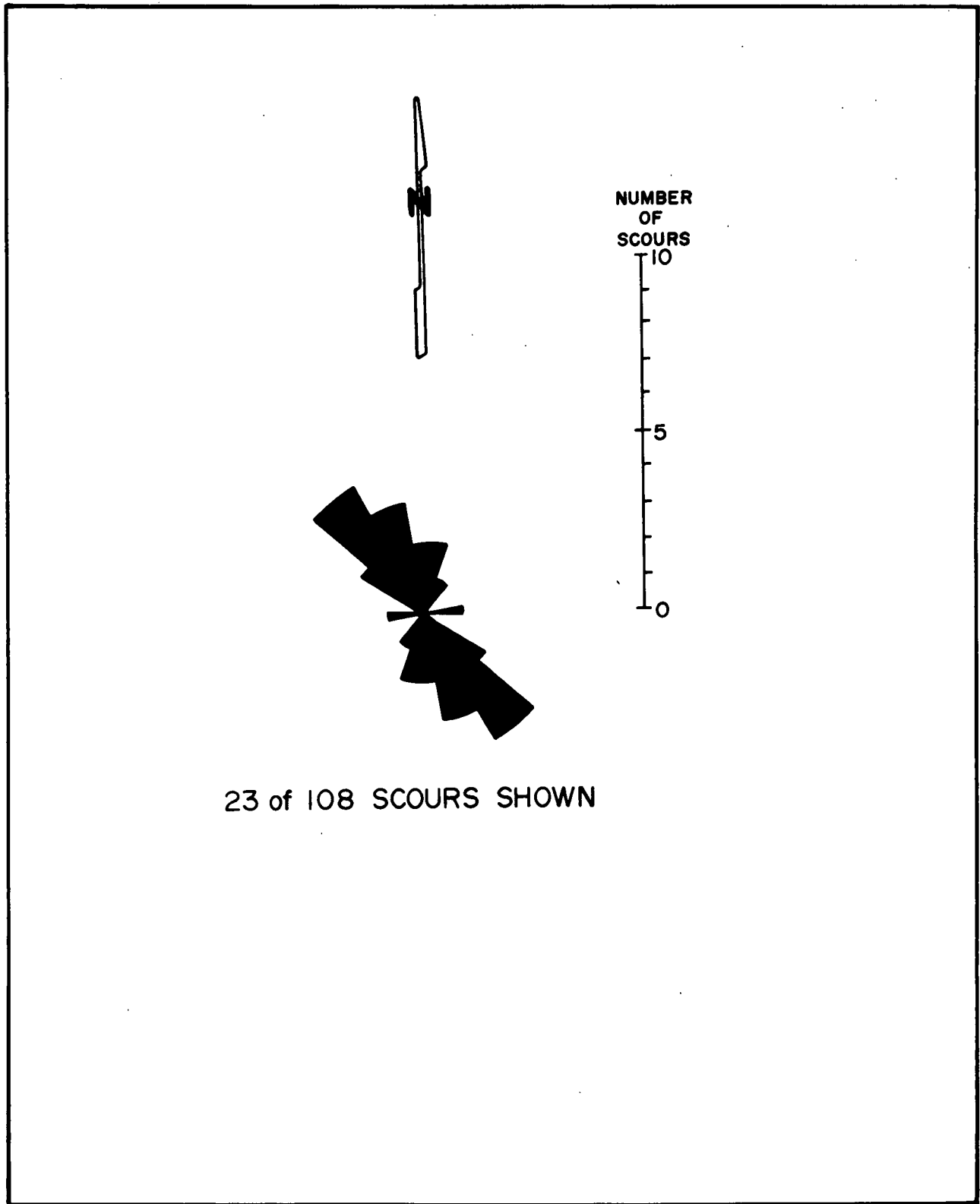


Figure 38. East HB wellsite mosaic orientations of isobath-traversing scours.

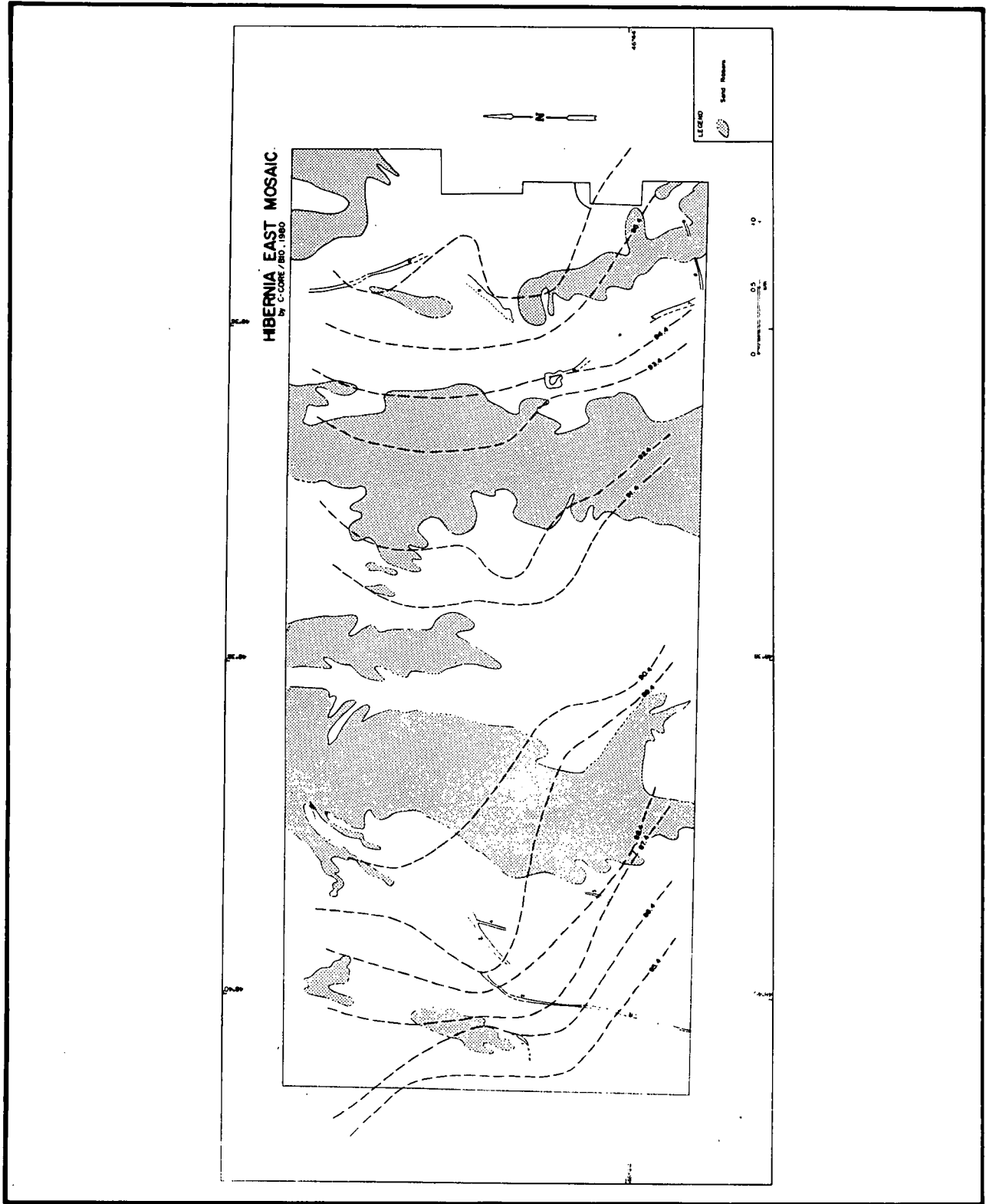


Figure 39. Hibernia East mosaic scour map.

diurnal and diurnal tides were oriented in an east-west direction. At this site the maximum currents speeds were 70 cm/sec, 60 cm/sec and 55 cm/sec at depths of 25 m, 45 m and 60 m, respectively. The mean speeds were 30 cm/sec, 25 cm/sec and 17 cm/sec. The residual currents at the site for each depth were west, west and northwest respectively.

Similar results were found from the measurements at location 46° 51'N, 48° 44'W. At this mooring site, the currents were measured at depths of 26 m, 47 m and 75 m. The semi-diurnal constituent had values of 13 cm/sec, 10 cm/sec and 9 cm/sec whereas the luni-solar diurnal (K_1) constituent had values of 8 cm/sec, 39 cm/sec and 54 cm/sec and the mean speeds were 21 cm/sec, 40 cm/sec and 15 cm/sec, respectively. The residual currents for each depth were southwest, west and northwest respectively.

Meaningful discussion of only two scour orientations with respect to currents cannot be made for this mosaic. However, it is worth noting that the scours only occur in the areas between the sand ribbons. It is possible that scours developed in the sandy facies would be obliterated by migration and infilling of sand moved during periods of storm-generated currents (50-80 cm/sec.).

THEORETICAL MODELLING OF UPSLOPE, DOWNSLOPE SCOUR

In the absence of reasonable alternatives (such as experimental modelling and extensive field data), mathematical simulation provides a powerful aid to intuition, delivering likely ranges for important parameters of the process modelled. In considering the possibility of upslope and downslope scour from a theoretical point of view, simplified mathematical simulations of upslope and downslope scour are presented.

Mechanisms of scour require an understanding of the stability of a floating body. Two scouring mechanisms are discussed: first "Unstable Roll" of an iceberg to an orientation of deeper draft allows contact with the seabed to be made and scouring to begin (upslope or downslope). Secondly, "Tilt" induced by soil pressures allowing draft adjustment to accommodate variations in the seafloor.

Evidence for the assumptions on which the modelling is based is presented. Two other simulation studies are described and a critical analysis is offered. The section concludes with a possible stochastic approach to the problem of determining likely draft increases for unstable icebergs.

A mathematical model of iceberg scour that emphasizes iceberg dynamics rather than soil mechanics is presented. The model is used to simulate upslope and downslope scouring, and to demonstrate a variety of phenomena associated with scouring icebergs, such as cratering. Results are presented showing the effects of various parameters on upslope and downslope scouring.

STABILITY

Figure 40 shows a floating homogeneous body. The force of gravity acting through G (the centre of gravity) and the force due to buoyancy acting through B (the centre of buoyancy) are equal and opposite. For equilibrium, G is vertically above B. The stability of that equilibrium position can be determined in any one of several ways. One of the simplest, intuitively, is to use the concept of potential energy. The potential energy of a floating body is defined to be the difference between the potential energy of the body (relative to some datum line) and that of the fluid it displaces. In precise terms, it is $Mg(h_B - h_G)$ where h_B and h_G are the distances of the centres of buoyancy and gravity, respectively, from the waterline. If, at some orientation, the potential energy is at a minimum (locally), then the body is in stable equilibrium, but not otherwise. If the potential energy is constant (locally) then the body is in neutral equilibrium. The degree of stability at a particular equilibrium orientation is best described by a

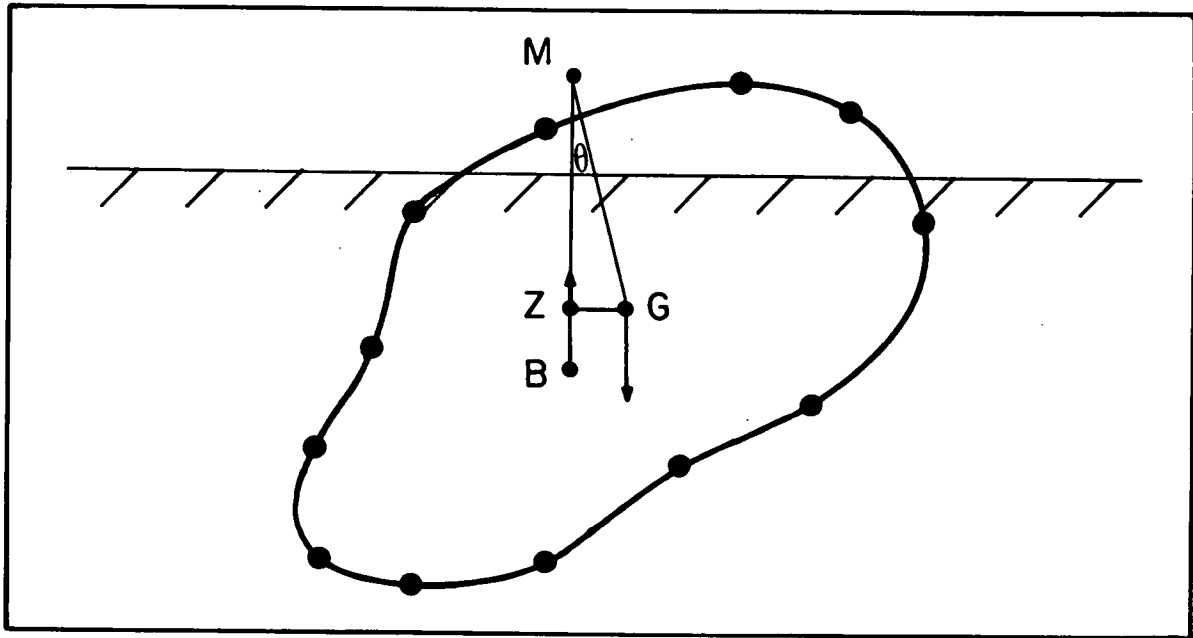


Figure 40. Iceberg profile showing node points.

single parameter, GM known as metacentric height. M is the point on the vertical line through G, about which the centre of buoyancy appears to rotate for small angles of inclination. Assuming G is fixed for this small rotation, one may derive a simple expression for the lever GZ (Figure 40) of the couple formed by the opposing forces of gravity and buoyancy. Namely GZ is approximately $GM\theta$ for small inclinations θ . Thus for GM large, there is a large couple restoring the body to its initial orientation, i.e. the body is very stable. Clearly if GM is negative (i.e. M is below G), the body will move farther from its equilibrium orientation if tilted (indicating instability).

TWO-DIMENSIONAL THEORETICAL MODELLING

Unstable roll

A computer program developed by Bass and Peters (1984a) can analyse the stability of arbitrary floating bodies. A brief description of that program and the way it has been used to simulate iceberg instability is given below (more details can be found in Bass and Peters, 1984a and b).

For a quantitative stability analysis of a specified "real" iceberg, the two-dimensional modelling is inadequate, but qualitatively more than sufficient.

In analysing the stability of an iceberg it is generally only necessary to consider stability relative to the axis about which it is most likely to roll. Because icebergs generally have one waterplane dimension significantly greater than any other, it has been assumed that the iceberg is most likely to roll about an axis in the direction of its major axis. The iceberg is then modelled by a two-dimensional profile representing the average vertical cross-section taken orthogonal to that axis. Using a piecewise linear representation of an iceberg profile, the nodes of that profile are input directly to the screen of a computer using a computer-driven "MOUSE". The computer program lifts the coordinates of these points from the screen and delivers a representation of the profile by vertical trapezoidal strips (Figure 41). This transformed data is input to a stability routine that calculates the GZ and potential curves for a preselected range of orientations. The user may then modify the iceberg profile by adding, deleting or moving "node points". In this way the user can simulate the process of ablation leading to destabilization. The melting simulation was generally applied so that maximum melting was achieved near the waterline and at the base of the profile. The resulting shapes, after various trial-and-error modifications, closely resemble iceberg profiles determined in the field using side-scan sonar (Figure 42) (Newfoundland and Labrador Petroleum Directorate, 1983).

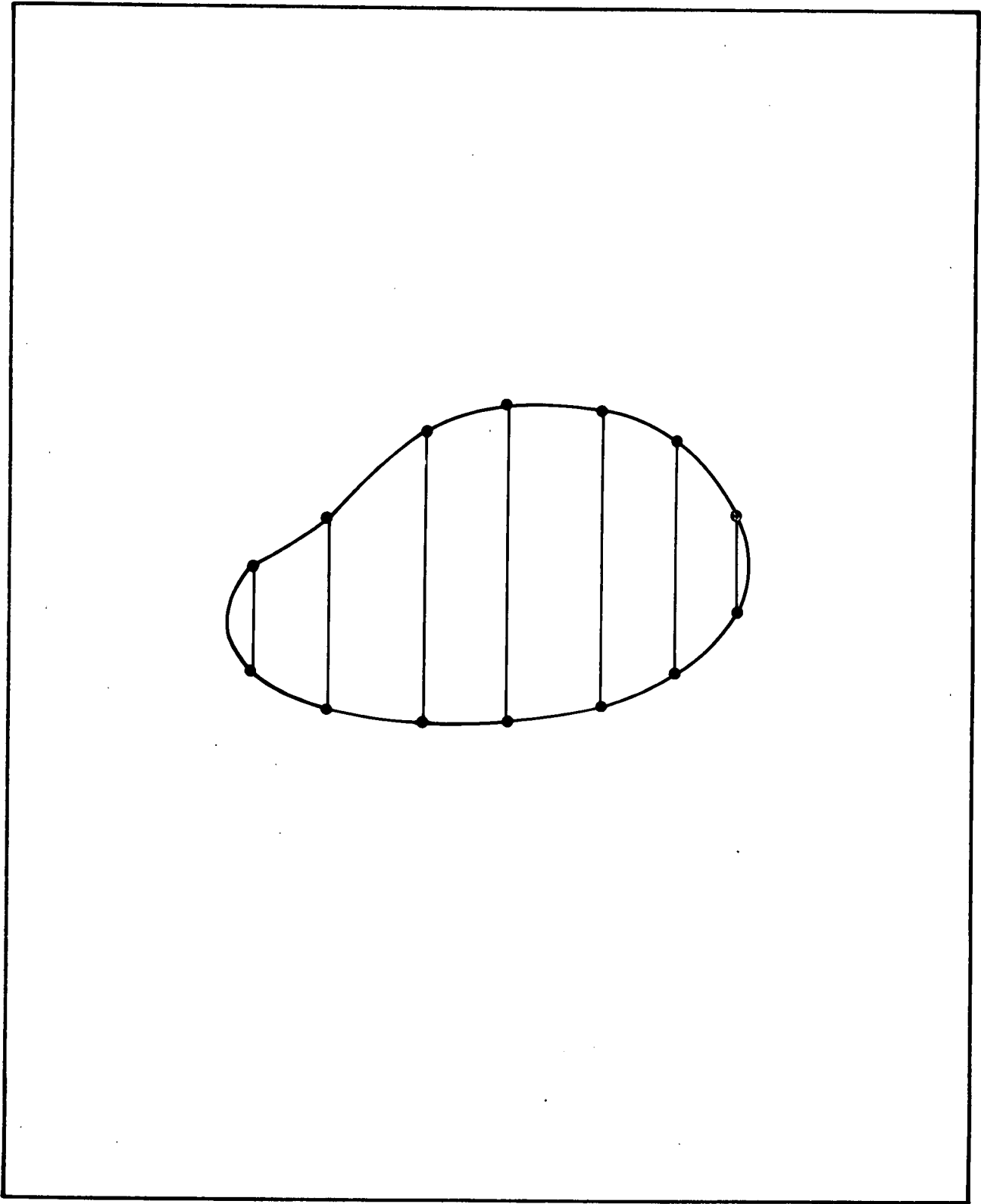


Figure 41. Trapezoidal representation of iceberg profile.

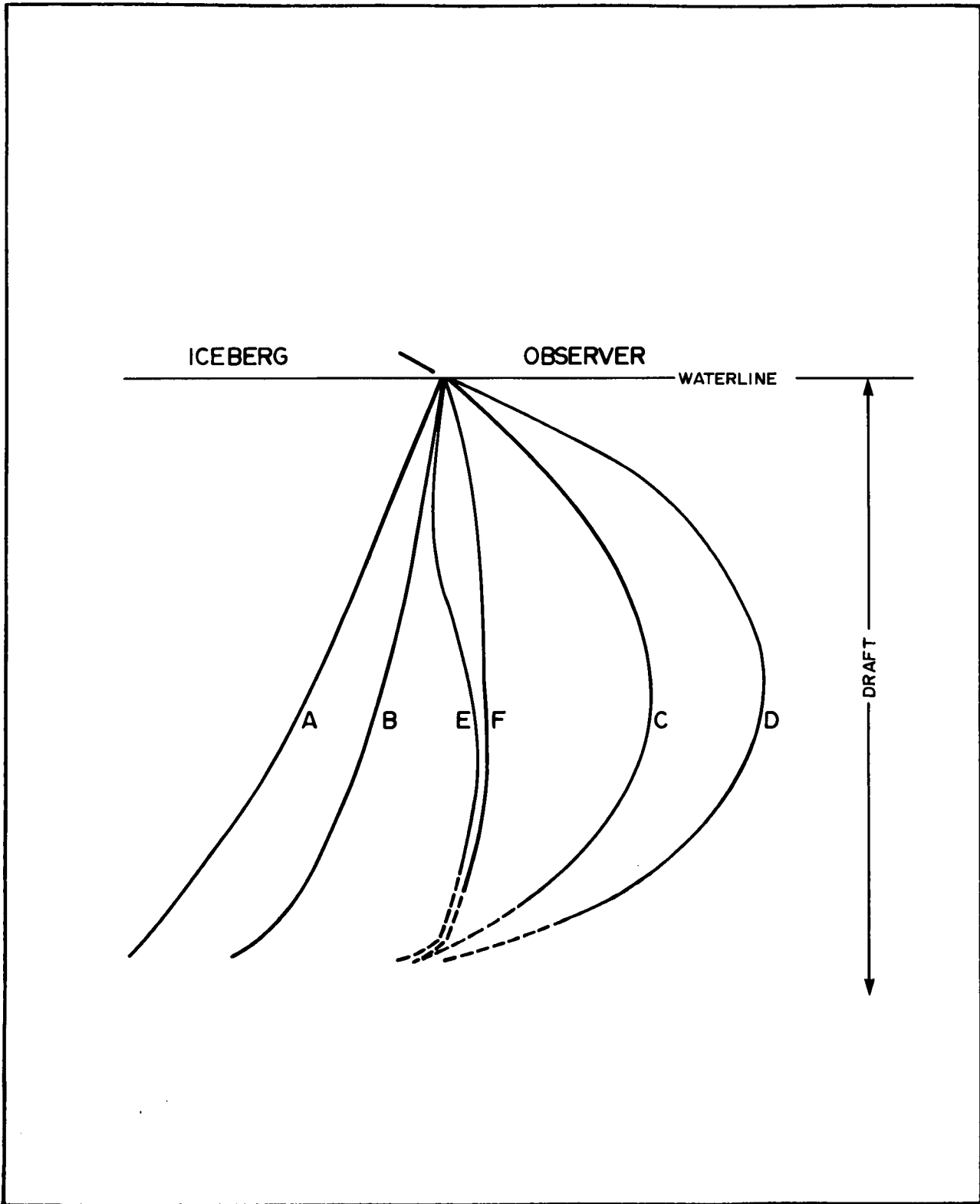


Figure 42. Partial underwater profiles of typical icebergs.

Elliptical, rectangular and trapezoidal initial profiles of various dimensions were used in the melting simulation. During the melting simulation, the iceberg developed a range of orientations over which it was near-neutrally stable. These ranges were generally flanked by regions of relatively high potential. Figures 43 (a), (b) and (c), show the development of this near-neutral range in a simulated melting of a trapezoidal profile. The profile obtained with the range of near-neutral stability may be regarded as a typical representative of a class of similarly shaped icebergs. For this class of icebergs the maximal draft increase possible following unstable roll is determined by the maximal draft variation within the near-neutral range. Maximal draft increases for a variety of trapezoid classes are given in Bass and Peters (1984a). The trapezoids were the most interesting of the initial profiles considered, in that they exhibited the greatest draft increases on roll.

Cogent arguments can be made as to why the trapezoid class of icebergs showed the most significant draft increases. Although there is no definitive proof that such icebergs present the greatest threat to seabed installations it is worthwhile presenting those arguments so that some estimates of the probability of occurrence of seabed collisions by rolling icebergs can be obtained.

The most readily apparent shape characteristic of the trapezoidal class of icebergs is their degree of "bulge" underwater - that is the width of the iceberg is greater below the waterline than at the waterline. Bass (1980) described this shape characteristic using a numerical descriptor known as the "underwater shape coefficient" (USC). A $USC < 1$ implies a bulging shape (e.g. an elliptical shape) whereas $USC = 1$ represents a vertical-sided rectangular shape and $USC > 1$ represents a tapering shape (e.g. an inverted triangle). For two icebergs of the same above-water dimensions, the one with a tapering underwater shape will have a greater draft than the one with a bulging shape. Clearly the class of icebergs that in general increase their draft on roll is characterized by $USC < 1$. In fact for such icebergs USC increases on roll.

Within this class of icebergs there are two other parameters of some significance; the bulge width (BW) and bulge depth (BD). They are difficult to define precisely for highly irregular shapes. BW is the ratio of the maximum "significant" width of the underwater shape to the width of the waterline (again the model is assumed two-dimensional for simplicity). BD is the ratio of the depth of this maximum significant width level, to the draft of the iceberg. For highly asymmetric icebergs it may be necessary to define a left or right ratio, or possibly to take the maximum value obtainable from each "side". Figures 44 (a), (b) and (c) show typical idealized representatives of these classes,

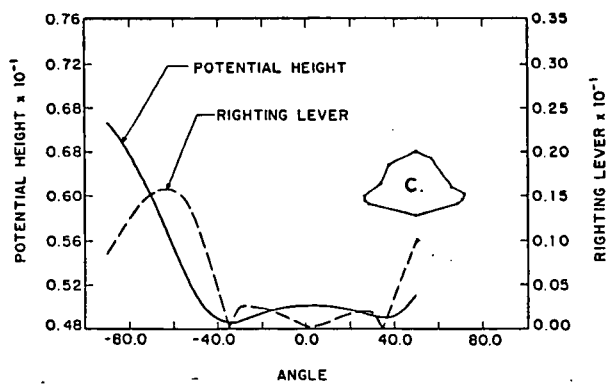
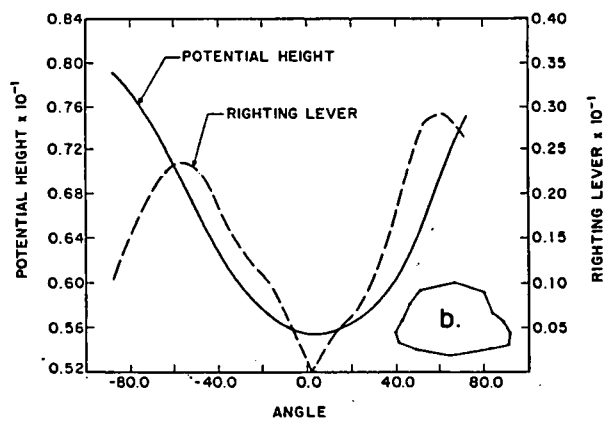
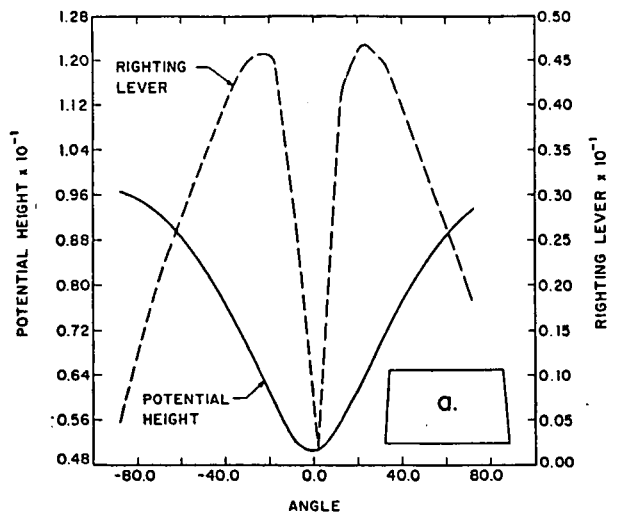


Figure 43. Melting of iceberg leads to near-neutral stability.

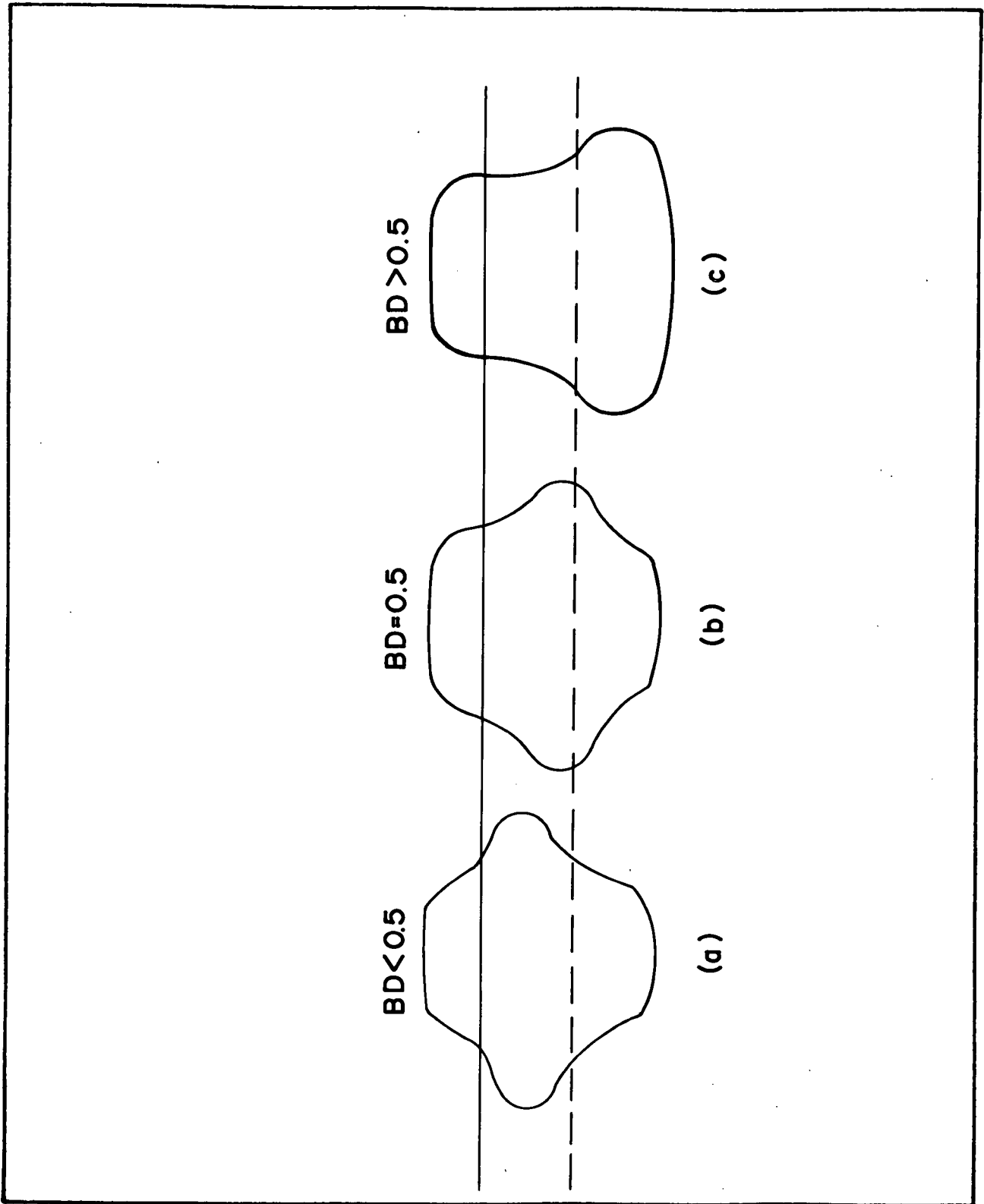


Figure 44. Profiles having similar bulge-width (BW) ratios but different bulge-depth ratios (BD).

showing, for a fixed bulge width ratio, various bulge depth ratio profiles. Assuming each is close to its limit of stability, the significance of the BD ratio in determining draft increases can be seen. As the iceberg in 44 (a) rotates, the waterline width increases rapidly thereby increasing the righting moment GZ. Thus, the effect of a small BD ratio is to limit the range of near-neutral stability. There is, therefore, little chance that the iceberg would roll sufficiently for a significant draft increase to occur. The iceberg in Figure 44 (c) also has a somewhat limited range of near-neutral stability, but for very different reasons. As it rotates the draft increases rapidly, causing a rapid rise in potential. Thus there is a significant draft increase on roll. The parameter BW in this case clearly affects not only the range of neutral stability but also the actual increase in draft attained. The icebergs in 44(a) and (c) presumably represent extremes with 44(b) representing the norm. The iceberg shown in Figure 45 was discussed in Bass and Peters (1984a) and gave a maximum draft-increase of nearly 50%. For this iceberg, $BD \approx 1$ and $BW \approx 2$.

The effect of increasing BW beyond a certain critical value is to increase the stability of the iceberg at the extremities of the near-neutral range and, more importantly, to limit the extent of that range. That critical value depends on the ratio BD. Figure 46 is another iceberg taken from Bass and Peters (1984) with a BD ratio of 0.75 and a BW ratio of 2.4. The maximum increase in draft for this type of iceberg was only 15%.

It may be possible to delineate more precisely the relationship of BW, BD and USC to changes in draft. At present, it can only be conjectured that these are the most significant parameters of the underwater shape determining draft increases for near unstable icebergs. An analysis of a large number of iceberg profiles is needed.

To determine the probability that icebergs with certain BW, BD and USC values exist is much more difficult. The evidence from available sidescan sonar profiles suggests that icebergs with USC values less than one ("bulging") are common, but too few of these records exist for the evidence to be conclusive. A further source of evidence comes from laboratory and field studies of iceberg ablation which suggest the shapes typical of those most prevalent in the sonar records (Josberger, 1977; Russel-Head, 1980). Finally evidence from measured draft-height ratios for a number of icebergs is indicative of the prevalence of bulging underwater shapes. Assuming a glacial ice to sea water density ratio of 0.875, an ideal rectangular cuboid iceberg would have a draft-to-height ratio of 7 to 1. Thus, for a tabular iceberg with a draft-height ratio of 5 to 1 (say) it is possible to conclude it is of bulging ($USC < 1$) underwater-type. Moreover, the smaller the draft-height

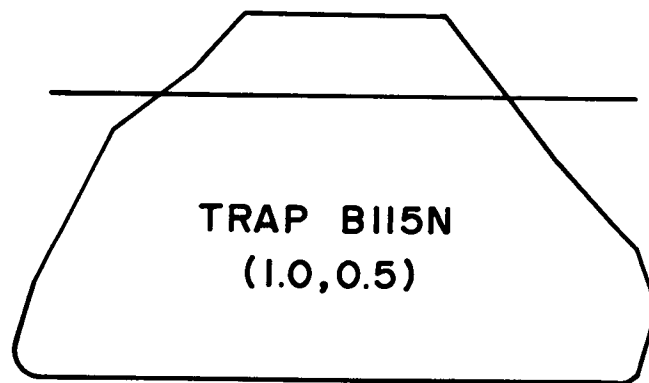


Figure 45. Iceberg profile increases its draft by nearly 50% on roll.

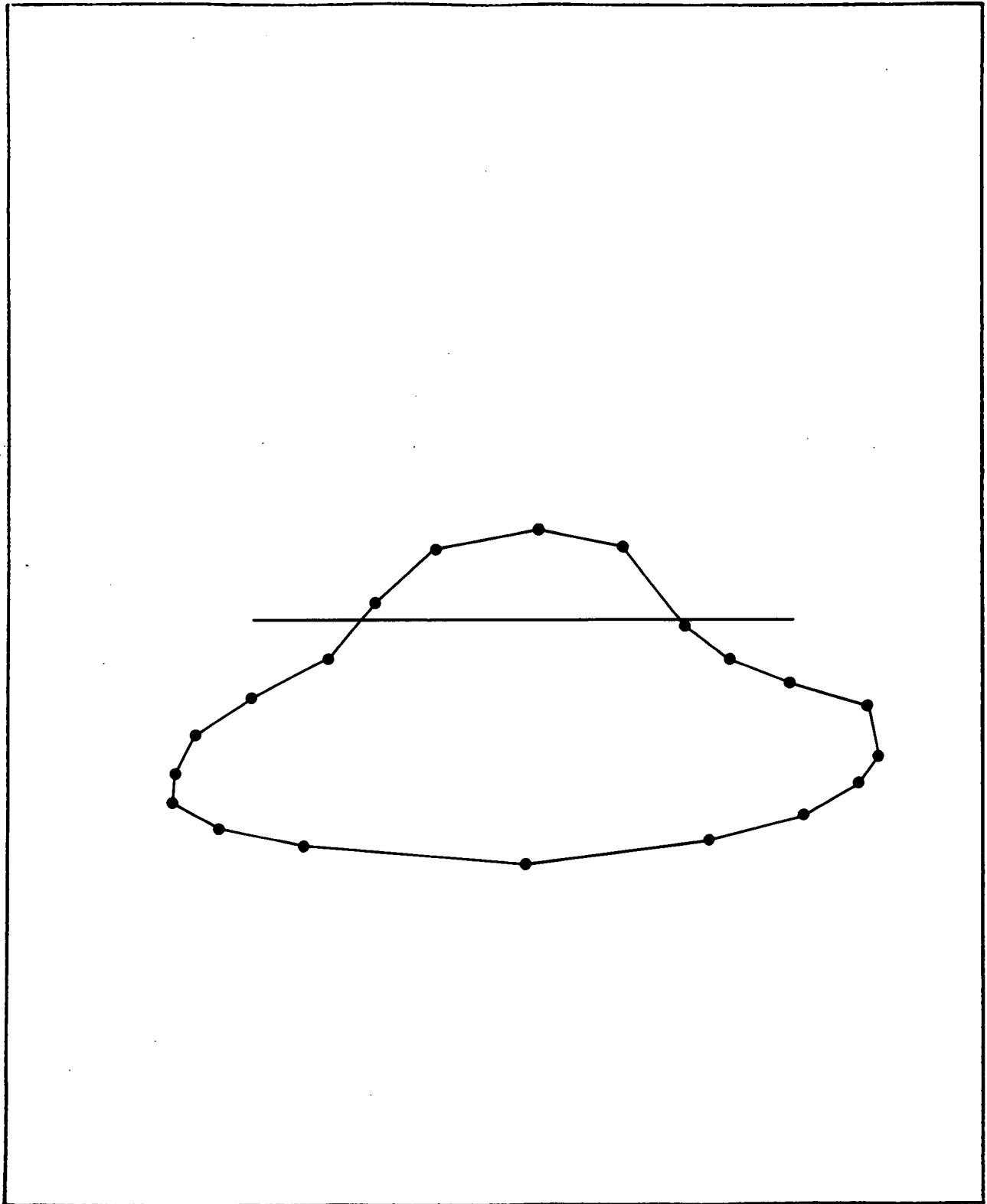


Figure 46. Iceberg profile increases its draft by 15% on roll.

ratio, the greater is the bulge-width ratio BW. The evidence from measured draft-height ratios for tabular bergs indicates an average value of <6 (Miller and Hotzel, 1982; Robe, 1975). For non-tabular icebergs, the evidence is no longer clear. For blocky and domed icebergs, draft-height ratios of less than 6 to 1 are probably indicative of bulging shapes. For pinnacled icebergs (etc.), height above the waterplane is not a good indicator of volume underwater. Thus for highly irregular above water shapes, draft to height ratios can vary a great deal, even if the underwater shapes are the same. Figure 47 shows the distribution of draft-height ratios for various iceberg categories (El-Tahan and Davis, 1982). The generally low values tend to support the evidence for the prevalence of bulging underwater shapes.

Estimates for a likely range of values for the bulge-depth ratio are much more difficult to obtain. From the evidence of sidescan sonar profiles the most likely values appear to be around 0.5. Assuming random variations, with a suitable probability distribution, would enable an estimate of the likelihood of BD ratios >0.5 to be made. Whatever else, the possibility of random variations in the BD ratio about 0.5, is indicative of the existence of the trapezoid class of bergs.

An alternative approach to the modelling presented here is given by Lewis and Bennett (1984). Briefly, these authors treat the problem from a stochastic point of view. They generate randomly a large number of convex polygons representing iceberg profiles. For each profile they calculate the draft change associated with each change in orientation from a metastable (locally stable) to the absolute stable equilibrium. By doing this for a large number of icebergs they are able to compile probabilities of occurrence of various changes in draft.

There are two problems with this approach. First, a stochastic approach requires the generation of large numbers of profiles. If the problem is to be completed in finite time, a restriction is necessary on the complexity of the shapes to be analysed. The profiles in their study are restricted to n -sided convex polygons with $n \leq 10$. None of the profiles in the Bass and Peters (1984a and b) study has less than 15 sides and very few are convex. The omission of what is possibly a major class of icebergs renders the conclusions of their study suspect. Moreover, each profile in their study is taken to be "equally likely" - again an assumption that could be reasonably questioned.

Secondly, a more serious problem is their assumption that, for each iceberg, each change of orientation from a metastable to an absolute stable one is equally likely and moreover, that changes in orientation from metastable to metastable are not likely (and therefore omitted in their

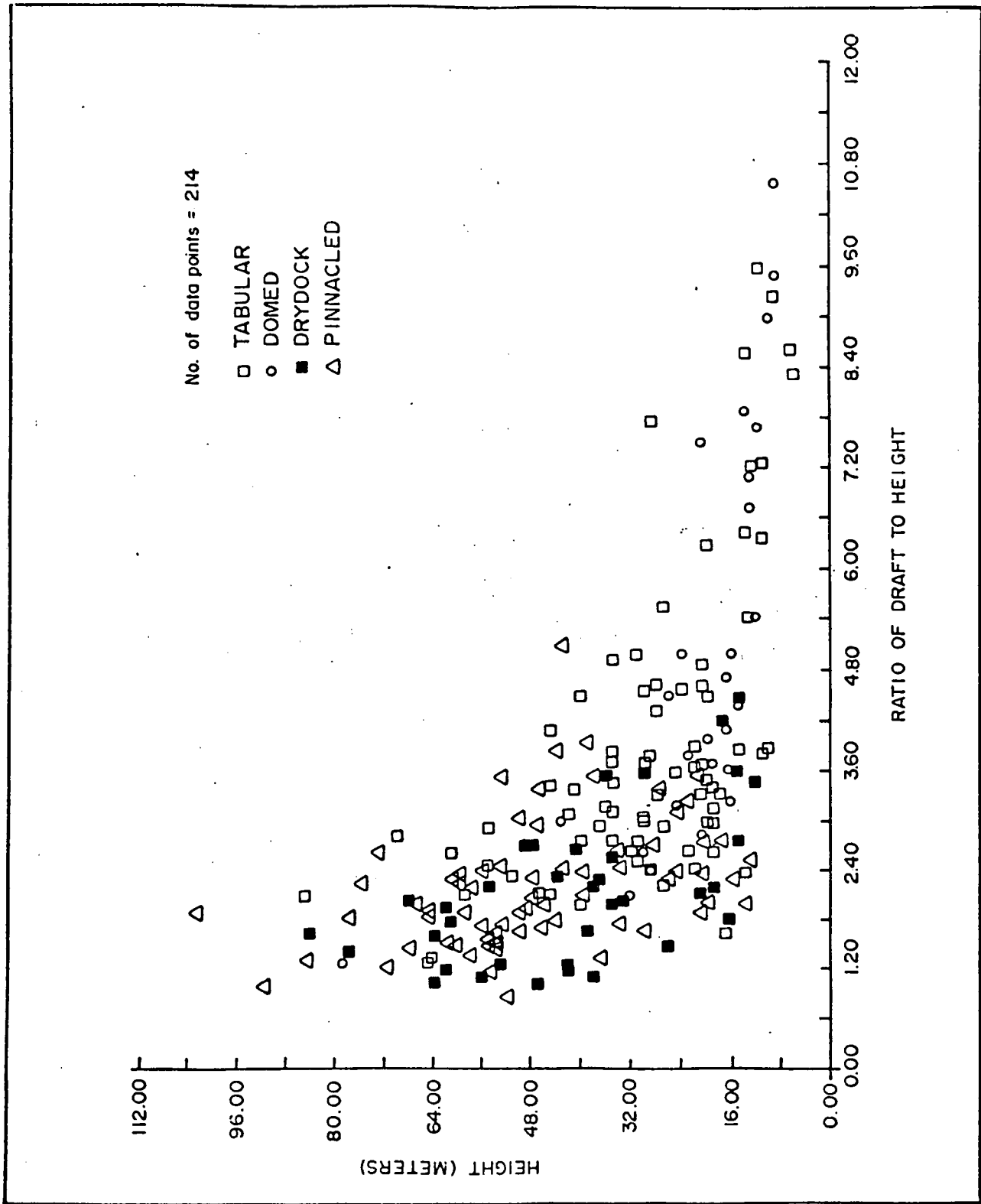


Figure 47. Distribution of draft-to-height ratios for different types of icebergs.

analysis). This assumption automatically precludes the changes in draft that occur in the near-neutral range for many of the icebergs in the trapezoid class (and many others), because many are absolutely stable at an orientation 180° removed from the near-neutral range (i.e. upside down). To accomplish this radical change in orientation would require a great deal of calving and melting, after which the profile could no longer be supposed to bear any resemblance to the original one. Such massive calvings are in fact, according to experienced ice-observers, often accompanied by a total break-up of the iceberg. Thus, probabilities for various changes in draft occurring for real icebergs cannot be reasonably extrapolated because first, the profiles in their study are not equally likely; secondly, the changes in orientation for the profiles considered are not equally likely; thirdly, likely changes in orientation are excluded.

The modelling carried out by Grande and Guillaud (1984) has little to offer. They considered only four basic simple profiles, none of which is near-unstable. They calculated draft changes that could occur if the iceberg were forced to roll and concluded that no significant increase would occur. They also considered the effect of calving large ice chunks from their model profiles and calculated the changes in draft that would occur after such destabilizing events. However, it is not clear just how much ice is calved in their simulation. If it is too large, their results are subject to some uncertainty for they concluded that draft changes of up to 15% could occur in such calving events.

If a probability distribution for bulge depth ratios (BD) and bulge width ratios (BW) could be established, then it might be possible to determine the probability of occurrence of certain increases in draft. Part of that analysis would require a reassessment of the type of results obtained in Bass and Peters (1984b) where maximum possible draft increases were calculated for each iceberg type. The results need to be reassessed from a probabilistic point of view. An example is given in Table 3 of the type of reanalysis required for four typical icebergs in the trapezoid class. The analysis is based on two assumptions. The first is that each orientation in the near-neutral range for the iceberg, is equally likely. The second is that on being perturbed from an equilibrium orientation in the near-neutral range, the iceberg moves to one of the two extremities of that range (each of which is equally likely) where the draft is greatest. The four icebergs considered are defined by the trapezoid type from which they were derived (Figure 48).

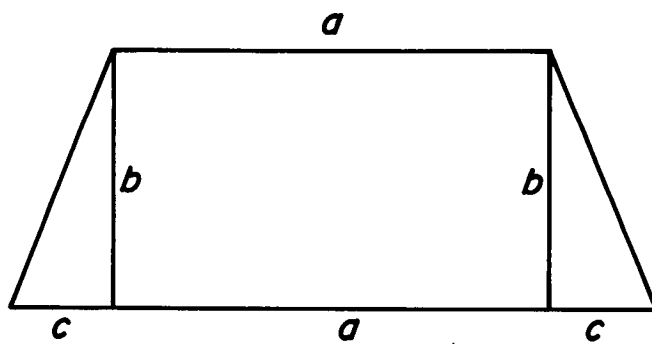


Figure 48. Trapezoidal iceberg of type (a,c).

TABLE 3

Probability of exceeding certain percentage draft increases for four typical trapezoidal icebergs.

Iceberg Type (a/b, c/b)	Draft Increase > 15%	Draft Increase > 10%	Draft Increase > 15%	Draft Increase > 20%	Draft Increase > 25%
(1.0, 0.3)	72%	47%	34%	31%	8%
(1.3, 0.4)	75%	56%	38%	15%	0%
(1.6, 0.5)	75%	57%	27%	2%	0%
(1.9, 0.3)	85%	72%	57%	44%	4%
Average	77%	58%	39%	23%	3%

Tilt

A model of iceberg scour with three-degrees of freedom of motion has been developed in which all motions are assumed to take place relative to a single vertical plane. The model was developed to determine the effects of a collision, with the seabed, of an iceberg rolling to an orientation of deeper draft. The model also predicts the subsequent motion and, in fact, may be used to model the dynamics of a scouring iceberg. The emphasis in the modelling has been on the dynamics of the iceberg rather than the dynamics of the surficial sediment shifted during scour. The forces associated with the soil pressures developed during scour have been derived on a quasi-statical basis. Those forces impeding horizontal motion of the iceberg are based on the simple quasi-statical model of Chari (1979), whereas the forces impeding vertical motion are derived from simple bearing capacity formulae (Scott, 1963). Both sets of forces are dependent on the cohesive shear strength (τ) and the submerged unit mass (γ) of the surficial sediment. The angle of soil shear resistance is taken to be very small. For the purpose of discussion, τ was taken to be between 2.0 kPa and 50.0 kPa, and γ was set at 1.5 tonnes/m³. The range of values chosen for τ reflect the generally weak surficial sediments found in the Labrador area.

Body-fixed axes are taken at the centre of mass of the iceberg, moving relative to some inertial frame (x, y) with the x -axis horizontal and positive in the direction of iceberg motion (assumed moving initially with the ocean current at 0.5 m/s). The vertical y -axis is positive downwards and the direction of rotation about an axis orthogonal to the x - y plane, positive in the anticlockwise direction. The soil resistance forces are dependent on the depth of penetration (S_2) of the scouring keel in the seabed and the distance traversed (S_1) by the scouring keel. The iceberg profile used in the analysis is shown in Figure 49. It is a profile used in the study by Bass and Peters (1984a) of icebergs that increase their draft on rolling. The profile represents the average vertical cross-section of an iceberg taken orthogonal to its major axis. The section of the three-dimensional iceberg that actually comes into contact with the seabed can be assumed to be of any shape, because any protrusions, spurs or notches are averaged out in taking the two-dimensional profile. The keel used in this model is taken to be a three-dimensional trapezoid of variable base angles and variable lower face (see Figure 49) TF1 determines the width of scour and is assumed to be 30 m in the simulation. The base angles of the trapezoid sections ϕ_1 and ϕ_2 are taken to be approximately 60°. The keel is assumed to "drag behind" in the motion. Although this is not the only possible motion of a scouring iceberg, it is likely to be the more stable relative to yaw motion. It has also been assumed that the scouring keel is centrally

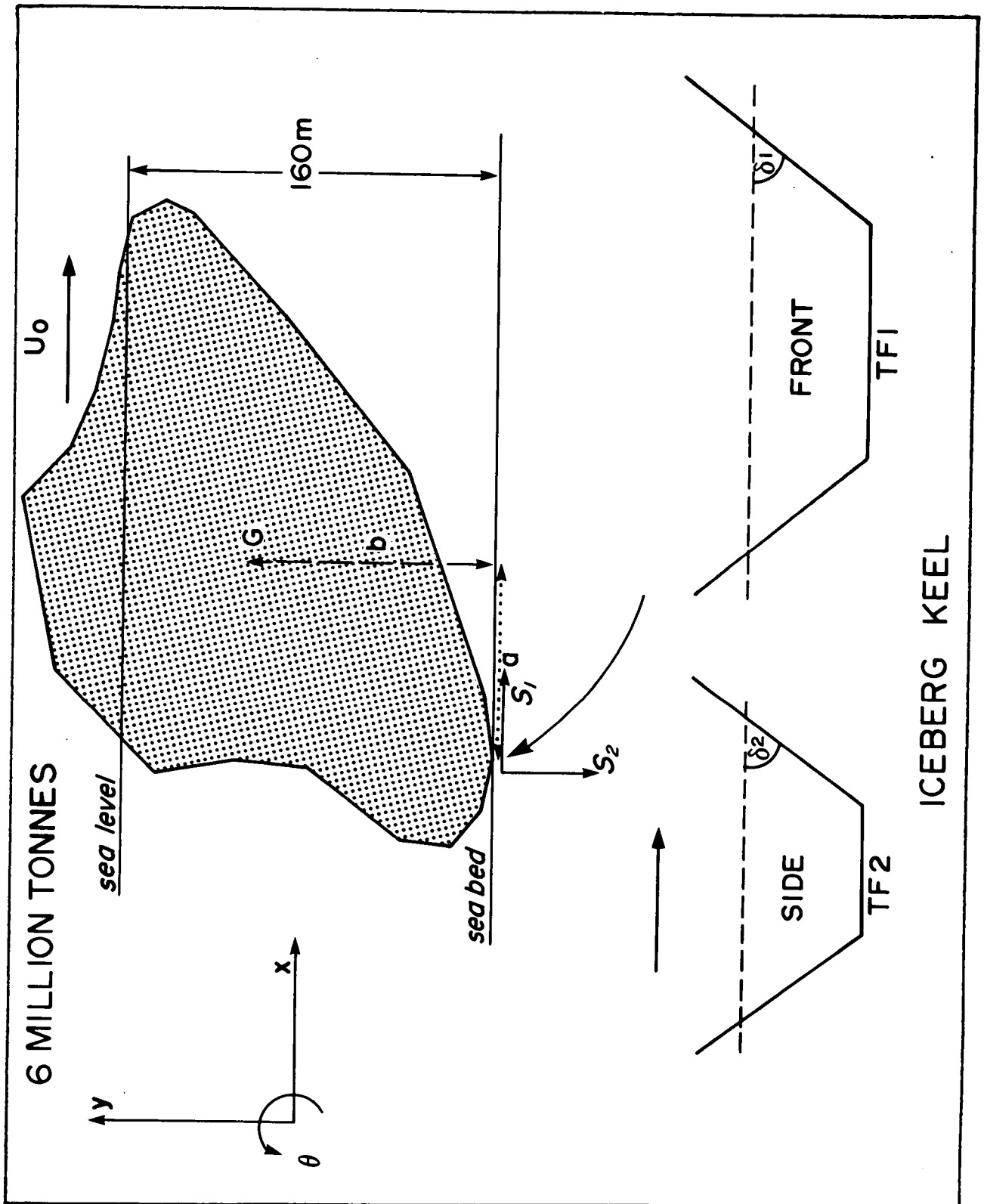


Figure 49. Iceberg profile used in simulation.

located on the major axis of the iceberg. Again this assumption is necessary because yaw has been omitted from the motion equations. Clearly a more comprehensive analysis requires the inclusion of yaw in the motion equations. The effect on the analysis is to at least double the number of parameters that have to be taken into account and is, therefore, a major undertaking. The calculation of the hydrodynamic coefficients for the motion equations is described in Bass and Sen (in prep.). In fact terms such as added mass may be considerably underestimated by the techniques employed, because the effects of underkeel clearance are difficult to quantify, but generally magnify such quantities as added mass (Blok and Dekker, 1979).

The motion equations are:

$$(M + \delta M_1) \ddot{x} + b_1 \dot{x} - \frac{1}{2} C_D \rho S_A (U_o - \dot{x}) |U_o - \dot{x}| = -F_1(S_1, S_2)$$

$$(M + \delta M_2) \ddot{y} + b_2 \dot{y} + A_{wp} \rho g y = -F_2(S_1, S_2)$$

$$(I + \delta I) \ddot{\theta} + b_3 \dot{\theta} + M g GM\theta = -a F_2(S_1, S_2) - b F_1(S_1, S_2)$$

$$\dot{S}_1 = b\dot{\theta} + \dot{x}$$

$$\dot{S}_2 = a\dot{\theta} + \dot{y}$$

where:

M_1, M_2, I = added mass terms

b_1, b_2, b_3 = damping terms

C_D = a drag coefficient

S_A = underwater surface area

U_o = velocity of the ocean current

A_{wp} = waterplane area

GM = transverse metacentric height

a and b = the horizontal and vertical distances of the centre of gravity from the 'centre' of the scouring keel.

The forces F_1 and F_2 are given as follows;

$$F_1(S_1, S_2) = \frac{\gamma g (S_2')^2}{2.0} + 2\tau S_2' B + \sqrt{2} S_2'^2 \tau$$

where: $B = (TF1 + S_2 \cot \delta_1)$, $S_2' = S_2 + S_1 \text{ grad}$

and grad is the slope of the seabed.

$$F_2(S_1, S_2) = (\tau(\pi + 2) + \gamma g S_2') ACON$$

where: $ACON = (TF1 + S_2' \cot \delta_1)(TF2 + S_2' \cot \delta_2)$

The horizontal soil pressure force (F_1) is dependent on the depth of keel penetration beneath the seabed and the 'average width' of that keel (B). As the iceberg moves forward into a seabed slope, the width (B) will vary. Similarly, the vertical soil pressure force (F_2) is dependent on the depth of penetration and the horizontally projected surface area in contact with the seabed ($ACON$).

In the simulation, an iceberg of mass 6 million tons and draft 160 m was used. To demonstrate upslope and downslope scour a gentle incline of slope 1 in 100 over a distance of 200 m was chosen followed by a downward slope of gradient 1 in 100. Despite the simplicity of the modelling, the results shown in Figures 50 and 51 amply demonstrate the significance of the parameters GM , τ and keel size. The low and the high values of GM are 1.7 m and 8.6 m and the low, medium and high values of soil strength τ are 2, 25 and 50 kP respectively. For an iceberg that is only weakly stable, there is clearly no difficulty traversing much higher ridges. However, for such icebergs, the depth of scour on the downward slope can be significantly smaller (as can the length of scour), than that on the upward slope. Just how much smaller (and shorter) depends on GM , τ and keel size. The contact face ($TF1 \times TF2$) was taken as 30 m x 4 m in the simulations of Figure 50 (small keel) and as 30 m x 10 m in Figure 51. The reason for the less deep, shorter scours on the downward slope, is that on the upward slope, the increasing soil depth (and, therefore, lateral force) and forward motion tilts the iceberg clockwise, but on the downward slope it has insufficient stored energy to regain the depth lost on the upward slope.

Figure 52 shows a particularly interesting case of an iceberg that rolled to an orientation of deeper draft. At the base of the slope it has an angular velocity of 0.005 rad/sec. Its equilibrium orientation is a further 0.01 radians (anticlockwise) from its orientation at the base of the slope. The iceberg then rolls past its equilibrium orientation to a depth of nearly 5 m before swinging back out of the seabed and then back in again. The oscillation is quickly dampened by soil pressures and the iceberg

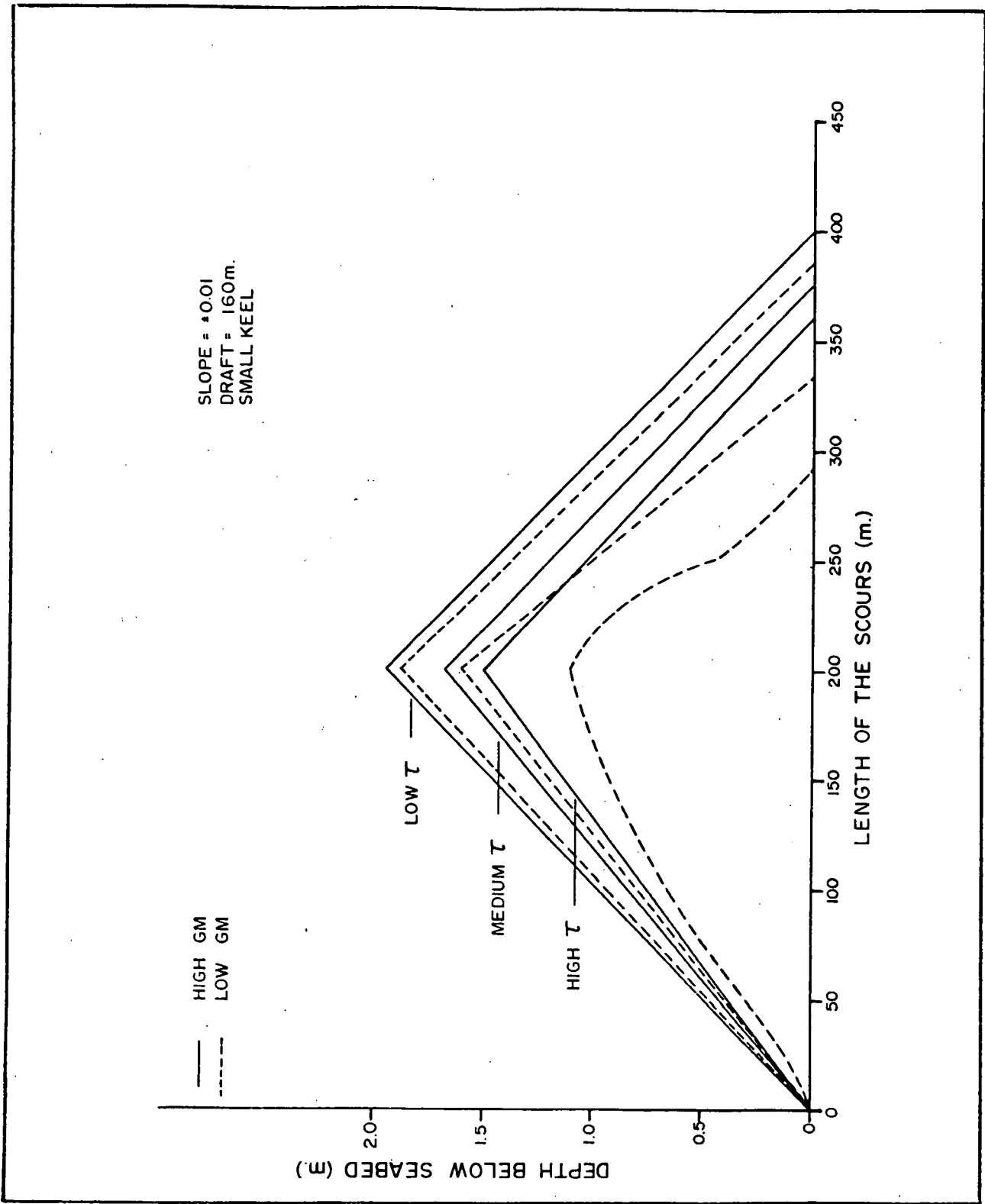


Figure 50. Scour depth verses distance travelled by a small keel.

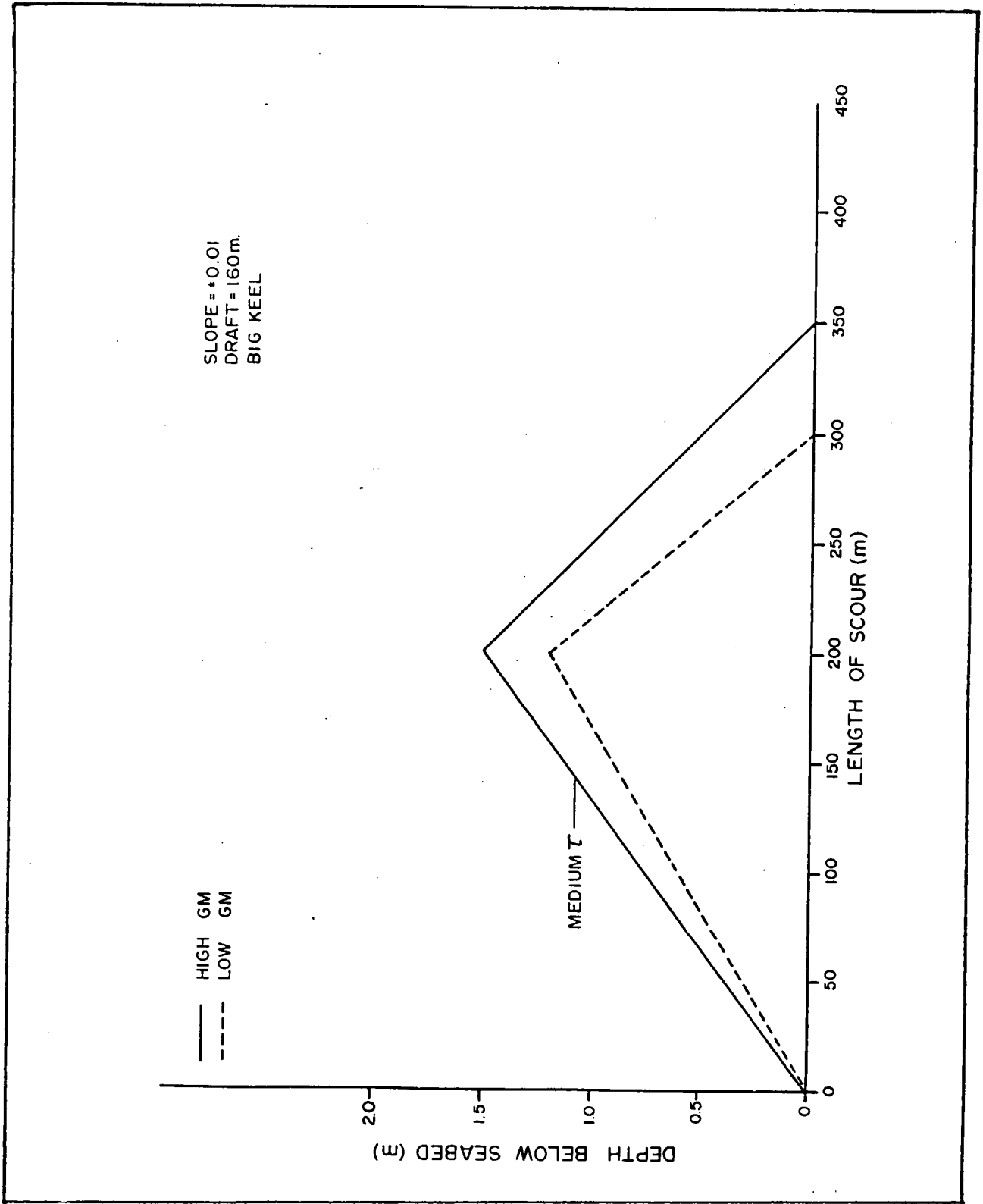


Figure 51. Scour depth versus distance travelled by a large keel.

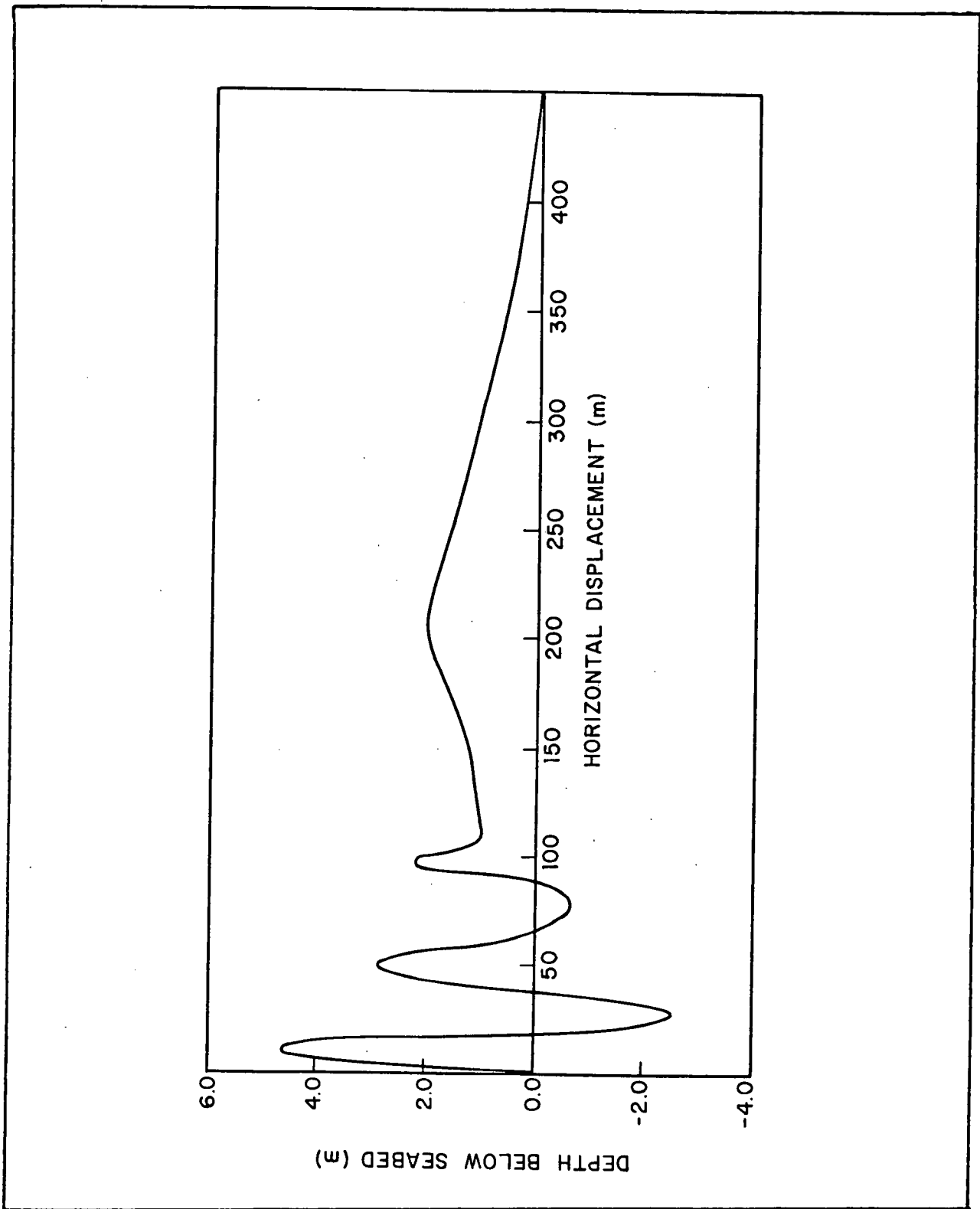


Figure 52. Scour by a rolling iceberg.

continues to scour upslope. In this situation the scour depth is at least equal on the downward slope to that on the upward slope and, in fact, scours farther than any of the bergs in the other simulations.

DISCUSSION AND POSSIBLE FUTURE WORK

The mosaics and scour maps used in this inventory provide a geological record of past scouring events from which the bathymetric range traversed by scouring bergs can be determined.

Changes in scour depth (where these data are available) can be recorded and compared with isobath crossings to define systematic or non-systematic depth changes. Changes in scour depth may not only reflect variations in the geological and geotechnical properties of the seabed (e.g. Chari, 1979) but also changes in the dynamic behaviour of a berg as it scours across isobaths (e.g. Woodworth-Lynas, et al. 1985). Depth changes may also indicate zones of infilling or erosion following the scouring event which is probably true for many old scours.

Changes in scour width may also be compared with isobath crossings. Scour morphology can be related back to berg movement patterns; for example, straight, curved or angled scours may yield information on local iceberg trajectories and currents. The correlation of current direction with scour orientation is not a straightforward matter. It must be remembered that the scours identified from the mosaics represent a spectrum in time possibly from the glacial era to the present and that temporal variations in ocean currents are quite possible. Because of sparse coverage the current regime for some study areas had to be extrapolated from distant collection points, and most data were collected during the summer and early fall. Thus, the data reflect only partial current regimes and perhaps should not be used to predict flow during the rest of the year or to infer the oceanic regime since glacial times.

The mode of scouring can be inferred: for example, normal linear scours imply continuously bottom-touching keels; crater or pit-like scours imply oscillating rotation as keels alternately penetrate and rotate free of the seabed; scours with transverse cusped features may imply "wobbling" bergs (e.g. Lien, 1982; Reimnitz et al., 1973). Keel morphology (single, double, or multi-keeled) can be inferred from scours that contain striations and grooves within the trough.

Scour length, together with upslope and downslope information, can be used to define the gradient of isobath-traversing scours, and may suggest certain ranges in gradient that are most likely to be scoured. In most cases scour lengths measured from the mosaics and scour maps are usually only partial lengths, complete scours being rarely seen in such relatively small survey areas (consequently scour length data from these surveys should not be used to infer maximum possible scour length). However, long scour tracks can be inferred from the radar data. Because the

main objective of this study is to provide a database a statistical analysis of these parameters has not been attempted.

The iceberg movement data from Labrador wellsite radar logs have been studied intensely in recent years, with the aim of developing iceberg drift hindcast and eventually forecasting models (e.g. Banke and Smith, 1984; Ball et al., 1981; Gaskill and Rochester, 1984; Sodhi and El-Tahan, 1980). More recently, the same data were used by Woodworth-Lynas et al. (1985) and El-Tahan et al. (1985) to estimate rates of iceberg scouring and grounding on the eastern Canadian shelf area. Two advantages of this data set over the mosaics and scour maps are, first, that longer interpreted scour tracks can be inferred, many of which reach great lengths (more than 10 km and possibly as great as 220 km); secondly, the complete amount of bathymetric range traversed by bergs interpreted to be scouring can be estimated (traverses as great as 45 m have been interpreted from radar data). Disadvantages are that the scour tracks are interpretations and have not been verified using acoustic surveys. Data on scour depth, changes in width and some morphological descriptions (e.g. crater chain scours and multi-keeled scours) cannot be gathered from the radar trajectories. However, the wellsite data place the seabed information in context and provide a very useful regional picture of modern day scouring.

The modelling of iceberg stability demonstrates, through theory, the upslope and downslope scouring ability of certain bergs and places the results of the inventory in perspective. The inventory data can be analysed not only in their own right, as discussed previously, but also can be used to further the development of theoretical knowledge of the physical responses of bergs to environmental forces during scouring. Discussion of draft increases after rolling of different iceberg types is important because it indicates that iceberg keels are not necessarily brought into contact with the seabed simply by running into a sloping seafloor. The presence of craters and in particular crater chains within mosaic areas is clear evidence of draft increase.

Variations in soil strength and changes in GM of modelled bergs (e.g. Figures 50 and 51) allows a variety of different scour tracks to be modelled. In areas of more competent seabed sediments, the results of modelling scouring over a symmetrical ridge suggests that bergs scouring downslope may float free of the seabed at shallower water depths than the initial point of contact on the upslope side. This observation suggests that in areas where both ends of scour tracks are visible where they traverse ridges and troughs, the direction of iceberg movement could be deduced.

Importantly, it can be seen that continual variation in scour depth can be expected in isobath-traversing scours, and this must be considered when analysing scour depths. Variations in scour depth means that a single measurement is insufficient to describe each individual scour. Further, measured scour depth may not necessarily reflect the original incision depth because of the possibility of post-scour infilling and erosion.

It has been demonstrated that icebergs can scour both upslope and downslope and evidence for the assumptions of the theoretical modelling has been presented. A more detailed analysis of three-dimensional iceberg models with full six-degrees of motion simulation equations is needed, to better quantify the results of the simulation presented here. It is doubtful whether the qualitative analysis would be very different but that could only be ascertained for certain following a full analysis of the three-dimensional modelling.

REFERENCES

- Ball, P., H.S. Gaskill and R.J. Lopez. 1981. Iceberg motion: an analysis of two data sets collected at drill sites in the Labrador Sea. C-CORE Technical Report 81-2, 121 p.
- Banke, E.G. and S.D. Smith. 1984. A hindcast study of iceberg drift on the Labrador Coast. Canadian Technical Report of Hydrography and Ocean Sciences, No. 49, 161 p.
- Barrie, J.V. 1980. Iceberg-seabed interaction (Northern Labrador Sea). *Annals of Glaciology*, 1:71-76.
- Barrie, J.V., C.M.T. Lynas and G. Gidney. 1982. Iceberg grounding review from wellsite observations. Geological Survey of Canada Open File Report 880.
- Barrie, J.V., C.F.M. Lewis, G.B. Fader and L.H. King. 1984. Seabed processes on the northeastern Grand Banks of Newfoundland; modern reworking of relict sediments. *Marine Geology*, 57: 209-227.
- Bass, D.W. and G.R. Peters. 1984a. Computer simulation of iceberg instability. *Cold Regions Science and Technology*, 9: 163-169.
- Bass, D.W. and G.R. Peters. 1984b. Simulation of capsizing icebergs. Proceedings of the Conference 'Applied Identification, Modelling and Simulation', New Orleans, 159-163.
- Bass, D.W. and D. Sen (In preparation). Added mass and damping coefficients for certain iceberg models.
- Blok, J.J. and J.N. Dekker. 1979. On the hydrodynamic aspects of ship collision with rigid or non-rigid structures. #3664, Proc. of the Offshore Technology Conference, Houston.
- Chari, T.R. 1979. Geotechnical aspects of iceberg scours on ocean floors. *Canadian Geotechnical Journal* 16(2): 379-390.
- Chari, T.R. and G.R. Peters. 1981. Estimates of iceberg scour depths. In Proc. Symposium, Production and Transportation Systems for the Hibernia Discovery, Feb. 16-18th., St. John's, p 178-188.
- Chari, T.R., G.R. Peters and K. Muthukrishnaiah. 1980. Environmental factors affecting iceberg scour estimates. *Cold Regions Science and Technology*, 1:223-230.

- Comfort, G. and B. Graham (In press). Evaluation of sea bottom ice scour models. Environmental Studies Revolving Funds, Study No. 098-23-05.
- Darwin, C.R. 1855. On the power of icebergs to make rectilinear, uniformly-directed grooves across a submarine undulatory surface. London, Edinburgh and Dublin Philosophical Magazine and Journal of Science 10:96-98.
- Dempster, R.T. 1984. The measurement and modelling of iceberg drift. Ocean '74 IEEE Conference on Engineering in the Ocean Environment, Halifax, Aug. 21-23, p. 125-129.
- Dobrocky Seatech (Nfld.) Ltd. 1981. 1981 Labrador physical oceanographic program. Prepared for Petro-Canada Exploration.
- Dobrocky Seatech (Nfld.) Ltd. 1983. 1983 Offshore Labrador physical oceanographic program data report. Prepared for Petro-Canada Inc.
- El-Tahan, M. and H.L. Davis. 1982. Correlation between iceberg draft and above water dimensions. NRC, Iceberg Scour Workshop, Montebello, Quebec, 1982.
- El-Tahan, M., H. El-Tahan, D. Courage and P. Mitten. 1985. Documentation of iceberg groundings. Environmental Studies Revolving Funds Report No. 007, Ottawa, 162 p.
- Fillon, R.H. and R.A. Harmes. 1982. Northern Labrador Shelf glacial chronology and depositional environments. Canadian Journal of Earth Sciences 19(1):162-192.
- Fissel, D.B. and D.D. Lemon. 1982. Analysis of physical oceanographic data from the Labrador Shelf. Summer 1980. OLABS Program Report, 155 p.
- Gaskill, H.S. and J. Rochester. 1984. A new technique for iceberg drift prediction. Cold Regions Science and Technology, 8:223-234.
- Geomarine Associates Ltd. 1975. Operations report, sea bottom survey, Labrador Shelf, July-August, 1975. Contract report prepared for Eastcan Exploration Ltd., 71 p.
- . 1976a. Snorri Wellsite bathymetry and iceberg scours. Report prepared for Eastcan Exploration Ltd., 126 p.
- . 1976b. Bjarni Wellsite bathymetry and iceberg scours. Contract report prepared for the Labrador Group, 137 p.

- _____. 1980a. Wellsite survey report, Rut, Saglek Bank, Labrador, September 2-September 5, 1980. Contract report prepared for the Labrador Group.
- _____. 1980b. Wellsite survey report, North Bjarni F-06, Makkovik Bank, Labrador, August 20-August 25, 1980. Contract report prepared for the Labrador Group.
- _____. 1980c. Wellsite survey report, East HB, Harrison Bank, Labrador, September 11-September 13, 1980. Contract report prepared for the Labrador Group.
- _____. 1980d. Wellsite survey report, D.B., Hamilton Bank, Labrador, September 14-September 16, 1980. Contract report prepared for the Labrador Group.
- Gilbert, G. and J.V. Barrie. 1985. Provenance and sedimentary processes of ice scoured surficial sediments, Labrador Shelf. *Canadian Journal of Earth Sciences*, 22(7):1066-1079.
- Grande, N. and C.H. Guillaud. 1984. Iceberg stability and draft changes. *Proc. Cold Regions Speciality Conf.*, April, Canadian Society of Civil Engineers, Montreal, p. 459-471.
- Hodgins, D.O. and H. Westergard. 1981. Internal waves in Davis Strait and their measurements with a real-time system. *Proc. 6th International Conference on Port and Ocean Engineering under Arctic Conditions*, '81, Quebec. 423-432.
- Jollymore, P.G. 1974. A medium range sidescan sonar for use in coastal waters: design criteria and operational experiences. *OCEAN '74 Conference Record*, Halifax, Nova Scotia, Aug. 21-23, 2:108-114.
- Josberger, E.G. 1977. A laboratory and field study of iceberg deterioration. *Proc. of 1st International Conference on Iceberg Utilization*, Ames, Iowa. 254-264.
- Josenhans, H.W. and J.V. Barrie. 1982. Preliminary results of submersible observations on the Labrador Shelf. *Geological Survey of Canada Paper 82-1B*: 269-276.
- Lewis, J.C. and G. Bennett. 1984. Monte Carlo calculations of iceberg draft changes caused by roll. *Cold Regions Science and Technology*, 10:1-10.

- Lien, R.L. 1982. Seabed features in the Blaaenga area, Weddell Sea, Antarctica. 6th International Conference on Port and Ocean Engineering under Arctic Conditions, Quebec, Canada, July 27-31. Proceedings, p. 706-716.
- Lopez, R., T.R. Chari, E. Moore, G.R. Peters and A. Zielinski. 1981. Hydrodynamic effects on iceberg gouging. Cold Regions Science and Technology, 4:55-61.
- MacLaren Marex Inc. 1980. Current meter data analysis of long term current meter moorings. Prepared for Total Eastern Exploration Ltd.
- MacLaren Plansearch Lavalin. 1981. Data analysis from current meter arrays at Sedco 706 and Zapata Uglan on the Grand Banks - October 2 to December 5, 1980. Report No. 8. Prepared for Mobil Oil Canada Ltd., 73 p.
- MacLaren Plansearch Lavalin. 1982. Data analysis from a current meter mooring at Sedco 706 on the Grand Banks - October 9 to December 12, 1981. Report No. 16. Prepared for Mobil Oil Canada Limited, 43 p.
- Miller, J.D. and I.S. Hotzel. 1982. Physical dimensions of icebergs in the Labrador Sea. NRC Workshop on Iceberg Scour, Montebello, Quebec: 103-113.
- Mountain, D.G. 1980. On predicting iceberg drift. Cold Regions Science and Technology 1:273-282.
- Newfoundland and Labrador Petroleum Directorate. 1983. A preliminary study on the integrity of a gravity base platform at Hibernia.
- NORDCO Ltd. 1979. Current data analysis - drill site Bjarni O-82. Prepared for Total Eastcan Ltd.
- NORDCO Ltd. 1981. Analysis of current data from the Hopedale Saddle. Prepared for Chevron Standard Ltd.
- NORDCO Ltd. 1981. Current and CTD Profiles on the Labrador Shelf. Prepared for Petro-Canada Exploration Inc., 167p.
- NORDCO Ltd. 1982. A Catalogue of Iceberg Scours and Ice Related Features on the Grand Banks of Newfoundland. Confidential report prepared for the Hibernia Joint Venture participants, 46 p.
- NORDCO Ltd. 1984. Surficial Geology of the Labrador Continental Shelf. Report prepared for Petro-Canada Exploration Inc. Geological Survey of Canada Open File Report 1081, 3 vols.

- Pereira, C.P.G., C.M.T. Woodworth-Lynas, J.V. Barrie, and C.F.M. Lewis. (In press). Iceberg scouring and sedimentological investigations of the southeast Baffin Island continental shelf.
- Praeg, D.B., B. MacLean, I.A. Hardy and P.J. Mudie. (In press). Quaternary geology of the Southeast Baffin Island Continental Shelf, N.W.T. Geological Survey of Canada Paper 85-14.
- Reimnitz, E., P.W. Barnes and T.R. Alpha. 1973. Bottom features and processes related to drifting ice on the Arctic Shelf, Alaska. United States Geological Survey, Miscellaneous Field Studies Map MF-532.
- Robe, R.Q. 1975. Height to draft ratios of icebergs. Proc. 3rd International Conference on Port and Ocean Engineering under Arctic Conditions, '75, Fairbanks, Alaska. 1:407-415.
- Russel-Head, D.S. 1980. The melting of free drifting icebergs. Annals of Glaciology, 1:119-122.
- Scott, R.F. 1963. Principles of soil mechanics. Addison Wesley.
- Seaconsult Marine Research Ltd. 1982. Analysis of oceanographic conditions at Raleigh N-18, 1982. Prepared for Canterra Energy Ltd., 238 p.
- Sodhi, D.S. and R.T. Dempster. 1975. Motions of icebergs in water currents. OCEAN '75 conference record, San Diego, California, Sept. 22-25:348-350.
- Sodhi, D.S. and M. El-Tahan. 1980. Prediction of an iceberg drift trajectory during a storm. Annals of Glaciology 1:77-82.
- Woodworth-Lynas, C.M.T. 1983. The relative age of ice scours using cross-cutting relationships. C-CORE Technical Report 83-3, 54 p.
- Woodworth-Lynas, C.M.T. and J.V. Barrie. 1985. Iceberg scouring frequencies and scour degradation on Canada's Eastern Shelf areas using sidescan remapping techniques. In: Proc. 8th International Conference on Port and Ocean Engineering Under Arctic Conditions, Sept. 6-13, 1:419-442.
- Woodworth-Lynas, C.M.T., A. Simms and C.M. Rendell. 1984a. Grounding and scouring icebergs on the Labrador Shelf. Iceberg Research, 7:13-20.

----- . 1984b. Iceberg grounding and
scouring frequency, Labrador Sea. OCEANS '84.
Conference Proceedings, Washington, D.C. Sept. 10-12.

----- . 1985. Iceberg grounding and
scouring on the Labrador Continental Shelf. Cold
Regions Science and Technology 10:163-186.